Topics in model building and phenomenology beyond the standard model

by Johannes Heinonen

This thesis/dissertation document has been electronically approved by the following individuals:

Csaki,Csaba (Chairperson)

Perelstein,Maxim (Minor Member)

Wittich,Peter (Minor Member)

TOPICS IN MODEL BUILDING AND PHENOMENOLOGY BEYOND THE STANDARD MODEL

A Dissertation

Presented to the Faculty of the Graduate School

of Cornell University

in Partial Fulfillment of the Requirements for the Degree of

Doctor of Philosophy

by

Johannes Heinonen

August 2010

TOPICS IN MODEL BUILDING AND PHENOMENOLOGY BEYOND THE
STANDARD MODEL

Johannes Heinonen, Ph.D.

Cornell University 2010

The origin of electroweak symmetry breaking is about to be explored by the LHC, which has started taking high-energy data this spring. In this thesis, we explore several theories proposed to extend the standard mode (SM) of particle physics and their phenomenological consequences for the LHC.

First we show that there exists an anomaly-free Littlest Higgs model with an exact T-parity by explicitly constructing such a weakly coupled UV completion. We show that an extended gauge and fermion sector is needed and estimate the impact of new TeV scale particles on electroweak precision observables. We also give both a supersymmetric and a five-dimensional solution to the remaining hierarchy problem up to the Planck scale.

We then examine the feasibility of distinguishing a fermionic partner of the SM gluon from a bosonic one at the LHC. We focus on the case when all allowed tree-level decays of this partner are 3-body decays into two jets and a massive, invisible particle. We show that the dijet invariant mass distributions differ significantly in the two models, as long as the decaying particle is substantially more massive than its invisible daughter.

Finally we analyze the theory and phenomenology of anomalous global chiral symmetries in the presence of an extra dimension. We propose a simple extension of the standard model in 5D whose signatures closely resemble those of supersymmetry with gauge mediation.

BIOGRAPHICAL SKETCH

Johannes Heinonen was born in Hamburg, Germany, on September 8 1979 as the first child of his father Rauno, an engineer, and his mother Gudrun, a medical technical assistant and homemaker.

Together with his younger brother Karl Henrik, he spent his childhood and adolescence in his hometown of Oering, Germany. He graduated at top of his class, receiving his "Abitur" degree from the Dahlmannschule in Bad Segeberg in 1998. After completing 13 month of obligatory alternative service in a hospital, he enrolled at the Ruprecht-Karls University of Heidelberg and started his training as a physicist in the fall of 1999.

In the academic year 2002/03 he spent an exchange year at Cornell University. Back in Heidelberg, he specialized in theoretical physics and graduated in July 2005 with a "Diplom" thesis on the "Renormalization flow in the Hubbard model" under the supervision of Prof. Christof Wetterich. From 2000 until the completion of his degree in 2005 he was supported by the German National Merit Foundation ("Studienstiftung des Deutschen Volkes").

In 2005, he returned to Cornell University to pursue a Ph.D. in theoretical particle physics under the supervision of Prof. Csaba Csáki. He worked on building models of electroweak symmetry breaking and exploring their phenomenology. After receiving his degree, he will join the high energy theory group at the University of Chicago as postdoctoral research associate with a McCormick fellowship.

Rauzille.

ACKNOWLEDGEMENTS

TABLE OF CONTENTS

LIST OF TABLES

LIST OF FIGURES

CHAPTER 1

INTRODUCTION

1.1   History and the big picture

The last century has seen tremendous success in uncovering the fundamental interactions that govern our world. At the end of the 19th century, the only known forces were gravity and the electromagnetic force. Nevertheless, to a large part it was believed that the fundamental physics was understood. So much that in 1874 Max Planck was told not to study theoretical physics, as this field was completely known and only small gaps needed to be filled. At the turn of the century, this changed quickly when quantum mechanics was discovered and its mathematical foundations revealed within only two decades by brilliant young theoretical physicists. Together with the new theory of relativity, this fundamentally changed our view of the world, shaking our beliefs of an absolute time and of a deterministic description of nature.

Shortly after radioactive decays were found and it was realized that there is even more unknown underlying physics than previously assumed. In the following half century, a whole "zoo" of particles was discovered and studied in great detail. This led to a deeper understanding of the world and finally to the weak force explaining radioactive decays and the strong force responsible for the confinement of nuclei. All together this culminated in the standard model of particle physics summarizing our understanding of the fundamental building blocks of nature. Now, at the beginning of the 21st century, we are at a similar situation as a little over hundred years ago: the standard model has been tested, verified and no deviations have been found. However, we have reasons to be-

lieve that the "small gaps" we know about are not actually that small and that there is some, more fundamental, physics we do not know about yet.

Fortunately, there is hope that we will soon be able to answer this question and deepen our understanding of nature. The Large Hadron Collider (LHC) has started running at CERN in fall 2009 and is right now taking data at unprecedented energies. Counted in manpower, this is probably the largest scientific effort mankind has ever undertaken and undoubtably the upcoming years will give us more insight into the fundaments of the universe. We will either learn about the particles and mechanisms that are responsible for electroweak symmetry breaking or, much less likely but not impossible, our understanding of the world will be challenged by a completely unknown kind of physics we cannot even imagine.

In this work we want to explore some of the possibilities of new particle models that extend the standard model as we know it. The following two sections of this chapter we will introduce the standard model of particle physics in more detail and explain why we believe the LHC will see new particles. Sections 1.4, 1.5 and 1.6 will then each introduce in more detail one of the remaining chapters of this thesis.

1.2   The Standard Model of Particle Physics and Electroweak Symmetry Breaking

One of the most astounding accomplishments of the last century is the establishment of the standard model of particle physics, a quantum theory of all known

fundamental forces except gravity. In this section we give a brief overview of the standard model.

The standard model (SM) is a renormalizable quantum field theory describing three of the four known forces in nature: the strong, the weak and the electromagnetic force. It allows one to calculate the interactions of about a dozen fundamental particles (quarks, leptons and gauge bosons) in terms of only a few very basic principles and parameters.

- **The forces:** The forces between elementary particles are described by gauge symmetries, i.e. local, internal rotation symmetries with associated gauge bosons. In particular the standard model describes three sets of gauge bosons: the gluons for the strong force and the weak and hypercharge gauge bosons for the electroweak forces. Their gauge groups are

$$SU(3)_C \times SU(2)_L \times U(1)_Y. \tag{1.2.1}$$

- **The matter fields:** All fundamental matter fields transform under specific representations of these gauge symmetries. There are five different fundamental fermionic fields, Q, u, d, L, e. Each of these exist in three different flavors or families, i.e. a field with the same quantum numbers and charges, but different masses. In addition, we believe that there exists a scalar field, the Higgs boson H . The charge assignments of all these fields are summarized in table 1.1.

Using these two principles, we can write down the most general, gauge invariant and renormalizable Lagrangian that governs the propagation of particles and their interactions. The only extra ingredient is to specify the numerical value of about ~ 20 parameters associated with the couplings and masses.

Table 1.1: Standard model gauge charges of the fundamental matter fields, all the spin 1/2 fields come in three families with the same charges, but different masses.

field	spin	family members	$SU(3)_c$	$SU(2)_L$	$U(1)_Y$
Q	1/2	$\left\{\begin{pmatrix} u_L \\ d_L \end{pmatrix}, \begin{pmatrix} c_L \\ s_L \end{pmatrix}, \begin{pmatrix} t_L \\ b_L \end{pmatrix}\right\}$	**3**	**2**	1/6
u	1/2	$\{u_R, c_R, t_R\}$	$\bar{\mathbf{3}}$	**1**	2/3
d	1/2	$\{d_R, s_R, b_R\}$	$\bar{\mathbf{3}}$	**1**	$-1/3$
L	1/2	$\left\{\begin{pmatrix} \nu_e \\ e_L \end{pmatrix}, \begin{pmatrix} \nu_\mu \\ \mu_L \end{pmatrix}, \begin{pmatrix} \nu_\tau \\ \tau_L \end{pmatrix}\right\}$	**1**	**2**	$-1/2$
e	1/2	$\{e_R, \mu_R, \tau_R\}$	**1**	**1**	-1
H	0	$-$	**1**	**2**	1/2

The standard model as described so far still has one shortcoming: gauge invariance forbids all mass terms except for the Higgs mass. However we know that all the fermions and the W- and Z-bosons are massive. One might think that adding a mass term by hand and abandoning the concept of gauge invariance might be possible (or even necessary), but gauge symmetry ensures the consistency of the whole theory. For example, the A_0 component of the gauge field has negative norm, yet gauge invariance ensures that its contribution always cancels with the one coming from the longitudinal polarization.

A very elegant solution for this problem is provided by the Higgs mechanism: *electroweak symmetry breaking* (EWSB). Gauge invariance is maintained in the Lagrangian, but the Higgs field obtains a vacuum expectation value (vev) that breaks part of the gauge symmetry. It is very easy to implement this idea by requiring that the Higgs has a so called "Mexican hat potential"

$$V(H) = -\mu^2 |H|^2 + \lambda |H|^4. \tag{1.2.2}$$

The negative mass term results in a nonzero minimum of the Higgs field at

$$\langle H \rangle = \frac{1}{\sqrt{2}} \begin{pmatrix} 0 \\ v \end{pmatrix}, \tag{1.2.3}$$

where we used the $SU(2)_L$ gauge freedom to rotate the vev into the real, lower component and $v = \mu/\sqrt{2\lambda}$. This vev breaks $SU(2)_L \times U(1)_Y$ down to the electromagnetic $U(1)_{EM}$, which is generated by $Q = T_3 + Y$ (electric charge), where T_3 is the diagonal generator of $SU(2)_L$ and Y the one for hypercharge. The gauge boson corresponding to this unbroken group remains massless and is called the photon. The remaining three broken generators of $SU(2)_L \times U(1)_Y$ correspond to the massive gauge bosons $W^\pm$ and Z, where the latter also couples to a combination of T_3 and Y like the photon. Their mass fixes the size of the Higgs vev to be $v \approx 246$ GeV. Unlike massless gauge bosons, massive ones have an additional physical longitudinal polarization component. During EWSB this degree of freedom is provided by the Higgs field.[*] This mechanism breaks gauge invariance only spontaneously and it can be shown that this theory still posses all the desired properties of a consistent quantum field theory, e.g. unitarity or renormalizability.

Remarkably, all particle physics experiments have confirmed the standard model as described in the previous section, some to astounding accuracy [1]. The only deviation we know is the existence of dark matter, which has been proven through gravitational measurements [2], and the fact that the Higgs boson has not yet been discovered[†].

---

[*]As one can be seen explicitly in transverse R_ξ-gauge ($\xi = 1$).
[†]Neutrino masses and oscillations are not strictly speaking part of the SM, however they can be incorporated easily by adding right handed sterile neutrinos ν_R with no gauge charges.

1.3 The Hierarchy Problem

Even though the standard model has been verified by experiments with the exception of a Higgs discovery, there are still some theoretical issues that need to be addressed: Why are the masses of the three families so different and the mixings between them so small? What is the nature of the dark matter (and dark energy) we observe in the universe on astrophysical scales? Why are there exactly three generations? Why do they group in the representations of the gauge groups as they do? Why is charge quantized? ...

Nevertheless, these are all fundamental questions about the size of parameters and the setup of the theory. There is one real problem that questions the consistency of our whole approach, called the large hierarchy problem. Summarized in one sentence it says: Why is the scale of electroweak symmetry breaking $M_W \sim 100$ GeV and therefore 17 orders of magnitude lower than the scale of quantum gravity $M_{Pl} \sim 10^{19}$ GeV?

This poses a problem for the following reason: In any quantum field theory, we know that observables get corrections from the exchange of virtual particles. This is also true for the bare parameters entering the Lagrangian, in particular the masses of the particles. However, the masses of the gauge bosons and the fermions are protected by gauge invariance and chiral symmetry, respectively. By this we mean that they receive only corrections that are proportional to their own mass. In contrast, the Higgs mass is not protected by any mechanism in the SM, so one expects the loop corrections (see fig. 1.1) to be on the order of the highest scale in the theory. In the standard model this is the Planck scale $M_{Pl} \sim 10^{19}$ GeV at which one expects gravitational quantum effects to become
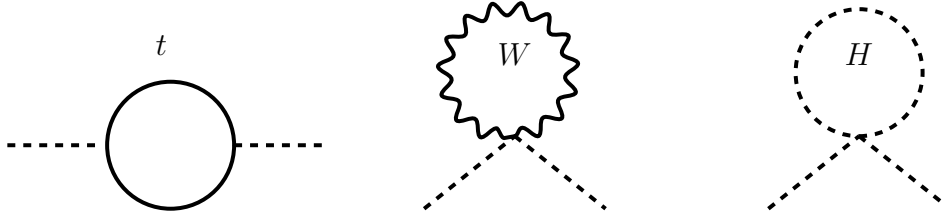
Figure 1.1: Loop diagrams yielding the biggest contributions to the Higgs mass.

important. Therefore, one would expect the Higgs mass to be of order M_{Pl}.

This is in contradiction, or at least strong tension, with both experimental data and theoretical considerations:

- **Experiment**: Even though there has been no direct detection of the Higgs boson yet, there have been a lot of measurements in which the Higgs boson enters indirectly through loop contributions . The dependence on the Higgs mass due to these higher order corrections is only small (and logarithmic at one-loop level, as opposed to the top quark, whose mass enters quadratically), but many of these measurements have been carried out with such high precision ($\sim 0.1\%$ for some) that present data can be used to constrain the Higgs mass. Figure 1.2 shows the $\Delta\chi = \chi^2 - \chi^2_{\min}$ distribution of a global fit to all precision data as performed by the GFitter group [3]. Note that the best fit value is already excluded by direct searches and that the best global fit yields an upper limit of $m_H \lesssim 170 - 210$ GeV at 95% confidence level (the upper limit depends on the analysis performed [4]).

- **Theory**: The Higgs has been introduced to explain electroweak symmetry breaking, i.e. to spontaneously break gauge invariance maintaining renormalizability and unitarity of unbroken gauge theories. One manifestation is that the tree-level scattering cross section of longitudinal W bosons on
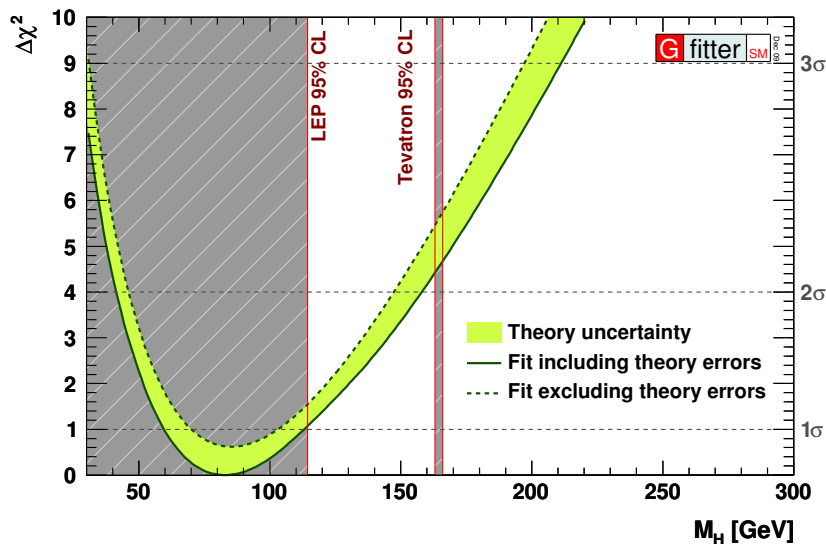
Figure 1.2: Experimental bounds: Best global fit to electroweak data (from
the GFitter group [3]). The shaded regions are excluded by di-
rect LEP and Tevatron searches [5,6].

each other grows with energy like E^2 if the theory contains no Higgs. Only
after intermediate Higgs states are taken into account the cross section lev-
els off, the divergence being cut off by the Higgs mass. As cross sections
translate into scattering probabilities, a too heavy Higgs would therefore
mean the loss of perturbative unitarity. This yields an upper bound for
the Higgs mass of order 800-1000 GeV [7–11]. This is one of the strongest
reasons to believe that we are about to see new physics at the TeV scale.

There are two possible ways out of this: For one, the bare mass in the Lagrangian
and the loop corrections could almost precisely cancel to yield a light Higgs.
However, this would require the fine tuning of two very large numbers to 17
digits.[‡] This fine tuning of parameters seems to be neither an elegant solution
nor one motivated by any principle. Much more satisfying would be to find
an underlying reason or a symmetry that ensures a light Higgs boson. This

---

[‡]For comparison: the most precise measurement to date in *any* system is only to 10^{-15}!

has been one of the main goals in theoretical high energy physics in the last three decades. In the following we will briefly describe some of the proposed solutions.

Supersymmetry

One of the most elegant solutions for the hierarchy problem is supersymmetry (SUSY). The idea is to introduce a new spacetime symmetry between bosonic and fermionic particles, so that each fermion has a bosonic partner and vice versa. A consequence is, that the SUSY partners have the same mass and that their couplings are related to each other. Since fermionic masses are protected from getting loop corrections of order M_{Pl} by chiral symmetry, the fermionic SUSY partner of the Higgs (and thus also the Higgs itself) is protected from receiving large contributions. In computations this protection manifests in cancellations of loop contributions between SM particles and their superpartners, for which the fact that they have the same mass and related couplings is crucial.

As we have not observed partners with opposite spin and the same mass in nature, we know that SUSY must be broken at some higher scale, rendering the cancellation incomplete and creating a massive Higgs. Most of the model building effort is consequently put into finding mechanisms that break SUSY in a way that is consistent with data. It is usually assumed that the supersymmetric standard model is decoupled from the sector that breaks supersymmetry and that the breaking is mediated by different messengers, e.g. gravity or gauge fields.

Randall-Sundrum models

Another approach to solve the large hierarchy problem is the introduction of a compact extra dimension with a non-trivial metric. A possible solution is to have a slice of Anti-de-Sitter space, where the four usual dimensions are flat and the metric has a warp factor e^{-2ky} that depends on the position y in the extra dimension

$$ds^2 = e^{-2ky}\eta_{\mu\nu}dx^\mu dx^\nu - dy^2. \tag{1.3.4}$$

In the simplest versions of this model, only gravity propagates in the bulk, while all SM fields are localized on one brane bounding the extra dimension (the IR brane). Choosing the size r_c of the extra dimension such that $kr_c \approx 30$ will then effectively warp down the Planck scale from the UV brane to the IR brane by a factor $e^{-30} \approx 10^{-15}$, explaining the large hierarchy of sales.

Little Higgs models

A third (and only partial) solution to the hierarchy problem is to understand the hierarchy problem as hint that the SM Higgs is not a fundamental scalar, but only the low-energy, effective description of some unknown physics at the TeV scale. In the SM we already know a mechanism that provides us with massless scalar modes, namely Goldstone's theorem. Whenever a scalar vev spontaneously breaks a global symmetry, some modes of this scalar field will become exactly massless. If the symmetry in question is only approximate, then the modes will not be massless, but still light. This is the idea of Little Higgs models. These models do not completely solve the hierarchy problem, but just answer the question, why new physics might be at the TeV scale rather than the

weak scale. This is sometimes also called *little* hierarchy problem.

Since a big portion of this thesis is dedicated to the construction of a particular Little Higgs model, we will describe this mechanism in more detail in the next section.

1.4 Little Higgs models and collective symmetry breaking

As mentioned in the last section, realizing the Higgs as a pseudo-Goldstone boson can solve the little hierarchy problem. For extensive reviews see [12,13]. To understand the mechanism, it is easiest to look at the simplest case of a complex scalar field,

$$\mathcal{L} = |\partial_u \phi|^2 - V(\phi^* \phi), \tag{1.4.5}$$

where the potential is given by the "Mexican hat potential" from eq. (1.2.2) and the field has a global symmetry $U(1)$ symmetry $\phi \to e^{i\alpha}\phi$. Expanding the field around the vev $\langle \phi \rangle = \frac{f}{\sqrt{2}}$ we we can write it as

$$\phi = \tfrac{1}{\sqrt{2}} \left[f + r(x) \right] e^{-i\pi(x)/f}, \tag{1.4.6}$$

where $r(x)$ parametrizes the radial direction and $\pi(x)$ the Goldstone boson from the symmetry breaking. Under the global $U(1)$ these two components transform as

$$r(x) \to r(x)$$
$$\pi(x) \to \pi(x) + \alpha f. \tag{1.4.7}$$

This means that all couplings to $\pi(x)$ have to be derivative couplings, since it possesses a shift symmetry under the broken global symmetry. This is exactly

what Goldstone's theorem states: $\pi(x)$ is an exactly massless field to all orders in perturbation theory [14–16].

The Coleman-Wess-Zumino theorem [17, 18] generalizes the description of the effective low-energy modes in (1.4.6) to a global symmetry breaking with an arbitrary group. If any group is broken by the vev f of a scalar field Φ, the low-energy effective theory, i.e. the Goldstone bosons π^a can be described using the parametrization

$$\tilde{\Phi} = \exp[i\pi^a X^a / f] \star \langle \Phi \rangle \,, \tag{1.4.8}$$

where X^a are the broken generators and the star $\star$ is representing the action of the group element $\exp[i\pi^a X^a / f]$ on the vev $\langle \Phi \rangle$. The field $\tilde{\Phi}$ describes the theory after all massive scalar degrees of freedom have been integrated out below the symmetry breaking scale f.

To obtain a realistic model, the global symmetry we started out with cannot be exact, as we know that the Higgs boson cannot be exactly massless. However, breaking the global symmetry explicitly usually reintroduces the quadratic divergences we were set out to eliminate. A solution to this is provided by *collective symmetry breaking*: We introduce two couplings that each break the global symmetry, but if only one of these two coupling is non-zero, the Higgs will still be an exact Goldstone boson. Hence one needs both couplings in any diagram to generate a mass to the Higgs. This then forbids quadratically divergent diagrams at one-loop and only allows them at higher order.

Models of this type are called *Little Higgs models*: the Higgs is a pseudo-Goldstone boson and gets mass only by collective symmetry breaking. These models are effective theories below the symmetry breaking scale $f \sim$ TeV and do not solve the large hierarchy problem. The scale of new physics is pushed

in the TeV range, thus only solving the little hierarchy problem. Little Higgs models contain additional gauge bosons (amongst other additional particles), which are necessary to cancel the contribution to the quadratic divergence coming from SM gauge bosons. As new gauge bosons also enter in electroweak precision data, it is helpful to introduce a new parity under which (at least the lighter) new gauge bosons are odd. In the case of Little Higgs models, this is called T-parity and the lightest T-odd particle is also a dark matter candidate.

However, as Little Higgs theories are effective theories it was pointed out by C. and R. Hill [19] that it is not clear whether the complete fundamental theory possesses this symmetry or whether it is anomalous and thus leads to the decay of the lightest T-odd particle (analogous to the decay $\pi^0 \to \gamma\gamma$ in the SM).

In chapter 2 we explicitly construct a UV completion for one of the most popular Little Higgs models, the Littlest Higgs [20], in which T-parity is an exact symmetry. We show that our weakly coupled UV completion is manifestly free of any T-parity anomalies and necessarily leads to an extension of both the gauge and the fermion sector [21].

1.5 Distinguishing theories at the LHC: Determining the spin of standard model partners

After years of preparation and anticipation the LHC has finally started running and is taking high-energy data since this year. As we have described in section 1.3, we have strong reasons to believe that we are going to finally explore the full physics of EWSB and see new particles at the TeV scale. But this is when

the real job just starts. Just knowing that there are new particles will not be enough to determine the underlying physics. In this section we will describe a question that needs to be addressed: How can we distinguish between super-symmetric model and extra dimensional models?

A popular extra dimensional model is the model of an universal extra dimension (UED). The extra dimension is compact, of inverse size $L^{-1} \sim 1 \, \mathrm{TeV}$ and, in contrast to Randall-Sundrum models, the metric is flat. In this theory all the SM fields are promoted to 5D bulk fields, with Neumann boundary conditions. Therefore, all 5D wave functions are flat before electroweak symmetry breaking. There is a whole tower of of equally-spaced higher-mass modes for each field, $m_n = n\pi/L$. Unlike the models described in section 1.3, UED does *not* solve the hierarchy problem, but only serves as a good and reliable tool for model building. The question we want to address is: how can we distinguish a UED model from a SUSY theory?

One hope would be that in extra dimensional models one could see multiple partners per SM particle, namely more than just one particle of the whole KK-tower. However, for realistic sizes of the extra dimension it will be difficult to detect even the second KK-mode. To make things worse, it is known that it is possible to mimic the mass spectrum of a SUSY theory with the first KK-modes of a UED model [22]. The most obvious distinction between these models is that in SUSY theories SM particles have partners of opposite spin, while in extra dimensional models the partners have the same spin. Therefore, one will need to measure the spin of a new particle to say something about the underlying physics. In principle it is possible to determine the spin a particle, from the angular distribution of its decay products. But in order to do this, one needs

to now the center of mass frame of the decaying particle, either from the experimental setup that permits this knowledge or from the measurement of all the decay products reconstructing the original four momentum. The first possibility is not feasible at the LHC since it is a hadron collider. The second is excluded in most models, as they contain a dark matter candidate that is at the end of most of the decay chains and escapes the experiment without detection.

In chapter 3 we investigate the possibility of distinguishing between the decay of the gluon partner to two jets and missing energy in SUSY theories and UED models using the invariant mass distribution of the two observable jets. We assume that no two-body decays are kinematically allowed and that this three-body decay is off-shell. We find that a distinction using the invariant mass distribution is possible, if the mother particle and the invisible one have a large enough mass ratio (a factor of ∼5 to 10) [23].

1.6 Mimicking characteristic gauge-mediated SUSY breaking with a flat extra dimension

A second way how identification of a model could fail is if our ignorance of possible models led us to believe that some signal was unique to this model, where in fact it is not. We will describe a special case of this scenario situation in the following.

A very popular class of supersymmetric models are models with gauge mediated SUSY breaking (GMSB). A good review is given in [24]. In these SUSY models, the the MSSM sector and the SUSY breaking sector decouple, if the SM

gauge couplings are taken to zero. This means that the SUSY breaking is only mediated via SM gauge loops and the SUSY breaking scale can be as low as ~ 100 TeV. Therefore, there are no new sources of flavor-changing neutral currents in addition to the SM Yukawas. In GMSB models the lightest supersymmetric particle is usually the gravitino and the neutralinos decay to it mostly by emission of a photon

$$\chi_0 \to \gamma + \tilde{G}. \tag{1.6.9}$$

Thus, if GMSB should be realized in nature, we would see a lot of events at the LHC with photons and missing energy ($\not{E}_T$), since the gravitino escapes detection. It has been believed that this signal is characteristic for GMSB.

However, we will show in chapter 4 that this signal has nothing to do with GMSB (in fact not even SUSY) and will construct a non-SUSY model that shows the same characteristic. We will use a UED setup with a discrete reflection parity around the midpoint of the extra dimension called KK-parity. We mimic the signature of (1.6.9) using the decay of the first photon KK-mode to the photon and some KK-odd particle ζ_-[§]

$$\gamma^{(1)} \to \gamma + \zeta_-(\not{E}_T). \tag{1.6.10}$$

In our model this decay is generated by an anomalous vertex involving a broken and anomalous 5D gauge symmetry. We show how the light ζ_- mode arises from the 5D component B_5 of this gauge field and how the decay 1.6.10 can be calculated in analogy to the anomalous $\pi \to \gamma\gamma$ decay in SM [25].

[§]The subscript "-" does not refer to the charge of the particle, as it is neutral, but to its KK-parity.

CHAPTER 2

A WEAKLY COUPLED ULTRAVIOLET COMPLETION OF THE LITTLEST HIGGS WITH T-PARITY

2.1 Motivation

In Little Higgs models the Higgs is a pseudo-Goldstone boson of a global symmetry breaking at a few TeV. This does not solve the big hierarchy problem, but at least reconciles the new physics that keeps the Higgs light with electroweak precision observables (EWPO). One can also introduce a particle exchange parity, dubbed T-parity, which lessens tension with EWPO even further and in addition also provides a stable dark matter candidate. However, Little Higgs theories are described as effective theories below a symmetry breaking scale f and it had been pointed out in [19] that a full, UV complete theory might not posses this T-parity and thus not have a dark matter candidate.

In this section we are going to show, that it is possible to explicitly construct a UV completion of a particular little Higgs model, the so-called Littlest Higgs, and explicitly show that it has an exact T-parity [21].

2.2 Introduction

One of the most pressing issues facing particle theory is the little hierarchy problem. On the one hand, electroweak precision measurements at LEP and the Tevatron seem to indicate the existence of a weakly coupled light (below 200 GeV) Higgs boson. This Higgs would be unstable against large radiative cor-

rections, and one would expect new physics at or below the TeV scale to stabilize the Higgs potential. On the other hand, the same electroweak precision measurements have failed to provide any indirect evidence for such physics. For the case of supersymmetry (SUSY), a natural minimal model should have already been discovered at LEP2 or the Tevatron: null results of superpartner and Higgs searches imply that a fine-tuning of order 1% or worse is required to accommodate the data, which is the particular incarnation of the little hierarchy problem for SUSY.

The motivation for Little Higgs (LH) models is to solve this issue by pushing the scale of new physics that solves the "large" (weak/Planck) hierarchy problem up to 10 TeV, and provide a rationale for the cancelation of the remaining quadratic divergences in the Higgs mass between 1 TeV and 10 TeV. This is achieved by interpreting the Higgs as an approximate Goldstone boson corresponding to a spontaneously broken global symmetry of the electroweak sector. Gauge and Yukawa couplings of the Higgs must break the global symmetry explicitly; however, if this breaking is "collective" (meaning that no single coupling breaks all of the symmetry responsible for keeping the Higgs light), the extended theory can remain perturbative until the 10 TeV scale without fine-tuning [20, 26]. Several explicit realizations of this idea have appeared in the literature [12, 13]. Models with T-parity are especially promising, since they can be consistent with precision electroweak constraints without need for fine tuning in the Higgs mass [27, 28]. In this chapter, we will focus on the Littlest Higgs model with T-parity (LHT) [29], which is a fully realistic example of this class.

Like all existing Little Higgs models, the LHT has been constructed as an effective field theory, valid below the cutoff scale of order 10 TeV. This is sufficient

to discuss the model's consistency with precision electroweak data [30, 31], its signatures at the Tevatron [32] and the LHC [33, 34], and the dark matter candidate that naturally emerges in this model [31, 33, 35, 36]. However, in order to really complete the program outlined above one needs to find the ultraviolet (UV) completion of these models, i.e. embed it into a more fundamental theory valid at higher scales, possibly all the way up to the scale of grand unification (GUT) or the Planck scale. The main aim of this chapter is to present such a construction. As with most BSM models, there are two possibilities. The UV completion may be a strongly coupled theory, which happens to produce the LHT as its effective theory below the confinement scale of 10 TeV, or the UV completion remains perturbative, and the LHT emerges as a low-energy description of a renormalizable weakly coupled gauge theory. Here we choose to follow the second possibility, that is we present a linear UV completion of the LHT. In this approach, one needs to introduce supersymmetry to stabilize the hierarchy between the 10 TeV scale and the GUT/Planck scale; however, since SUSY is broken at 10 TeV, the model is free of the fine-tuning plaguing the MSSM. Alternatively one can have a Kaluza-Klein (KK) tower of a warped extra dimension starting at 10 TeV, which would also stabilize the large hierarchy. Our model explains the appearance and radiative stability of the global symmetry structure of the LHT, which at first sight appears rather unnatural. Furthermore, the model is manifestly free of anomalies, including both the familiar gauge/gravitational anomalies and the anomalies involving T-parity. Thus, the anomaly-induced T-parity violating operators, which recently received some attention in the literature [19, 37], are completely absent in our model and T-parity is an exact symmetry, at least as long as gravitational effects can be ignored. This illustrates the point that the existence of these operators depends crucially on the nature

of the ultraviolet completion of the LH model. This has also been emphasized very recently in [38], where it was also pointed out the UV completions with anomalous T-parity are unlikely to have the correct vacuum alignment. The model constructed here does not exhibit gauge coupling unification. Construction of unified models is outside the scope of this chapter.

Before presenting our model, let us briefly comment on its relation to previous work in this area. UV completions of the Littlest Higgs model have been until now based on either a strongly interacting theory or equivalently a warped extra dimension at the 10 TeV scale. Models without T-parity have been constructed [39,40], while recently an attempt to incorporate a discrete parity based on two throats of warped dimensions was presented in [41]. Our model is based on conventional, four-dimensional and perturbative physics, making it much easier to incorporate T-parity and to analyze anomalies. Supersymmetric ultraviolet completions of an alternative LH model, the "simplest" little Higgs, have also appeared in the literature [42–45]. However, in those models the electroweak precision constraints are so strong that one has to assume that SUSY is broken at the weak scale, and the LH scale is much higher. The role of the Little Higgs mechanism is to solve the little hierarchy problem within SUSY. In contrast, in our model the LH partners appear first, and SUSY is irrelevant until the 10 TeV scale. At the LHC, our model would look like the familiar LHT, with a few extra states. We will also present an extra dimensional model that is reminiscent of the structure of the minimal composite Higgs (MCH) models of [46], in which the Higgs will appear as the zero mode of the A_5 bulk gauge fields, which will pick up a finite radiatively generated potential. The main difference between the model presented here and the MCH models is that we will have the T-odd little Higgs partners appearing at the 1 TeV scale, which will allow

us to push the KK mass scale of the theory to 10 TeV without fine-tuning. Thus the KK tower only plays a role of UV completing the theory above 10 TeV and stabilizing the hierarchy between 10 TeV and the Planck scale, but it is not used to cut off the 1-loop quadratic divergences between 1 and 10 TeV.

The chapter is organized as follows. We first construct a four-dimensional, non-supersymmetric, renormalizable model which reduces to the LHT (plus a few extra states) below the 10 TeV scale. We discuss the bosonic (gauge and scalar) sector of the model in section 2.3, and show how to incorporate fermions in section 2.4. In section 2.5, we extend the model to achieve complete anomaly cancelation, including anomalies involving T-parity. In section 2.6, we discuss how the hierarchy between the 10 TeV scale and the Planck scale can be stabilized by either supersymmetrizing the model or embedding it into a theory with a warped fifth dimension à la Randall and Sundrum [47]. In section 2.7, we estimate the precision electroweak constraints on the model, and show that the model is realistic. In section 2.8, we show by an explicit diagrammatic calculation how the little Higgs cancelations occur in our renormalizable model. Finally, section 2.9 contains our conclusions.

2.3   The Scalar/Gauge Sector for $SU(5) \times SU(2) \times U(1)$

The bosonic (scalar and gauge) degrees of freedom of the LHT model are described by a gauged non-linear sigma model (nlσm). The scalars are the Goldstone bosons of the global symmetry breaking $SU(5) \to SO(5)$. The symmetry-breaking vev (or condensate) is in the symmetric representation **15** of the $SU(5)$. The symmetry breaking scale f_S is assumed to be about 1 TeV. To incorporate the

gauge degrees of freedom, an $[SU(2) \times U(1)]^2$ subgroup of the $SU(5)$ is gauged; for the fundamental representation, the gauged subgroup of $SU(5)$ is spanned by the generators

$$Q_1^a = \left(\begin{array}{c|c|c} \tau^a & & \\ \hline & 0 & \\ \hline & & 0 \end{array} \right), \qquad Y_1 = \frac{1}{10} \left(\begin{array}{c|c|c} \begin{array}{cc} 3 & \\ & 3 \end{array} & & \\ \hline & -2 & \\ \hline & & \begin{array}{cc} -2 & \\ & -2 \end{array} \end{array} \right) \qquad (2.3.1)$$

and $\quad Q_2^a = \left(\begin{array}{c|c|c} 0 & & \\ \hline & 0 & \\ \hline & & -\tau^{aT} \end{array} \right), \qquad Y_2 = \frac{1}{10} \left(\begin{array}{c|c|c} \begin{array}{cc} 2 & \\ & 2 \end{array} & & \\ \hline & 2 & \\ \hline & & \begin{array}{cc} -3 & \\ & -3 \end{array} \end{array} \right) \qquad (2.3.2)$

where $\tau^a = \sigma^a/2$. Below f_S, the gauge symmetry is reduced to the diagonal $SU(2) \times U(1)$, which is identified with the Standard Model (SM) electroweak gauge group $SU(2)_L \times U(1)_Y$. Under this group, the physical (uneaten) Goldstones decompose into a weak doublet, identified with the SM Higgs, and a weak triplet. The Higgs mass is protected from a one-loop quadratic divergence by the collective symmetry breaking mechanism. The nlσm is an effective theory valid up to the scale $\Lambda \sim 4\pi f_S \sim 10$ TeV. For a more detailed description of the LHT model, see Refs. [29, 30, 33].

The first step to a weakly coupled UV completion of the LHT is to replace the nlσm with a *linear* sigma model with the same symmetry breaking structure. This model contains a single scalar field S, transforming as **15** of $SU(5)$, which

is assumed to get a vev

$$\langle S \rangle = f_S \begin{pmatrix} & & \mathbb{1} \\ & 1 & \\ \mathbb{1} & & \end{pmatrix}, \qquad (2.3.3)$$

where $f_S \sim 1$ TeV. The Lagrangian is simply

$$\mathcal{L}_{\text{lin}} = \tfrac{1}{8}|D_\mu S|^2 - V(S), \qquad (2.3.4)$$

where D_μ is the covariant derivative, and the renormalizable potential $V(S)$ is assumed to lead to an S vev of the form (2.3.3). We will not need to specify this and other scalar potentials explicitly, for an example of a possible potential for S see eq. (2.8.3). The excitations around the vacuum (2.3.3) can be parametrized as

$$S = \langle S \rangle + i \begin{pmatrix} \phi_S & \sqrt{2}\,h_S & \chi_S + \frac{\eta_S}{\sqrt{5}} \\ \sqrt{2}\,h_S^T & -\frac{4\eta_S}{\sqrt{5}} & \sqrt{2}\,h_S^\dagger \\ \chi_S^T + \frac{\eta_S}{\sqrt{5}} & \sqrt{2}\,h_S^* & \phi_S^\dagger \end{pmatrix} + (\text{radial modes}), \qquad (2.3.5)$$

where χ_S is a hermitian, complex 2×2 matrix, η_S a real singlet, ϕ_S a complex, symmetric 2×2 matrix and h_S a complex doublet, which will be identified with the SM Higgs. These fields are pseudo-Goldstone bosons (they would be exact Goldstone bosons, if the gauge couplings were taken to zero). They contain 14 degrees of freedom, corresponding to the number of $SU(5)$ generators broken by the S vev. The other 16 degrees of freedom in S, the "radial" modes, obtain masses $\sim c f_S$, where c are order-one numbers determined by the coupling constants in $V(S)$. Integrating out the radial modes reproduces the nlσm description of the LHT, independent of the details of $V(S)$. This is guaranteed by the Coleman-Wess-Zumino theorem [17, 18]. In particular, the crucial feature of the LHT nlσm is the special structure of the Higgs coupling to gauge fields,

which guarantees the absence of a quadratic divergence in the Higgs mass at one loop. In section 2.8, we show by an explicit calculation how this structure emerges from the linear sigma model.

The model defined by eq. (2.3.4) is of course renormalizable, and can be valid up to an arbitrarily high scale, for example the Planck scale. In this sense, it is a viable UV completion of (the bosonic sector of) the LHT. However, it has two significant shortcomings:

- The symmetry structure of this model is *very unnatural*. Because gauge interactions break the global $SU(5)$ explicitly, renormalization-group evolution generates $SU(5)$-violating operators in the Lagrangian. In the LHT model, the global $SU(5)$ has to be a good symmetry at the 10 TeV scale. This would require the linear model to contain a very special combination of $SU(5)$-violating terms at the Planck scale, finely tuned just so that the $SU(5)$ is miraculously restored at 10 TeV.

- SM fermions *cannot* be incorporated in this model in a way consistent with T-parity. T-parity requires that for every field transforming under one of the two $SU(2) \times U(1)$ gauge groups of the LHT model, there must be another field transforming in the same way under the other $SU(2) \times U(1)$. Since the SM weak group is the diagonal combination of the two $SU(2)$ factors, this means that the model must have an even number of weak doublets of the same hypercharge and color charge. Therefore this model cannot lead to the chiral fermion content of the SM in the low energy limit.

To avoid the first problem, we would like to start at high energies with a model in which the full $SU(5)$ is promoted to a *gauge* symmetry. Further, to

Table 2.1: Scalar fields and their gauge charge assignments.

	$SU(5)$	$SU(2)_3$	$U(1)_3$
$\Phi_{1,2}$	Adj	1	0
S	⊡	1	0
K_1	□	□	$-1/2$
K_2	$\bar{\square}$	□	$-1/2$

incorporate chirality, we must enlarge the gauge structure to contain an odd number of gauged $SU(2)$ factors. The most obvious and easiest choice is to add one extra gauge $SU(2)$. As we will see below, obtaining the correct hypercharge assignments for all SM fermions also requires an additional $U(1)$ gauge group.

Thus, the full gauge group of our model, at high energies, is

$$SU(5) \times SU(2)_3 \times U(1)_3, \tag{2.3.6}$$

where we labeled the extra $SU(2) \times U(1)$ factor with a subscript "3" to distinguish it from the $[SU(2) \times U(1)]^2$ subgroup of the $SU(5)$ that survives below 10 TeV. To break the $[SU(2) \times U(1)]^3$ subgroup to the SM electroweak gauge group, we also need additional bifundamental scalars under $SU(5) \times SU(2)_3$, K_1 and K_2, which will acquire the appropriate vevs (see eq. (2.3.9)).

To reproduce the symmetries of the LHT model at low energies, we introduce a set of scalar fields, summarized in Table 2.1. At the 10 TeV scale, the Φ

fields get vevs of the form

$$\langle \Phi_1 \rangle = f_\Phi \begin{pmatrix} -3 & & & & \\ & -3 & & & \\ & & 2 & & \\ & & & 2 & \\ & & & & 2 \end{pmatrix}, \quad \langle \Phi_2 \rangle = f_\Phi \begin{pmatrix} 2 & & & & \\ & 2 & & & \\ & & 2 & & \\ & & & -3 & \\ & & & & -3 \end{pmatrix} \quad (2.3.7)$$

where $f_\Phi \sim 10$ TeV. These vevs break the $SU(5)$ down to $[SU(2) \times U(1)]^2$, the gauge group of the LHT model, and leave the $SU(2)_3 \times U(1)_3$ unbroken. If the scalar potential has the form

$$V = V(\Phi_1, \Phi_2) + V(S, K_1, K_2), \quad (2.3.8)$$

so that there are no direct couplings between Φ's and other scalars, the model will possess an $SU(5)$ global symmetry below 10 TeV, broken only by gauge interactions. This is the idea that was first employed in the context of $SU(6)$ GUT models in [48–50], and also in the "simplest little Higgs" model in [51,52]. With this assumption, the full gauge/global symmetry structure of the LHT is reproduced. Of course, this construction is only natural, if there is a symmetry reason for the absence of direct potential couplings between Φ's and the other scalars. In section 2.6, we will show that the Φ-vevs can be stabilized at the 10 TeV scale, either by supersymmetrizing the model or by embedding it into a five-dimensional model with warped geometry. In both cases, the couplings between Φ and the other scalars can be naturally suppressed.

At the 1 TeV scale, the field S gets a vev given in eq. (2.3.3), while the bifun-

damental fields get vevs

$$\langle K_1 \rangle = f_K \begin{pmatrix} 1 \\ & 1 \\ & & \\ & & \\ & & \\ & & \end{pmatrix}, \quad \langle K_2 \rangle = f_K \begin{pmatrix} \\ & \\ & & \\ & & 1 \\ & & & 1 \end{pmatrix}, \quad (2.3.9)$$

where $f_K \sim 1$ TeV. Together, these vevs break the $[SU(2) \times U(1)]^3$ gauge symmetry down to a single $SU(2) \times U(1)$, identified with the SM. The unbroken generators are simply $Q_D^a = Q_1^a + Q_2^a + Q_3^a$ and $Y_D = Y_1 + Y_2 + Y_3$.

The global symmetry breaking by the K-vevs results in additional pseudo-Goldstone bosons. We will assume that the tree-level scalar potential does not contain direct couplings between the fields: $V = V(S) + V(K_1, K_2)$. With this assumption, the Goldstones contained in different fields do not mix. Most of the Goldstones are not protected by the collective symmetry breaking mechanism. They will therefore receive quadratically divergent masses at the one-loop level from gauge loops, and their masses are in the TeV range. The only exceptions are the SM Higgs h_S, and a set of three real Goldstones transforming as a real triplet under the SM $SU(2)$ gauge group. Two of these triplets are eaten by the heavy $SU(2)$ gauge bosons, while the third one remains physical. The physical mode is a linear combination of the Goldstones coming from S, K_1 and K_2. In fact, one can think of our model below 10 TeV as a three-site deconstruction of a five-dimensional model, with the moose diagram shown in Fig. 2.1. In this picture, the light triplet mode is simply the counterpart of A_5, and can only receive a mass from non-local effects due to compactification. However, the Yukawa couplings of our model (discussed in the following section) do not have such an "extra-dimensional" structure, and the triplet mass is *not* protected from the
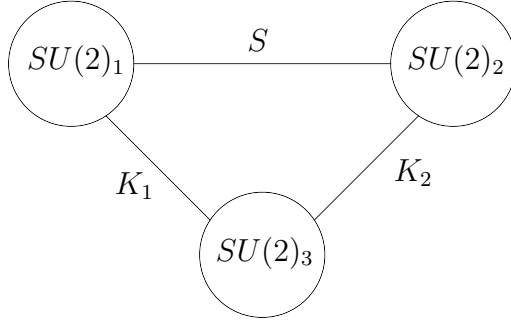
Figure 2.1: The gauge symmetries and scalar field content of the model below the 10 TeV scale.

one-loop diagrams involving the Yukawas. Thus, this mode will also receive a TeV-scale mass. The only pseudo-Goldstone protected by the collective symmetry mechanism is the SM Higgs.

In addition to the gauge symmetries, we impose that the model is invariant under a discrete T-parity, which acts on the gauge and scalar fields as follows:

$$
\begin{aligned}
W_{SU(5)} &\rightarrow \Omega(W_{SU(5)})\Omega^\dagger \,, \\
W_{SU(2)} &\rightarrow \omega(W_{SU(2)})\omega^\dagger = W_{SU(2)} \,, \\
B_{U(1)} &\rightarrow B_{U(1)} \,, \\
\Phi_1 &\leftrightarrow \Omega\Phi_2\Omega^\dagger \,, \\
S &\rightarrow \Omega S^\dagger \Omega^T \,, \\
K_1 &\leftrightarrow \Omega K_2 \omega^T \,,
\end{aligned}
\tag{2.3.10}
$$

where $W_{SU(5)}$, $W_{SU(2)}$ and $B_{U(1)}$ are the SU(5), SU(2)$_3$ and U(1)$_3$ gauge fields, respectively, and

$$
\Omega = \begin{pmatrix} & & -\mathbb{1} \\ & 1 & \\ -\mathbb{1} & & \end{pmatrix} \quad \text{and} \quad \omega = -\mathbb{1}. \tag{2.3.11}
$$

Note that $\Omega \in SU(5)$ and $\omega \in SU(2)$. The kinetic terms are automatically invariant under this parity, while the scalar potential must be restricted to the terms consistent with it. The vevs in eqs. (2.3.3), (2.3.7) and (2.3.9) do not break T-parity. It is easy to check that the T-parity defined in this way acts in the desired way on the fields of the LHT model: the two $SU(2) \times U(1)$ factors inside the $SU(5)$ are interchanged, the Higgs boson h_S is T-even, while the weak triplet is T-odd, as required by precision electroweak fits.

Now, let us discuss the spectrum of the bosonic states. Sixteen out of the 24 $SU(5)$ gauge bosons get masses at the 10 TeV scale. These states are too heavy to have any phenomenological consequences, and we will not discuss them further. Below 10 TeV, we have three sets of $SU(2)$ gauge bosons:

$$
\begin{aligned}
m_{W_{SM}}^2 = 0: & \qquad W_{SM} = \frac{1}{\sqrt{2g_3^2+g_5^2}}[g_3(W_1+W_2)+g_5 W_3] \\
m_{W_{\text{even}}}^2 = \frac{g_5^2+2g_3^2}{4}f_K^2: & \qquad W_{\text{even}} = \frac{1}{\sqrt{2g_5^2+4g_3^2}}[g_5(W_1+W_2)-2g_3 W_3] \qquad (2.3.12) \\
m_{W_{\text{odd}}}^2 = \frac{g_5^2}{4}(2f_S^2+f_K^2): & \qquad W_{\text{odd}} = \frac{1}{\sqrt{2}}[W_1-W_2],
\end{aligned}
$$

as well as three $U(1)$ bosons:

$$
\begin{aligned}
m_{B_{SM}}^2 = 0: & \qquad B_{SM} = \frac{1}{\sqrt{2g_5'^2+g_3'^2}}[g_3'(B_1+B_2)+g_5' B_3] \\
m_{B_{\text{even}}}^2 = \frac{g_5'^2+2g_3'^2}{4}f_K^2: & \qquad B_{\text{even}} = \frac{1}{\sqrt{2g_5'^2+4g_3'^2}}[g_5'(B_1+B_2)-2g_3' B_3] \qquad (2.3.13) \\
m_{B_{\text{odd}}}^2 = \frac{g_5'^2}{100}(10f_S^2+f_K^2): & \qquad B_{\text{odd}} = \frac{1}{\sqrt{2}}[B_1-B_2].
\end{aligned}
$$

Here g_5, g_3 and g_3' are the $SU(5)$, $SU(2)_3$ and $U(1)_3$ coupling constants, respectively, and in proper normalization $g_5' = \sqrt{5/3}\, g_5$.

Note that the model contains a set of T-even gauge bosons at the TeV scale, due to the presence of an extra $SU(2) \times U(1)$ gauge factor, which is T-even. These states can be problematic for electroweak precision constraints, but are

inevitable in our model. However, they do not participate in the cancelation of the quadratic divergences in the Higgs boson mass. Therefore, they can be substantially heavier than the T-odd states, without spoiling naturalness. This occurs if $g_3', g_3 \gg g_5$; if the T-odd states are at 1 TeV, requiring that $g_3', g_3 \sim$ 3-5 g_5 is sufficient to avoid precision electroweak constraints, and the model remains weakly coupled, but for these parameters, the Weinberg angle is fixed at a wrong value: $\sin^2 \theta_W = 5/8$ in the limit $g_3', g_3 \gg g_5$. However, as we will discuss in section 2.4.2, reproducing the top sector of the LHT from a renormalizable model will require introduction of additional scalar vevs at the TeV scale, which will affect the gauge boson spectrum. It turns out that in the full model the correct value of the Weinberg angle can be easily reproduced without conflict with precision electroweak data, as we will show in detail in section 2.7.

2.4 The Fermion Sector

In this section we describe the fermion sector of our model that contains the SM fermions plus a number of heavier states. Our convention is to write all fermion fields as left-handed two-component spinors.

2.4.1 The SM fermions

It is straightforward to include the SM $SU(2)_L$ singlets as T-even fermionic singlets, u_R, d_R and e_R. (The SM generation index will be omitted throughout this chapter.) For each SM doublet, we introduce two fermions in the representa-

Table 2.2: Fermion fields required to incorporate one generation of SM quarks, and their gauge charge assignments. Here $Y = 1/6$ is the SM quark doublet hypercharge. For a generation of leptons, the same set of fields is required, except $d_R \to e_R$, u_R is omitted if the neutrino is Majorana (or $u_R \to \nu_R$ if it is Dirac), and $Y = -1/2$.

	$SU(5)$	$SU(2)_3$	$U(1)_3$
Ψ_1	$\overline{\square}$	1	$Y + 1/2$
Ψ_2	$\square$	1	$Y + 1/2$
ψ_3	1	$\square$	$-Y$
$\psi_{4,5}$	1	$\square$	$-Y - 1$
$U_{R1,2}$	1	1	$-Y - 1/2$
u_R	1	1	$-Y - 1/2$
d_R	1	1	$-Y + 1/2$

tions $\mathbf{5}$ and $\overline{\mathbf{5}}$ of $SU(5)$

$$
\Psi_1 = \begin{pmatrix} \psi_1 \\ U_{L1} \\ \chi_1 \end{pmatrix} \text{ and } \Psi_2 = \begin{pmatrix} \chi_2 \\ U_{L2} \\ \psi_2 \end{pmatrix}. \tag{2.4.1}
$$

A linear combination of ψ_1 and ψ_2 will become the SM doublet. To decouple the extra components, we need 5 extra fermions: ψ_3, ψ_4 and ψ_5 are $SU(2)_3$ doublets, and U_{R1} and U_{R2} are singlets. We also need two extra scalar fields, $F_1 \in \mathbf{5}$ and $F_2 \in \overline{\mathbf{5}}$ of $SU(5)$. Both are uncharged under $SU(2)_3 \times U(1)_3$. Under T-parity,

$$
\Psi_1 \leftrightarrow \Omega^\dagger \Psi_2
$$

$$
\psi_3 \to \omega \psi_3
$$

$$
\psi_4 \leftrightarrow \omega \psi_5
$$

$$
U_{R1} \leftrightarrow U_{R2} \tag{2.4.2}
$$

$$
u_R \to u_R
$$

$$
d_R \to d_R
$$

$$
F_1 \leftrightarrow \Omega F_2.
$$

The Yukawa couplings allowed by gauge symmetries and T-parity are:

$$\mathcal{L}_{\text{Yuk}} = \kappa_1 \left[\Psi_1 K_1 \psi_3 + \Psi_2 K_2 \psi_3 \right] + \kappa_2 \left[\Psi_1^\dagger K_2 \psi_4^\dagger + \Psi_2^\dagger K_1 \psi_5^\dagger \right]$$
$$+ \kappa_3 \left[\Psi_1 F_1 U_{R1} + \Psi_2 F_2 U_{R2} \right] + \text{h.c..}$$
(2.4.3)

The invariance under T-parity can be easily shown using $\Omega^\dagger \Omega = \mathbb{1}$ and $\omega^\dagger \omega = \mathbb{1}$. This form of the Yukawas, together with the requirement of the correct hypercharges for the SM fields, unambiguously fixes the $U(1)_3$ charges for all fermions. The gauge quantum numbers of the fermions are summarized in Table 2.2.

The fundamental scalars get vevs consistent with T-parity:

$$\langle F_1 \rangle = \langle F_2 \rangle = (0, 0, f_F, 0, 0)^T \,,$$
(2.4.4)

where $f_F \sim$ TeV. These vevs break Y_1 and Y_2 seperately, but leave $Y_1 + Y_2 + Y_3$ unbroken, so that no gauge symmetries not already broken by S and K vevs are broken.

For each SM doublet, our model contains five massive Dirac fermions at the TeV scale[*], three T-odd and the other two T-even. Their masses are $m_{1-} = \sqrt{2}\kappa_1 f_K$, $m_{2\pm} = \kappa_2 f_K$ and $m_{3\pm} = \kappa_3 f_F$, where the signs denote the T-parity of each state. There is one massless T-even doublet, $\psi_{SM} = \frac{1}{\sqrt{2}}(\psi_1 - \psi_2)$, which is identified with the SM quark or lepton doublet. In the next subsection, we will explain how the SM Yukawa couplings can be generated in this model.

---

[*]Note that the T-odd fermion masses are bounded from above by constraints on four-fermion operators [30], and cannot be much heavier than a TeV.

2.4.2 The Yukawa couplings

We will start with the top Yukawa. Due to the large value of this coupling in the SM, naturalness requires it to be implemented in a way that only breaks the global symmetries of the LHT collectively. It is straightforward to incorporate the top Yukawas of the LHT model in our linear model. For the third generation quarks, we use the set of fields listed in Table 2.2. In addition to the terms in (2.4.3), we include the following operators:[†]

$$\mathcal{L}_{\text{t}} = \lambda_1 \frac{1}{M} \left[\epsilon^{ijk} \epsilon^{xy} \Psi_{1i} S^\dagger_{jx} S^\dagger_{ky} + \epsilon_{i'j'} \epsilon_{x'y'z'} \Psi_2^{x'} S^{y'i'} S^{z'j'} \right] u_R + \text{ h.c.} \qquad (2.4.5)$$

where we restrict the summation to $i, j, k \in \{1, 2, 3\}$, $x, y \in \{4, 5\}$ and $i', j' \in \{1, 2\}$, $x', y', z' \in \{3, 4, 5\}$ and M is the mass scale suppressing this dimension-5 operator. Note that eq. (2.4.5) is T-parity invariant, although this is not immediately manifest; taking the T-parity transformation of the first term yields

$$\epsilon^{ijk} \epsilon^{xy} \Psi_{1i} S^\dagger_{jx} S^\dagger_{ky} \rightarrow \epsilon^{ijk} \epsilon^{xy} (\Omega^\dagger \Psi_2)_i (\Omega^\dagger S \Omega^*)_{jx} (\Omega^\dagger S \Omega^*)_{ky}$$

$$= \left[\epsilon^{ijk45} \Omega^\dagger_{ix'} \Omega^\dagger_{jy'} \Omega^\dagger_{kz'} \Omega^\dagger_{41} \Omega^\dagger_{52} \right] \left[\epsilon^{123xy} \Omega^*_{41} \Omega^*_{52} \Omega^*_{33} \Omega^*_{i'x} \Omega^*_{j'y} \right] \Psi_2^{x'} S^{y'i'} S^{z'j'} \quad (2.4.6)$$

$$= \left[\epsilon_{x'y'z'} \det \Omega^\dagger \right] \left[\epsilon_{i'j'} \det \Omega^* \right] \Psi_2^{x'} S^{y'i'} S^{z'j'},$$

which together with $\det \Omega = 1$ gives exactly the second term in eq. (2.4.5). The expansion to summing over 1 to 5 (and then restricting again to partial summation as in eq. (2.4.5)) in this derivation is possible due to the special structure of Ω. After the S field gets a vev and the radial modes are integrated out, eq. (2.4.5) reduces to the top Yukawa term of the usual nlσm LHT model (see e.g. [29, 30, 33]). These Yukawa couplings incorporate the collecitve symmetry breaking mechanism, which protects the Higgs mass from large renormalization by top loops.

[†]By convention fundamental $SU(5)$ indices are upper, antifundamental are lower. SU(2) indices are raised and lowered with ϵ^{ab} and ϵ_{ab} as usual.

We now want to obtain the operators in eq. (2.4.5) from an $SU(5)$-invariant, renormalizable Lagrangian. To restore $SU(5)$ invariance, let us introduce two scalar fields,

$$A_1 \in \overline{\mathbf{10}}\,, \quad A_2 \in \mathbf{10}\,, \tag{2.4.7}$$

with T-parity action

$$A_1 \leftrightarrow \Omega^\dagger A_2 \Omega^*. \tag{2.4.8}$$

These fields get vevs

$$\langle A_1 \rangle = f_A \begin{pmatrix} 0 & & \\ & 0 & \\ & & \varepsilon \end{pmatrix}, \quad \langle A_2 \rangle = f_A \begin{pmatrix} \varepsilon & & \\ & 0 & \\ & & 0 \end{pmatrix}, \quad \text{where } \varepsilon = \begin{pmatrix} 0 & 1 \\ -1 & 0 \end{pmatrix}. \tag{2.4.9}$$

These vevs do not break T-parity or the gauged $SU(2)$s, but break the Y_1 and Y_2 gauged generators. So, the A's need to be charged under $U(1)_3$ with charges chosen such that the broken linear combinations are orthogonal to the one identified with hypercharge, $Y_1 + Y_2 + Y_3$. This requires $Q_3(A_1) = Q_3(A_2) = -1$. In addition to their role in the top sector, the antisymmetric fields also help resolve the problem with the correct value of the Weinberg angle mentioned earlier. For a disussion of this issue, see section 2.7.

Eq. (2.4.5) can now be thought of as the low-energy limit of the following ($SU(5)$-invariant, but still non-renormalizable) Lagrangian:

$$\mathcal{L}_{\mathrm{t}} \propto \left[\epsilon^{abcde} \Psi_{1a} S^\dagger_{bx} S^\dagger_{cy} (A_1)_{de} (A_1^*)^{xy} + \epsilon_{abcde} \Psi_2^a S^{bx} S^{cy} (A_2)^{de} (A_2^*)_{xy} \right] u_R + \text{ h.c.}, \tag{2.4.10}$$

where the summations are no longer restricted and run from 1 to 5.

One possible way to obtain a renormalizable model is to introduce four scalar fields, $\eta, \eta', \xi,$ and ξ'. These are uncharged under $SU(2)_3 \times U(1)_3$, and

transform under $SU(5)$ as follows:

$$\eta \in \square, \ \ \eta' \in \bar{\square}, \ \ \xi, \xi' \in \ \text{Adj}. \tag{2.4.11}$$

T-parity acts in by-now familiar way:

$$\eta \leftrightarrow \Omega \eta', \ \ \xi \leftrightarrow \Omega^\dagger \xi' \Omega. \tag{2.4.12}$$

The renormalizable Lagrangian is then given by

$$
\begin{aligned}
\mathcal{L}_{\text{t}} \propto{}& \Psi_{1a}\eta^a u_R + \epsilon^{abcde}\eta_a^\dagger S_{bx}^\dagger \xi^x{}_c (A_1)_{de} + m_0(\xi^\dagger)_x{}^c S_{cy}^\dagger (A_1^*)^{xy} \\
&+ \Psi_2^a \eta'_a u_R + \epsilon_{abcde}\eta'^{\dagger a} S^{bx}(\xi'^\dagger)_x{}^c (A_2)^{de} + m_0 \xi'^x{}_c S^{cy}(A_2^*)_{xy} + \text{ h.c.}
\end{aligned}
\tag{2.4.13}
$$

plus mass terms for the scalars. Assuming that the scalars are heavier than f, integrating them out reproduces eq. (2.4.10).

With the above quantum numbers there is no Yukawa coupling possible for the leptons and the down quarks, which resembles the top Yukawa in eq. (2.4.5). However, it is possible to write down a dimension-6 operator to generate these Yukawa couplings. For the down quarks, this operator has the form

$$\mathcal{L}_{\text{d}} \sim \frac{\lambda}{M_d^2} \left(\epsilon_{ijk}\epsilon_{xy}\Psi_2^x K_1^{ia} K_{1\,a}^j S^{ky} + \epsilon^{i'j'}\epsilon^{x'y'z'}\Psi_{1i'} K_{2x'}^a K_{2y'a} S_{z'j'}^\dagger \right) d_R + \text{ h.c.}, \tag{2.4.14}$$

where the summation is restricted to $i, j, k \in \{1, 2, 3\}$, $x, y \in \{4, 5\}$ and $i', j' \in \{1, 2\}$, $x', y', z' \in \{3, 4, 5\}$, and M_d is the mass scale at which this operator is generated. The lepton Yukawas are of the same form. In complete analogy to the top sector, the desired operators can be obtained from a renormalizable and $SU(5)$ invariant lagrangian by introducing new heavy states (scalars or fermions) and integrating them out.

2.4.3 A non $SU(5)$ invariant theory

One might wonder if the rich structure of the model we built is just due to the requirement of $SU(5)$ gauge invariance at high energies. If one is willing to assume that the $SU(5)$ global symmetry accidentally emerges at the 10 TeV scale, a model with ungauged $SU(5)$ can be considered. Could this dramatically simplify the particle content needed to reproduce the LHT? A detailed look at the previous section reveals that only very few states could actually be omitted in such a non-$SU(5)$ invariant model:

- We could use incomplete $SU(5)$ representations in (2.4.1) and omit the states $\chi_{1,2}$.

- We would not need the scalars $F_{1,2}$ to give mass to the $U_{L1,2}$ states.

- We would not need the scalars $A_{1,2}$, whose role is to make the coupling (2.4.5) $SU(5)$ invariant.

- Fewer massive scalars would be necessary to obtain the top Yukawas (2.4.5) from a renormalizable theory.

In total one would end up with a slightly smaller particle content, but overall the model would not simplify significantly.

2.5 Anomaly Cancellation

While the model presented above suffers from gauge anomalies, in this section we will present a simple extension of the model which is anomaly free. Further-

more, we will show that T-parity is an anomaly free symmetry of the quantum theory.

2.5.1 Gauge anomalies

First, we examine the gauge anomalies of the model. The chiral fermion content of a single generation is summarized in Table 2.2, where $Y = 1/6$ for quarks and $Y = -1/2$ for leptons. Note that the $SU(5)$ group is vectorlike, while $SU(2)$ representations are real, so all anomalies involving only these two groups vanish. However, anomalies involving $U(1)_3$ are *not* canceled with this fermion content. The simplest way to achieve anomaly cancelation is to extend the model in such a way that it contains a sector which is vectorlike under the full $SU(5) \times SU(2)_3 \times U(1)_3$ gauge group, plus a sector which is chiral under $SU(2)_3 \times U(1)_3$, but with charges identical to one generation of the SM fermions. This guarantees anomaly cancelation as in the SM. Since at low energies the matter content of our model coincides with the SM, this is in fact possible. In order to achieve this, we need to introduce mirror partners for all fields that don't already have SM quantum numbers. In particular for the quark sector we introduce the mirror partners Q_1', Q_2', q_4', q_5', U_{R1}', U_{R2}' and *two* fields q_3', q_3''. The two q_3 partners are necessary in order to exactly reproduce the chiral SM matter content under $SU(2)_2 \times U(1)_3$, guaranteeing complete anomaly cancelation. The total anomaly-free fermion content in the quark sector is summarized in Table 2.3 in the columns (a) and (b).

The additional states acquire TeV-scale masses through a Lagrangian of the

Table 2.3: The complete fermion sector (single generation) and the gauge charge assignments for the anomaly-free version of the model.

a)	$SU(5)$	$SU(2)_3$	$U(1)_3$	b)	$SU(5)$	$SU(2)_3$	$U(1)_3$
Q_1	$\bar{\square}$	1	$+2/3$	Q'_1	$\bar{\square}$	1	$-2/3$
Q_2	$\square$	1	$+2/3$	Q'_2	$\square$	1	$-2/3$
q_3	1	$\square$	$-1/6$	q'_3, q''_3	1	$\square$	$+1/6$
q_4	1	$\square$	$-7/6$	q'_4	1	$\square$	$+7/6$
q_5	1	$\square$	$-7/6$	q'_5	1	$\square$	$+7/6$
U_{R1}	1	1	$-2/3$	U'_{R1}	1	1	$+2/3$
U_{R2}	1	1	$-2/3$	U'_{R2}	1	1	$+2/3$
u_R	1	1	$-2/3$				
d_R	1	1	$+1/3$				

c)	$SU(5)$	$SU(2)_3$	$U(1)_3$
L_1	$\bar{\square}$	1	0
L_2	$\square$	1	0
ℓ_3	1	$\square$	$+1/2$
ℓ_4	1	$\square$	$-1/2$
ℓ_5	1	$\square$	$-1/2$
E_{R1}	1	1	0
E_{R2}	1	1	0
e_R	1	1	$+1$
$(\nu_R$	1	1	$0\ )$

form

$$\mathcal{L} \propto Q'_1 K_2^* q'_3 + Q'_2 K_1^* q''_3 + Q_1'^\dagger K_1^* q_4'^\dagger + Q_2'^\dagger K_2^* q_5'^\dagger + Q'_1 F_1 U'_{R1} + Q'_2 F_2 U'_{R2} \,. \quad (2.5.1)$$

Note that this is almost the same as eq. (2.4.3), except that the presence of the two *different* fields q'_3 and q''_3 guarantees that there is no light mode.

For the lepton sector with $Y = -1/2$ in Table 2.2 we automatically have a charge assignment that produces the SM chiral matter content under $SU(2)_3 \times U(1)_3$, so no additional mirror fields are needed. The matter content in the lepton sector is summarized in Table 2.3 (c).

Table 2.4: The chiral matter content for one generation of the anomaly-free version of the model.

	$SU(5)$	$SU(3)_c$	$SU(2)_3$	$U(1)_3$
q_3''	1	$\square$	$\square$	$+1/6$
u_R	1	$\bar{\square}$	1	$-2/3$
d_R	1	$\bar{\square}$	1	$+1/3$
ℓ_5	1	1	$\square$	$-1/2$
e_R	1	1	1	$+1$

The chiral matter content of one generation of the model is summarized in Table 2.4. Here $SU(3)_c$ denotes the color gauge group. As anticipated above, the quantum numbers of these fermions under $SU(3)_c \times SU(2)_3 \times U(1)_3$ are exactly the same quantum numbers as for the usual SM fermions under $SU(3)_c \times SU(2)_L \times U(1)_Y$. Hence all gauge and gravitational anomalies cancel.

The above construction should be viewed as a proof of principle, showing that it is possible to add a set of spectator fermions to our model to cancel all gauge and gravitational anomalies, and to give them large masses in a way consistent with the symmetries. The particular set of spectators chosen here is rather large, but has the advantage that the anomalies cancel in exactly the same way as in the SM. Its disadvantage is that the QCD β-function will become very large and the theory would rapidly develop a Landau pole. The exact location of the pole depends on the values chosen for the Yukawa couplings and vevs in eqs. (2.5.1) and (2.4.3). In the supersymmetric version of this model, which we will describe in section 2.6.1, this implies that once the Landau pole is hit an appropriate Seiberg duality [53] has to be performed and the theory will be a cascading gauge theory as in [54]. It would be interesting to see if a more minimal anomaly-free matter content can be found.

2.5.2 T-parity anomalies

Whenever physical Goldstone bosons appear in a theory, one has to check whether the global symmetries whose spontaneous breaking produces the Goldstones are anomalous. The presence of such anomalies would produce new couplings for the Goldstones, of the general form

$$\frac{1}{f}\pi^a \partial_\mu J^{a\mu}. \tag{2.5.2}$$

If the global current $J^{\mu a}$ is anomalous with respect to a gauge symmetry, then

$$\partial_\mu J^{a\mu} = \frac{Ag^2}{16\pi^2}\mathrm{Tr}F\tilde{F}, \tag{2.5.3}$$

where F is the gauge field, and the anomaly coefficient A can be calculated from the triangle diagrams involving fermion loops. In the low energy effective theory after the fermions are integrated out, a term involving the light gauge fields and the Goldstones has to be present, whose variation reproduces the anomalies of the global current. This is the Wess-Zumino-Witten (WZW) term [55, 56], whose coefficient can be found by matching to the triangle diagrams in the high energy theory. This WZW term may break discrete symmetries of the Goldstone sector. The canonical example is the $\pi^a \to -\pi^a$ symmetry of the pseudoscalar octet of QCD. The effect of the $SU(2)^2_A \, U(1)_{em}$ anomaly in the quark picture will imply the presence of the $\pi_0 F\tilde{F}$ coupling in the effective low-energy theory, which breaks the $\pi \to -\pi$ reflection symmetry. Using similar arguments Hill and Hill [19] argued that T-parity will also be broken in a similar way in little Higgs models. They have discussed several examples based both on more complicated versions of the $SU(3) \times SU(3) \to SU(3)_D$ breaking pattern, as well as the $SU(5) \to SO(5)$ and other little Higgs-type models, and have calculated the form of the Wess-Zumino-Witten terms in a variety of examples.

However, whether these T-parity breaking terms are ultimately present in the low-energy effective theory or not depends on the UV completion of the theory. If the global symmetries (and T-parity itself) are not anomalous, then the coefficient of the Wess-Zumino term vanishes, and T-parity remains a good symmetry at the quantum level. Therefore, in a complete model with T-parity one has to show that T-parity is not broken by any of the global anomalies present in the theory. While in an effective low-energy theory one may only speculate whether such anomalies are present or not, our UV completion allows us to address this issue straightforwardly. Since the $SU(5)$ global symmetry responsible for producing the Goldstones is also gauged, it has to be anomaly free. Indeed we have shown above that it is possible to choose the matter content such that all anomalies involving $SU(5)$ will disappear. Therefore there can be no Wess-Zumino-Witten term from $SU(5)$ anomalies present in this theory that would give rise to T-parity violation.

A final worry might be that the T-parity itself as a discrete symmetry might be anomalous. However, as we have seen before, T-parity is a combination of an $SU(5) \times SU(2)_3$ gauge transformation element with a discrete exchange symmetry. We have seen that the gauge transformations are anomaly free, but what about the exchange symmetry (which is a symmetry similar to charge conjugation)? Could that possibly be anomalous? The answer is clearly negative. The exchange symmetry in the path integral language merely corresponds to a relabeling of the integration variables. The integration measure is invariant under this relabeling. So, if the Lagrangian is invariant under the exchange symmetry, then the whole path integral is invariant. Therefore we do not expect T-parity violating anomalous terms to show up anywhere in the model.

2.6 Solutions to the Large Hierarchy Problem

We constructed a weakly coupled, four-dimensional UV completion of the LHT model, with T-parity exact at the quantum level. However, the model assumes a large hierarchy between the scale of scalar vevs (1 or 10 TeV), and the Planck scale. This hierarchy needs to be stabilized. In this section, we will explore two possible ways this can be achieved: by embedding the model into a supersymmetric theory above 10 TeV, and by promoting it to a warped-space five-dimensional model with the Planck scale at the infrared (IR) boundary of order 10 TeV.

2.6.1 A supersymmetric version

It is straightforward to supersymmetrize our model by promoting all fields to superfields, and assuming that the components that do not appear in our model receive soft masses at the 10 TeV scale. In addition, one needs to introduce a superfield $\bar{S}$, which has the same quantum numbers as $S^\dagger$. This fields gets interchanged with S under T-parity in the familiar way $S \leftrightarrow \Omega \bar{S} \Omega^T$. It ensures that it is possible to write down a superpotential that allows for the vev in eq. (2.3.3) and generates the Yukawa couplings (2.4.13). We assume the superpotential of the form

$$W = W_\Phi(\Phi_1, \Phi_2) + W_{\mathrm{Yuk}}(S, \bar{S}, K_1, K_2, \ldots), \qquad (2.6.1)$$

where W_Φ generates $SU(5)$ breaking vevs as in eq. (2.3.7) without breaking SUSY, and W_{Yuk} includes the Yukawa couplings of our model. This superpotential allows for the adjoint vevs in Eq. (2.3.7), with $\langle \sigma \rangle = 0$. At the same time, since the Yukawa couplings do not contain the Φ fields, it does *not* lead to direct

couplings between Φ and the other fields in the F-term scalar potential. As a result, the global SU(5) symmetry below the scale $f_\Phi \sim 10$ TeV is preserved at this level. Note that this structure of the F-term potential is technically natural, due to the standard non-renormalization theorems of SUSY.

The scalar potential also receives a D-term contribution. Since both Φ and the other scalar fields, including S and $\bar{S}$, are charged under SU(5), the D-term potential will in general couple them, violating the global SU(5). This can give a large contribution to the Higgs mass, potentially of order $g_5 f_\Phi$. However, it can be shown that this effect is suppressed in the limit when the soft masses for the adjoint fields are small compared to f_Φ, and the Higgs mass can remain at the weak scale without fine-tuning.

The argument is based on the following observation [57, 58]: In the limit of unbroken SUSY, the effective theory below the scale f_Φ is a supersymmetric theory with reduced gauge symmetry. This SUSY theory does *not* contain any D-terms for S or $\bar{S}$ corresponding to the broken generators, and does not contain any Φ fields as they are either eaten or get masses at the scale f_Φ. So, in this limit we are only left with D-terms for S and $\bar{S}$ corresponding to the unbroken subgroup. These terms do not generate a tree-level S or $\bar{S}$ mass, and moreover they break the SU(5) in exactly the same pattern as the unbroken gauge symmetries themselves. In particular, the Higgs (contained in S and $\bar{S}$) would still remain a Goldstone if only one of the two $SU(2)$ subgroups was gauged. Thus, in the unbroken-SUSY limit, the D-terms do not spoil the symmetries responsible for keeping the Higgs light.

Let us see explicitly how this works. Since for the protection of the higgs mass only the interactions between $S, \bar{S}$ and $\Phi_{1,2}$ are relevant, we will only focus

on these fields on the following discussion. Above f_Φ, the D-term potential has the form

$$V_D = \frac{g_5^2}{2} \sum_a (D_\Phi^a + D_S^a + ...)^2,$$

$$\text{with} \quad D_\Phi^a = \sum_i \text{Tr}\, \Phi_i^\dagger [T^a, \Phi_i]\,, \quad D_S^a = 2\,\text{Tr}\, S^\dagger T^a S - 2\text{Tr}\bar{S}^\dagger T^{aT} \bar{S}\,.$$

(2.6.2)

After the Φ's get vevs, this potential includes $SU(5)$ symmetry breaking terms for S and $\bar{S}$. However, to obtain the correct low-energy potential, we have to carefully integrate out the heavy "radial" modes of the Φ fields. The important radial modes are $R^{\hat{a}}$ along the generators $T^{\hat{a}}$ broken by $\langle \Phi_{1,2}\rangle$. These modes are the real parts of the superfield containing the Goldstones, and as such they must be F-flat directions.[‡] But since the Goldstones are eaten by the broken gauge bosons, the $R^{\hat{a}}$ fields will get masses from the D-terms, which must be precisely equal to the gauge boson masses in order to preserve SUSY. Furthermore, they are the only radial modes that receive a mass from the D-terms. The scalar potential has the form

$$V_{\text{SUSY}} = F^* F + \frac{g^2}{2} D^a D^a = \frac{1}{2} \sum_{\hat{a}} (M_{\hat{a}} R^{\hat{a}} + ... + g_5 D_S^{\hat{a}})^2 + ...,$$

(2.6.3)

where $\hat{a}$ labels the broken generators, $M_{\hat{a}}$ are the gauge boson masses and the dots denote terms that do not contain either $D_S^{\hat{a}}$ or $R^{\hat{a}}$. The equations of motion yield

$$R^{\hat{a}} = -\frac{g_5 D_S^{\hat{a}}}{M_{\hat{a}}},$$

(2.6.4)

which exactly cancels the unwanted D-terms for S and $\bar{S}$ corresponding to the broken generators.

In a realistic model, SUSY must be broken. Consider a situation when the SUSY-breaking soft masses for the Φ fields are lower than the $SU(5)$ breaking

---

[‡]Non-linearly realized Goldstones are completely F-flat. If realized linearly, however, one will encounter quartic and higher interactions in the F-term potential.

scale f_Φ. Assume that the soft breaking are of the form

$$V_{SUSY} = \frac{1}{2} \sum_{\hat{a}} m_{\hat{a}}^2 R^{\hat{a}\,2} + \dots, \qquad (2.6.5)$$

with $m_{\hat{a}} \ll f_\Phi$, and dots denote terms not containing $R^{\hat{a}}$. The important feature of these soft terms is that they do not contain a linear term in $R^{\hat{a}}$, and thus only affect the SUSY cancellation of the D-terms at subleading order in $m_{\hat{a}}/M_{\hat{a}}$. The equations of motion for $R^{\hat{a}}$ now yield

$$R^{\hat{a}} = -\frac{g_5 D_S^{\hat{a}} M_{\hat{a}}}{M_{\hat{a}}^2 + m_{\hat{a}}^2} + \dots \approx -\frac{g_5 D_S^{\hat{a}}}{M_{\hat{a}}} \left(1 + \frac{m_{\hat{a}}^2}{M_{\hat{a}}^2} + \dots\right). \qquad (2.6.6)$$

The resulting low-energy potential has the form

$$V_{\text{eff}} \sim \sum_{\hat{a}} \frac{m_{\hat{a}}^2}{M_{\hat{a}}^2} \left(g_5 D_S^{\hat{a}}\right)^2 + \dots \qquad (2.6.7)$$

where the dots denote terms of higher order in $m_{\hat{a}}/f_\Phi$. This potential gives a mass to the Goldstones in S and $\bar{S}$ (including the SM Higgs) of the order

$$m_h^2 \sim \frac{m_{\hat{a}}^2}{M_{\hat{a}}^2} f_S^2. \qquad (2.6.8)$$

This is phenomenologically acceptable as long as $m_{\hat{a}}/M_{\hat{a}} \lesssim 0.1$. One possibility is that $f_\Phi \sim M_{\hat{a}} \sim 10$ TeV as previously assumed, but the soft masses for Φ are an order of magnitude smaller than the other soft masses in the theory, $m_{\hat{a}} \sim 1$ TeV. This small mass hierarchy would be radiatively stable. Another possibility is that $m_{\hat{a}} \sim 10$ TeV along with the other soft masses, but $f_\Phi \sim 100$ TeV. In this case, all quadratic divergences are still cut off at 10 TeV due to SUSY, but SU(5)-violating logarithmic corrections are enhanced by running between 10 and 100 TeV scales. This leads to an additional contribution to the Higgs mass of order $\sim \frac{g^2}{16\pi^2} f_S^2 \log \frac{100\,\text{TeV}}{10\,\text{TeV}}$, which is of the same order as the top contribution.

The above discussion is completely general and does not depend on any particular representation of the $SU(5)$ breaking fields and their vevs, the specific form of the superpotential W_Φ, or the soft breaking potential V_{SUSY}. As an

example consistent with our model, we can use a T-parity invariant superpotential of the form

$$W = \kappa\sigma(\text{Tr } \Phi_1\Phi_1 + \text{Tr } \Phi_2\Phi_2 - 60f_\Phi^2) + W_{\text{Yuk}}(S, \bar{S}, K_1, K_2, \ldots), \qquad (2.6.9)$$

with σ a gauge-singlet chiral superfield, and the soft breaking terms

$$V_{SUSY} = M_\Phi^2 \left(\text{Tr } \Phi_1^\dagger\Phi_1 + \text{Tr } \Phi_2^\dagger\Phi_2\right) + M_\sigma^2|\sigma|^2. \qquad (2.6.10)$$

This potential has an extended $SU(5)^2$ global symmetry, and thus not all Goldstone bosons are eaten by the heavy gauge field. However, the uneaten Goldstones will receive a contribution to their mass of order $\frac{f_\Phi}{4\pi}$ at one loop, which is of order $1 - 10$ TeV.

2.6.2 A five-dimensional version

A popular alternative to supersymmetry for solving the weak/Planck hierarchy problem is the warped-space five-dimensional (5D) setup pioneered by Randall and Sundrum [47]. It is straightforward to embed our model into such a setup.[§]

The five-dimensional version of the model is illustrated in Fig. 2.2. We assume that the extra dimension has a warped AdS$_5$ gravitational background given by the metric

$$ds^2 = \left(\frac{R}{z}\right)^2 \left(\eta_{\mu\nu}dx^\mu dx^\nu - dz^2\right), \qquad (2.6.11)$$

The extra dimension is an interval bounded at $z = R$ by the "ultraviolet" (UV) boundary (or brane), and at $z = R'$ by the "infrared" (IR) brane. The AdS curvature R is assumed to be $1/R \sim \mathcal{O}(M_{Pl})$, while $1/R'$ is of order a few TeV.

_____

[§]A 5D version of the original Littlest Higgs model was given in [40].
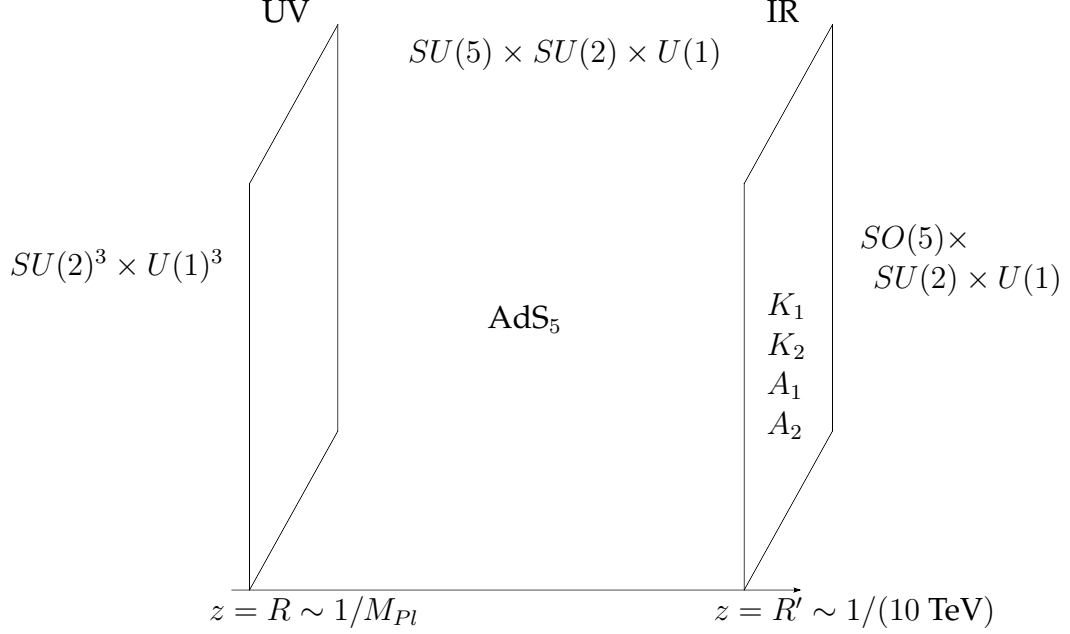
Figure 2.2: Geometric setup, gauge symmetries and matter content of the five-dimensional model.

The 5D theory should reproduce at ~ 1 TeV the T-odd particle spectrum necessary for the little Higgs mechanism. The cutoff scale of the 4D little Higgs theory is usually at around 10 TeV. In the 5D theory this will be identified with the scale m_{KK} where the additional KK resonances appear, thus UV completing the theory above 10 TeV. The cutoff scale of the 5D theory can be estimated via NDA to be of the order $\Lambda_{5D} \sim 24\pi^3/(g^2 R' \log R'/R)$, while the scale f is given by $f = 2/(gR'\sqrt{\log R'/R})$. In our case we want $f \sim 1$ TeV, then the cutoff scale is of order 100 TeV, while the KK mass scale is $m_{KK} \sim 2/R' \sim 10$ TeV.

The best handle for finding the right setup is to use the dictionary of the AdS/CFT correspondence. From that point of view we would be looking for the dual of a CFT with an $SU(5)$ global symmetry, where the $SU(2)^2 \times U(1)^2$ subgroup is gauged. As we discussed, this symmetry needs to be extended to $SU(5) \times SU(2)_3 \times U(1)_3$, with $[SU(2) \times U(1)]^3$ gauged, in order to incorporate T-

parity in the (chiral) fermion sector. So, the 5D setup we start with is an $SU(5) \times SU(2)_3 \times U(1)_3$ bulk gauge group. The action of T-parity on the gauge bosons is again given by eq. (2.3.10). We assume that the gauge symmetry is broken by boundary conditions (BC's) for the gauge fields, as in [59,60]: on the UV brane,

$$SU(5) \times SU(2) \times U(1) \to [SU(2) \times U(1)]^3 \quad (\text{UV}), \qquad (2.6.12)$$

while on the IR brane

$$SU(5) \times SU(2) \times U(1) \to SO(5) \times SU(2) \times U(1) \quad (\text{IR}). \qquad (2.6.13)$$

In the language of the 4D model, this is equivalent to placing the $\Phi_{1,2}$ fields on the UV brane and the S field on the IR brane, and integrating out the radial models of these fields after they get vevs. (Note that this geometric separation of Φ and S automatically guarantees the absence of the direct potential couplings between them, as needed in our model.) These BC's result in an unbroken $[SU(2) \times U(1)]^2$ gauge group at low energies and leave T-parity unbroken. The gauge fields in $[SU(2) \times U(1)]^3$ which are only broken by BC's on the IR brane will get a mass of order $f \sim 1$ TeV. These fields correspond to the T-odd gauge bosons of the LHT model. As discussed above, the full Kaluza-Klein (KK) tower starts at the somewhat higher scale $m_{KK} \sim 10$ TeV.

To reduce the group further (down to just the SM) we will assume that the scalars K_1, K_2 live on the IR brane, getting vevs of order $m_{KK} \sim 10$ TeV. Furthermore, to incorporate fermion masses in an $SU(5)$ invariant way, we also add the scalars A_1, A_2 on the IR brane,with vevs of order m_{KK}. (We will not need to introduce the scalars $F_{1,2}$ to give masses to $U_{L1,2}$.) Note that $m_{KK} \sim 10$ TeV is the natural scale for the vevs on the IR brane. It is an order of magnitude larger than the vevs for these fields in the 4D version of the model. However, these larger vevs do not lead to larger masses for the corresponding massless gauge

bosons: in fact, their contribution to the masses is at most of order $gf \sim 1$ TeV. This can be seen by observing that the limit of very large vevs is equivalent to breaking gauge symmetries by BC's on the IR brane, which produce masses of order gf.

The A_5 components of the gauge fields corresponding to the broken $SU(5)/SO(5)$ generators develop zero modes. These modes, which are scalars from the 4D point of view, include the weak doublet identified with the SM Higgs. The Higgs mass is protected by the collective symmetry breaking mechanism. To see this, consider a variation of the symmetry breaking pattern in eqs. (2.6.12), (2.6.13), with $SU(5)$ broken down to a *single* $SU(2) \times U(1)$ subgroup on the UV brane. This theory possesses an $SU(3)$ global symmetry, broken down to $SU(2)$ by the BC's on the IR brane. The A_5 components identified with the Higgs are the Goldstone bosons of this global symmetry breaking, and as such are exactly massless. Thus, the Higgs can only get a mass if *both* $SU(2) \times U(1)$ factors in $SU(5)$ are unbroken at the UV brane. That is, zero modes for at least two different gauge fields must enter into any diagram contributing to the Higgs mass. Just as in the 4D LHT, this implies cancelation of the quadratic divergence in the Higgs mass between the SM gauge bosons and their T-odd counterparts at scale f. The remaining logarithmic divergence is canceled by the KK states at the scale of order $1/R' \sim 10$ TeV, and a finite Higgs mass is generated, as guaranteed by non-locality and 5D gauge invariance. Note that there may be additional light states among the A_5 modes due to the large vevs of $K_{1,2}, A_{1,2}$ on the IR brane. However, those would not be protected by the collective breaking mechanism, but only by the 5D non-locality, so their masses would be of the order of $m_{KK}/4\pi \sim 1$ TeV, rather than the 100 GeV range for the doubly protected physical Higgs.

It is useful to compare this structure to that of the "minimal" holographic composite Higgs model of Agashe, Contino and Pomarol [46]. In that model, *all* divergences in the Higgs mass are canceled at the same scale, the KK scale $1/R'$. Precision electroweak (PEW) constraints push this scale up to at least 3 TeV, and some amount of fine-tuning is needed to obtain consistent EWSB. In contrast, in our theory, the quadratic divergence is canceled at the 1 TeV scale by the Little Higgs mechanism, without any tension with PEW constraints thanks to T parity. This allows us to push the KK scale to 10 TeV without fine-tuning. At this scale, the KK states themselves are completely safe from PEW constraints. Thus, the tension between fine-tuning and PEW constraints is eliminated. Of course, the price to pay is a larger symmetry group and matter content.

In principle, the fermion content of the five-dimensional model could be simplified compared to the 4D $SU(5)$-invariant model, if one were to take advantage of the symmetry breaking BC's and simply project out some of the unwanted zero modes for the fermions (such as, for example, U_i and χ_i components of the Ψ_i fields) instead of introducing new states for them to marry. However, one needs to be careful with this, if T-parity is to be maintained as an exact symmetry. 5D theories are automatically anomaly free in the sense that every bulk fermion is actually a 4D Dirac fermion, and so the theory is always vectorlike. However, once orbifold projections are introduced, *localized* anomalies can be generated on the boundaries, which would be locally canceled by an anomaly flow corresponding to the bulk Chern-Simons (CS) term [61]. These bulk CS terms would contain the A_5 field and thus could violate T-parity similarly to the WZW operators in the 4D case. In order to avoid such terms, we need to make sure that there are no localized anomalies in our theory. The most obvious way of achieving this is by putting a separate bulk fermion field for

every field in Table 2.3, with a zero mode forming a complete $SU(5)$ representation. This would imply that we pick a $(+, +)$ boundary condition for all the left handed components, and a $(-, -)$ BC for all the right handed components. This choice ensures that all localized anomalies cancel in the same way as in the 4D theory (see section 2.5), and there would be no bulk CS term appearing. The terms corresponding to the Lagrangian in eqs. (2.4.3) and (2.5.1) can then be mimicked by brane localized Yukawa terms involving the K_1, K_2 fields on the IR brane, and via UV brane localized mass terms of the form $U_{L1}U_{R1} + U_{L2}U_{R2}$ (remember that on the UV brane $SU(5)$ is broken and so these mass terms are not violating gauge invariance, so we do not need to introduce $F_{1,2}$). If we were to try to simplify the spectrum by using $(-, +)$ type boundary conditions for some of the fermions (and introducing fewer bulk fields), we would end up with a consistent theory, but with a bulk CS-term breaking T-parity.

In order to obtain Yukawa couplings, we need to make sure that the zero modes for the right-handed quarks also partly live in the right-handed component of $U_{L1,2}$. This can be achieved via the IR brane localized scalars corresponding to η, η', ξ, ξ' in eq. (2.4.11). A Lagrangian corresponding to eq. (2.4.13) can be also added to the IR brane, except for adding mass terms along the pattern of the $\langle S \rangle$ instead of the complete S field (which is allowed due to the symmetry breaking BC's). The effect of those boundary terms will be to partially rotate the u_R zero mode into Q_1, and thus generate our effective Yukawa coupling. Note, that since all global $SU(3)_{1,2}$ violating effects are non-local (as they need to involve both branes), the radiatively generated Higgs potential will be completely finite. We leave the detailed study of the EWSB and the phenomenology of the holographic T-parity models to future investigations.

2.7 Constraints from the Weinberg Angle, Precision Electroweak Fits, and Dark Matter

The model constructed in sections 2.3 and 2.4 correctly reproduces the particle content of the SM at low energies. At the TeV scale, the model reproduces the particle content and couplings of the LHT. This sector eliminates the little hierarchy problem, and is consistent with precision electroweak fits as long as $f_S \geq 500$ GeV, and the T-odd partners of the SM fermion doublets are not too far above the TeV scale [30]. In addition, our model contains a number of states at the TeV scale that were *not* present in the LHT. These states can produce additional contributions to precision electroweak observables. While a detailed analysis of the resulting constraints is outside the scope of this section, we would like to briefly discuss the most salient constraint and show that it can be satisfied.

Most TeV-scale non-LHT states in our model are vectorlike fermions, and their contributions to PEW observables are small. The dominant new contribution is from the massive T-even gauge bosons. As discussed in section 2.3, these states can be significantly heavier than the T-odd gauge bosons, if the gauge couplings of the $SU(2)_3 \times U(1)_3$ gauge groups are stronger than that of the $SU(5)$ group. Since the SM Higgs does not couple to the $SU(2)_3 \times U(1)_3$ gauge bosons, the little hierarchy problem is still solved in this limit, provided that the T-odd gauge bosons remain sufficiently light. However, as mentioned at the end of section 2.3, the potential problem with this limit is the Weinberg angle prediction: the SM coupling are related to the $SU(5) \times SU(2)_3 \times U(1)_3$

gauge couplings via

$$\frac{1}{g^2} = \frac{2}{g_5^2} + \frac{1}{g_3^2} \quad \text{and} \quad \frac{1}{g'^2} = \frac{6}{5g_5^2} + \frac{1}{g_3'^2}, \tag{2.7.1}$$

so that $\sin^2\theta = 5/8$ in the limit $g_3', g_3 \gg g_5$. Is it possible to satisfy precision electroweak constraints and at the same time reproduce the experimental value of the Weinberg angle, $\sin^2\theta_{\text{exp}} \approx 0.2315$?

The spectrum of the TeV-scale gauge bosons has been discussed in section 2.3, see eqs. (2.3.12) and (2.3.13). However, these equations did not take into account the effect of the additional breaking of the $U(1)$ gauge bosons by the vevs of $A_{1,2}$ and $F_{1,2}$. Including these vevs, the $U(1)$ gauge boson masses are

$$m_{B_{\text{even}}}^2 = \frac{g_5'^2 + 2g_3'^2}{4}(f_K^2 + 16f_A^2) \quad \text{and} \quad m_{B_{\text{odd}}}^2 = \frac{g_5'^2}{100}(10f_S^2 + f_K^2 + 16f_A^2 + 32f_F^2), \tag{2.7.2}$$

(where $g_5' = \sqrt{5/3}\,g_5$),while the $SU(2)$ gauge boson masses are still given by eq. (2.3.12). It is convenient to rewrite the gauge boson spectrum and the Weinberg angle in terms of dimensionless ratios:

$$\sin^2\theta = \left[1 + \frac{1}{5} \cdot \frac{6 + 5/r'}{2 + 1/r}\right]^{-1}$$
$$\frac{m_{W_{\text{even}}}^2}{m_{W_{\text{odd}}}^2} = \frac{1 + 2r}{1 + 2r_S}$$
$$\frac{m_{B_{\text{odd}}}^2}{m_{W_{\text{odd}}}^2} = \frac{1 + 10r_S + 16r_A + 32r_f}{60(1 + 2r_S)} \tag{2.7.3}$$
$$\frac{m_{B_{\text{even}}}^2}{m_{W_{\text{odd}}}^2} = \left[\frac{5}{3} + 2r'\right]\frac{1 + 16r_A}{1 + 2r_S},$$

where the ratios are defined as

$$r = g_3^2/g_5^2, \quad r' = g_3'^2/g_5^2, \quad r_S = f_S^2/f_K^2, \quad r_A = f_A^2/f_K^2, \quad r_F = f_F^2/f_K^2. \tag{2.7.4}$$

Tree-level shifts in precision electroweak observables can be computed in terms of the T-even gauge boson masses and the coupling constant ratios, r and

r'. For example, taking the Z mass, the Fermi constant G_F and the fine structure constant α as inputs, the shift in the W boson mass with respect to the reference value is given by

$$\Delta m_W \equiv m_W - c_w^{\text{ref}} m_Z = \frac{m_W}{4} \frac{\pi\alpha}{c_w^2 - s_w^2} \left(\frac{1}{r} \frac{v^2}{m_{W_{\text{even}}}^2} + \frac{5}{3} \frac{1}{r'} \frac{v^2}{m_{B_{\text{even}}}^2} \right) , \qquad (2.7.5)$$

where c_w^{ref} is the reference value of the cosine of the Weinberg angle, and $v \approx 246$ GeV is the Higgs vev. The structure of corrections to *all* observables is the same as in eq. (2.7.5): the contributions of the heavy $SU(2)$ states are proportional to $r^{-1} m_{W_{\text{even}}}^{-2}$, while those due to the heavy $U(1)$ states are proportional to $r'^{-1} m_{B_{\text{even}}}^{-2}$. This is because both the light-heavy gauge boson mixing, and the couplings of the heavy gauge bosons to light fermions, are inversely proportional to $\sqrt{r}$ or $\sqrt{r'}$.

This structure can be exploited to find the region of parameter space where the corrections are suppressed without fine-tuning. To avoid large corrections to the Higgs mass from the $SU(2)$ sector, the W_{odd} gauge bosons should be light, preferably around 1 TeV or below. At the same time, the W_{even} can be much heavier, if the parameter r is large. In this regime, the contribution to precision electroweak observables from the $SU(2)$ sector is suppressed both by the W_{even} mass and by its small mixing and couplings to the SM fermions, as noted above. The PEW constraint on the mass of an extra $SU(2)$ boson with SM-strength couplings (such as the KK gauge bosons in models with extra dimensions) is typically around 3 TeV. Using this value and assuming $m_{W_{\text{odd}}} = 1$ TeV and $f_S = f_K$, we estimate that the $SU(2)$ contributions in our model are sufficiently suppressed if $r \gtrsim 2$. The r parameter is limited from above by the requirement that the $SU(2)_3$ not be strongly coupled:

$$\frac{g_3^2}{4\pi} \lesssim 0.3 \quad \Leftrightarrow r \lesssim 5 . \qquad (2.7.6)$$

There is a wide rage of values where the model is perturbative and consistent with data.

Once r is fixed, the requirement of getting the correct Weinberg angle fixes r'; the range $2 < r < 5$ corresponds to $0.14 \lesssim r' \lesssim 0.16$, so that the $U(1)$ mixing angle is essentially fixed. Thus, the B_{even} boson *cannot* be decoupled by assuming large g_3'. Moreover, the couplings of the heavy $U(1)$ gauge boson to the SM fermions are actually enhanced compared to the SM hypercharge coupling. However, its mass is essentially a free parameter, and it can be heavy provided that $f_A \gg f_S, f_K$. For example, assuming again $m_{W_{\text{odd}}} = 1$ TeV and $f_S = f_K$, the value of $f_A = 3f_S$ gives $m_{B_{\text{even}}} \approx 10$ TeV, which should be completely safe for precision electroweak fits even with the enhanced coupling. At the same time, for the same parameters and $f_F = f_S$, the T-odd $U(1)$ boson B_{odd} has a mass just above 1 TeV, so that the Higgs mass divergence is still canceled at 1 TeV and there is no fine-tuning. Thus, we estimate that in the region

$$2 \lesssim r \lesssim 5, \quad r' \approx 0.15, \quad r_A \gtrsim 10, \tag{2.7.7}$$

and all other dimensionless ratios of order one, our model should be consistent with precision electroweak data without fine-tuning in the Higgs mass.

An interesting phenomenological feature of the spectrum needed to satisfy the constraints is that the B_{odd} boson is not necessarily the lightest T-odd particle (LTP), in contrast to the situation typical in the original LHT model. Cosmological considerations require that the LTP not be strongly interacting or electrically charged. In our model, the T-odd partner of the SM neutrino can also play the role of the LTP. The T-odd neutrino LTP has not been considered in the previous studies of Little Higgs dark matter, which focused on the B_{odd} as the dark matter candidate. Our model provides a motivation to analyze this alternative

possibility.

In addition to the gauge bosons, several new scalar states appear at the TeV scale in our model. These include pseudo-Goldstone bosons which receive a mass at the one-loop order, as well as the radial excitations of the fields S and $K_{1,2}$. Several of these states are triplets with respect to the SM weak SU(2). If allowed by T-parity and hypercharge conservation, gauge interactions will generate terms of the form $h^\dagger \phi_i h$, where ϕ_i are the triplets, in the one-loop Coleman-Weinberg potential. Such terms do indeed arise for some of the triplets in our model. Those triplets are forced to acquire vevs, which can give large corrections to precision electroweak observables. For example, this effect played an important role in constraining the original littlest Higgs model without T-parity [62]. In our model, the triplet vevs are not directly related to the magnitude of the Higgs quartic coupling, as was the case in the LH without T-parity. We expect that it should be possible to find phenomenologically consistent regions of parameter space where the triplet vevs are small.

2.8 Little Higgs Mechanism in the Linear Sigma Model

A key feature of little Higgs models is the protection of the SM Higgs mass from quadratic divergence at the one-loop level through collective symmetry breaking. We argued in sections 2.3 and 2.4 that, since our model below the 10 TeV scale reproduces the nlσm LHT, the same cancelations will occur. While our model has extra states at the TeV scale, the symmetric scalar field S, which contains the SM Higgs, has no direct couplings to those states. (It is uncharged under the extra gauge group $SU(2)_3 \times U(1)_3$ and has no Yukawa couplings

56
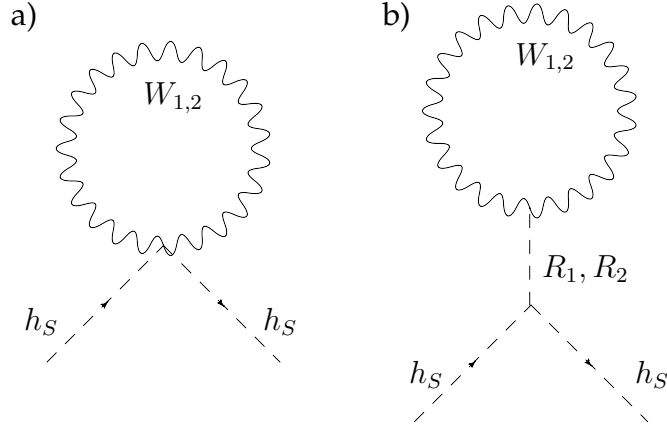
Figure 2.3: The Feynman diagrams contributing to the effective gauge couplings of the Higgs boson at low energies.

other than the top Yukawa already present in the LHT.) Thus, no new one-loop quadratic divergences arise. This argument ensures that in our model the little hierarchy problem is resolved in exactly the same manner as in the LHT. Nevertheless, it is interesting and instructive to see explicitly how the little Higgs cancelations occur in our weakly-coupled, UV-complete model. We will do so in this section.

First, let is consider the renormalization of h_S mass by gauge boson loops. We will focus on the $SU(2)$ gauge bosons; the analysis for the $U(1)$ bosons is essentially identical. In our model, the Higgs coupling to the gauge bosons includes the terms

$$\mathcal{L} \supset \tfrac{1}{8} h_S^\dagger h_S \left(g_1^2 W_1^1 + g_2^2 W_2^2 \right), \tag{2.8.1}$$

where g_i denotes the gauge coupling to the $SU(2)_i$ subgroup of $SU(5)$ (which are the same in our model, but potentially different in the original Littlest Higgs). These terms arise from the covariant derivative in eq. (2.3.4) and are required by gauge invariance. These couplings produce a quadratic divergence in the Higgs mass via the "bow-tie" diagrams in Fig. 2.3 (a). Recall that in the Lit-

tlest Higgs model, the structure of the four-point Higgs-gauge boson coupling is different [63]:

$$\mathcal{L}_{\text{LHT}} \supset \tfrac{1}{4} g_1 g_2 W_1 W_2 (h^\dagger h), \tag{2.8.2}$$

which does not lead to a quadratic divergence at one loop. Since our model must reduce to the LHT below the 10 TeV scale, there seems to be a contradiction.

This issue is resolved when the full set of diagrams contributing to the Higgs mass at one-loop in our linearlized model is included. Specifically, the relevant diagrams are the ones involving two radial (heavy) modes of S, coupling to the Higgs and the gauge bosons. These diagrams are shown in Fig. 2.3 (b). Let us assume that a potential for S has the form

$$V = -M^2 \text{Tr } SS^\dagger + \lambda_1 (\text{Tr } SS^\dagger)^2 + \lambda_2 \text{Tr } SS^\dagger SS^\dagger, \tag{2.8.3}$$

where $M^2 = 2(5\lambda_1 + \lambda_2) f_S^2$. This potential produces the desired pattern of symmetry breaking at scale f_S. It leads to the following pieces in the Lagrangian containing the heavy radial modes R_1 and R_2 (amongst others):

$$\begin{aligned}
\mathcal{L} \supset & -\tfrac{1}{2} M_{R_1}^2 R_1^2 - \tfrac{1}{2} M_{R_2}^2 R_2^2 + \frac{1}{\sqrt{5} f_S} \left(\tfrac{3}{2} M_{R_1}^2 R_1 + 2 M_{R_1}^2 R_2 \right) h_S^\dagger h_S \\
& + \frac{f_S}{4\sqrt{5}} (R_1 - 2R_2) \left(g_1^2 W_1^2 + g_2^2 W_2^2 - 2 g_1 g_2 W_1 W_2 \right),
\end{aligned} \tag{2.8.4}$$

where the radial modes have masses $M_{R_1}^2 = 32\lambda_2 f_S^2$ and $M_{R_2}^2 = 32(5\lambda_1 + \lambda_2) f_S^2$. Note that the couplings of the radial modes to $h_S^\dagger h_S$ are proportional to their masses. The effective Lagrangian below the scale f_S is obtained by integrating out the radial modes $R_{1,2}$ in eq. (2.8.4). The resulting Lagrangian contains terms that exactly cancel the gauge-Higgs four-point couplings in eq. (2.8.1). The remaining coupling has the form

$$\mathcal{L}_{\text{eff}} \supset \tfrac{1}{4} g_1 g_2 W_1 W_2 (h_S^\dagger h_S), \tag{2.8.5}$$
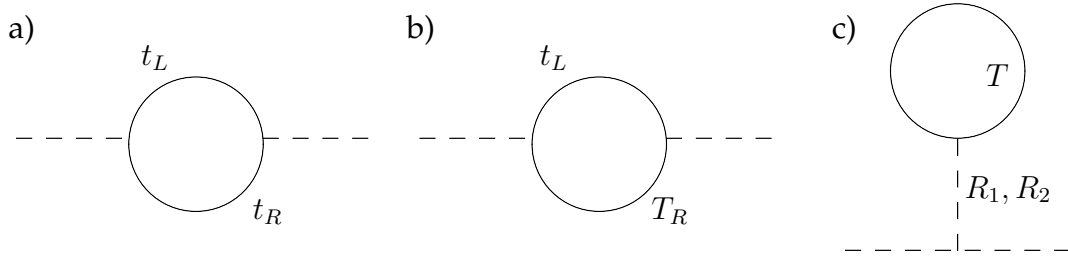
Figure 2.4: The Feynman diagrams contributing to the effective top couplings of the Higgs boson at low energies.

which exactly matches the non-linear Littlest Higgs Lagrangian and does not lead to quadratic divergences at one loop. Note that this result is independent of the couplings $\lambda_{1,2}$, as expected from the Coleman-Wess-Zumino theorem.

In a completely analogous way, one can show that the diagrams for cancelling the top loop divergence are generated by integrating out R_1, R_2 properly. These diagrams are shown in Fig. 2.4. Especially, we also recover the sum rule from [64] for the Yukawa coupling of the top quark with itself λ_t and with its heavy partner λ_T

$$\frac{M_T}{f_S} = \frac{\lambda_t^2 + \lambda_T^2}{\lambda_T}, \tag{2.8.6}$$

which ensures that the one-loop quadratic divergence due to the top quark cancel.

2.9   Conclusions and Outlook

In this chapter, we constructed a weakly coupled, renormalizable theory which reproduces the structure of the LHT model below the 10 TeV scale. This structure includes collective symmetry breaking mechanism to protect the Higgs mass from one-loop quadratic divergences, resolving the little hierarchy prob-

lem. The model is manifestly free of anomalies, and T-parity is an exact symmetry of the quantum theory. This leads to an exactly stable lightest T-odd particle, which can be either the T-odd hypercharge gauge boson or the partner of the neutrino. This particle can play the role of dark matter, and provide a missing energy signature at colliders. In addition, our model contains a few T-even extra states at the TeV scale, which can however be made sufficiently heavy to avoid conflict with precision electroweak data, without any fine tuning. Above the 10 TeV scale, our model can be embedded into either a supersymmetric theory or a five-dimensional setup with warped geometry, stabilyzing the large hierarchy between 10 TeV and the Planck scale. A remaining concern regarding the fully anomaly free matter content is that due to the large numbers of states required for anomaly cancelation a Landau pole in the QCD gauge coupling would rapidly develop. It would be very interesting to find a smaller anomaly canceling matter content that can avoid this issue.

In a weakly coupled UV completion of the LHT, a number of issues can be addressed which could not be analyzed in the original effective theory. One issue is gauge coupling unification, since in our model renormalization group evolution of all couplings is calculable within perturbation theory above 10 TeV. Unfortunately, in the explicit anomaly-free models constructed here, the range of validity of perturbation theory is limited by the rapid increase in the gauge couplings above 10 TeV. In these models, no gauge coupling unification occurs within the perturbative regime. If consistent UV completions with smaller matter content are found, the issue of gauge unification should be reexamined.

Another important issue is flavor physics, in particular flavor-changing neutral currents (FCNCs). There are two sources of FCNCs in the LHT model.

The first one is the effects generated by loops of heavy T-odd quarks and leptons, calculable within the effective theory. These effects have been considered in [65–68]. The second class are the effects generated at or above the cutoff scale of the effective theory. These effects should be represented by local operators in the effective theory, with coefficients obtained by matching to the UV completion at the cutoff scale. If the UV completion does not contain any flavor structure, one expects such operators to appear suppressed by powers of the cutoff scale, with order-one coefficients. In the LHT, the cutoff scale is 10 TeV, so several of these operators would strongly violate experimental bounds on the FCNCs. This indicates that additional flavor structure (e.g. flavor symmetries) is a necessary part of the UV completion of the LHT. It would be interesting to extend out model to obtain realistic flavor physics.

CHAPTER 3

TESTING GLUINO SPIN WITH THREE-BODY DECAYS

3.1   Motivation

If new particles are found at the LHC, one problem that arises is that their mass spectrum will not be completely known. This will not be enough to identify the underlying physics. For example, it has been shown that extra dimensional models (UED) can mimic the spectrum of supersymmetric (SUSY) theories. To distinguish between these models it will be thus necessary to measure their spin as well.

In this chapter we investigate the possibility of determining the spin of new particles from their decay products. In particular, we look at the case where the new particle can only decay via a 3-body decay to two jets and a massive invisible daughter, which escapes detection [23].

3.2   Introduction

Very soon, experiments at the Large Hadron Collider (LHC) will begin direct exploration of physics at the TeV scale. Strong theoretical arguments suggest that this physics will include new particles and forces not present in the Standard Model (SM). Several theoretically motivated extensions of the Standard Model at the TeV scale have been proposed. After new physics discovery at the LHC, the main task of the experiments will be to determine which of the proposed models, if any, is correct.

Unfortunately, there exists a broad and well-motivated class of SM extensions for which this task would be highly non-trivial. In these models, the new TeV-scale particles carry a new conserved quantum number, not carried by the SM states. The lightest of the new particles is therefore stable. Furthermore, the stable particle interacts weakly, providing a very attractive "weakly interacting massive particle" (WIMP) candidate for dark matter with relic abundance naturally in the observed range. Models of this class include the minimal supersymmetric standard model (MSSM) and a variety of other supersymmetric models with conserved R parity, Little Higgs models with T parity (LHT), and models with universal extra dimensions (UED) with Kaluza-Klein (KK) parity. All these models have a common signature at a hadron collider: pair-production of new states is followed by their prompt decay into visible SM states and the lightest new particle, which escapes the detector without interactions leading to a "missing transverse energy" signature. If this universal signature is observed at the LHC, how does one determine which of these models is realized?

One crucial difference between the MSSM and models such as LHT or UED is the correlation between spins of the new particles and their gauge charges. In all these models, all (or many of) the new states at the TeV scale can be paired up with the known SM particles, with particles in the same pair carrying identical gauge charges. However, while in the LHT and UED models the two members of the pair have the same spin, in the MSSM and other supersymmetric models their spins differ by 1/2. Thus, measuring the spin of the observed new particles provides a way to discriminate among models.

Experimental determination of the spin of a heavy unstable particle with one or more invisible daughter(s) in hadron collider environment is a difficult

task. One possibile approach, which recently received considerable attention in the literature [69–75], is to use angular correlations between the observable particles emitted in subsequent steps of a cascade decay, which are sensitive to intermediate particle spins. This strategy is promising, but its success depends on the availability of long cascade decay chains, which may or may not occur depending on the details of the new physics spectrum. It is worth thinking about other possible strategies for spin determination.

In this chapter, we explore the possibility of using 3-body decays of heavy new particles to determine their spin. The most interesting example is the 3-body decay of the MSSM gluino into a quark-antiquark pair and a weak gaugino,

$$\tilde{g} \to q + \bar{q} + \chi. \tag{3.2.1}$$

In a large part of the MSSM parameter space, this decay has a large branching ratio: this occurs whenever all squarks are heavier than the gluino. Under the same condition, gluino pair-production dominates the SUSY signal at the LHC. The main competing gluino decay channel in this parameter region is a two-body decay $\tilde{g} \to g\chi$, which first arises at one-loop level and generically has a partial width comparable to the tree-level decay (3.2.1). The gluino decay patterns in this parameter region have been analyzed in detail in Ref. [76]. We will argue that the invariant mass distribution of the jets produced in reaction (3.2.1) contains non-trivial information about the gluino spin, and can be used to distinguish this process from, for example, its UED counterpart, $g^1 \to q + \bar{q} + B^1/W^1$.

It is important to note that the jet invariant mass distribution we study depends not just on the spin of the decaying particle, but also on the helicity struc-

ture of the couplings which appear in the decay (3.2.1), as well as on the masses of the decaying particle, the invisible daughter, and the off-shell particles mediating the decay. If all these parameters were measured independently, the jet invariant mass distribution would unambiguously determine the spin. However, independent determination of many of the relevant parameters will be very difficult or impossible at the LHC. In this situation, proving the spin-1/2 nature of the decaying particle requires demonstrating that the experimentally observed curve cannot be fitted with any of the curves predicted by models with other spin assignments, independently of the values of the unknown parameters. This considerably complicates our task. Still, interesting information can be extraced. For example, we will show that, even if complete ignorance of the decaying and intermediate particle masses is assumed, the jet invariant mass distribution allows one to distinguish between the decay (3.2.1) in the MSSM and its UED counterpart (assuming the couplings specified by each model) at the LHC.

This chapter is organized as follows. After setting up our notation and reviewing the basics of three-body kinematics in Section 2, we present a simple toy model showing how dijet invariant mass distributions from three-body decays can be used to probe the nature of the decaying particle and its couplings in Section 3. Section 4 discusses using this observable for MSSM/UED discrimination, and contains the main results of the chapter. Section 5 contains the conclusions. Appendix A contains the polarization analysis of the decay $g^1 \rightarrow q + \bar{q} + B^1/W^1$ in UED, which sheds some light on the main features of the dijet invariant mass distribution in this case. Appendix B contains a brief review of the Kullback-Leibler distance, a statistical measure used in our analysis.

3.3 The Setup and Kinematics

We are interested in three-body decays of the type

$$A \to q + \bar{q} + B, \tag{3.3.1}$$

where A and B are TeV-scale particles. The main focus of this chapter will be on the case when A is the gluino of the MSSM or the KK gluon of the UED model, and B is a neutalino or chargino of the MSSM or a KK electroweak gauge boson of the UED; however the discussion in this section applies more generally. We assume that q and $\bar{q}$ are massless, and denote their four-momenta by p_1 and p_2 respectively. To describe the kinematics in Lorentz-invariant terms, we introduce the "Mandelstam variables",

$$
\begin{aligned}
m_{12}^2 &\equiv s = (p_1 + p_2)^2 = (p_A - p_B)^2 \,, \\
m_{1B}^2 &\equiv u = (p_1 + p_B)^2 = (p_A - p_2)^2 \,, \\
m_{2B}^2 &\equiv t = (p_2 + p_B)^2 = (p_A - p_1)^2 \,,
\end{aligned}
\tag{3.3.2}
$$

of which only two are independent since

$$s + t + u = m_A^2 + m_B^2. \tag{3.3.3}$$

The allowed ranges for the Mandelstam variables are determined by energy and momentum conservation; in particular,

$$0 \le s \le s^{\mathrm{max}} \equiv (m_A - m_B)^2. \tag{3.3.4}$$

We will assume that p_B cannot be reconstructed, either because B is unobservable or is unstable with all decays containing unobservable daughters. Moreover, since the parton center-of-mass frame is unknown, no information is available about the motion of particle A in the lab frame. Due to these limitations, the

analysis should use observables that can be reconstructed purely by measuring the jet four-momenta, and are independent of the velocity of A in the lab frame. The only such observable is s, and the object of interest to us is the distribution $d\Gamma/ds$. This is given by

$$\frac{d\Gamma}{ds} = \frac{1}{64\pi^3} \frac{s}{m_A^2} \int_{E_B - p_B}^{E_B + p_B} \frac{dy}{(m_A - y)^2} |\bar{\mathcal{M}}|^2 \,, \qquad (3.3.5)$$

where

$$\begin{aligned} E_B &= \frac{m_A^2 + m_B^2 - s}{2m_A} \,, \\ p_B &= \sqrt{E_B^2 - m_B^2} \,, \end{aligned} \qquad (3.3.6)$$

and $\mathcal{M}$ is the invariant matrix element for the decay (3.3.1), with the bar denoting the usual summation over the final state spins and other quantum numbers and averaging over the polarization and other quantum numbers of A. This procedure should take into account the polarization of A, if it is produced in a polarized state. In the examples of this chapter, production is dominated by strong interactions and A will always be produced unpolarized. For a more detailed discussion of polarized decays see Appendix A.1.

The quantity $|\bar{\mathcal{M}}|^2$ can be expressed in terms of the variables (3.3.2); substitutions

$$t \to m_A^2 - \frac{s m_A}{m_A - y}, \quad u \to \frac{sy}{m_A - y} + m_B^2 \qquad (3.3.7)$$

should be made in $|\bar{\mathcal{M}}|^2$ before performing the integral in Eq. (3.3.5). Notice that Eq. (3.3.5) is valid in the rest frame of the particle A; however, since s is Lorentz-invariant, its Lorentz transformation is a trivial overall rescaling by time dilation, and the shape of the distribution is unaffected. The strategy we will pursue is to use this shape to extract information about the decay matrix element $\mathcal{M}$, which is in turn determined by the spins and couplings of the particles A and B.
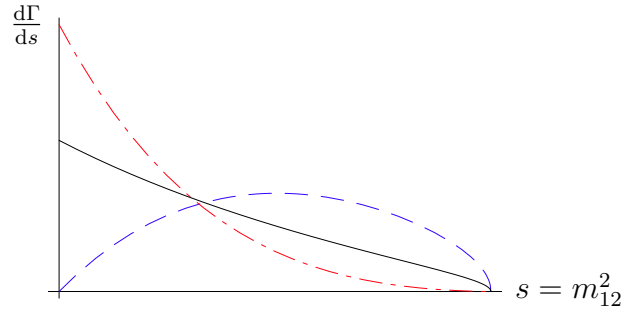
Figure 3.1: Dijet invariant mass distribution for the toy model 1 (blue/dashed) and model 2 (red/dot-dashed) compared to phase space (black/solid) for $M_*/m_A = 1.5$ and $m_B/m_A = 0.1$.

To separate the effects of non-trivial structure of the decay matrix element from those due merely to kinematics, it will be useful to compare the dijet invariant mass distributions predicted by various theories to the "pure phase space" distribution, obtained by setting the matrix element to a constant value. From Eq. (3.3.5), the phase space distribution is given by

$$\frac{d\Gamma}{ds} = \frac{1}{32\pi^3} \frac{|\mathbf{p}_B|}{m_A} \propto \sqrt{(s - m_A^2 - m_B^2)^2 - 4m_A^2 m_B^2}. \tag{3.3.8}$$

This distribution* is shown by a solid black line in Fig. 3.1. Notice that the phase space distribution has an endpoint at $s = s^{\mathrm{max}}$, with the asymptotic behavior given by

$$\frac{d\Gamma}{ds} \sim (s - s^{\mathrm{max}})^{1/2} \tag{3.3.9}$$

as the endpoint is approached.

3.4 Chiral Structure in Three-Body Decays: a Toy Model

To illustrate how the chiral structure of the couplings involved in the decay (3.3.1) can be determined from the dijet invariant mass distribution, consider a situation when the particles A and B are real scalars. Introduce a massive Dirac fermion Ψ of mass $M_* > m_A$, and consider the following two models: model 1 defined by

$$\mathcal{L}_1 = y_A A \bar{\Psi} P_L q + y_B B \bar{\Psi} P_R q + \text{h.c.} \tag{3.4.1}$$

and model 2 defined by

$$\mathcal{L}_2 = y_A A \bar{\Psi} P_L q + y_B B \bar{\Psi} P_L q + \text{h.c.} \tag{3.4.2}$$

The matrix element for the decay (3.3.1) in model 1 is given by

$$\sum_{\text{spin}} |\mathcal{M}_1|^2 = 2 y_A^2 y_B^2 (M_*^2 \, s) \left(\frac{1}{(t - M_*^2)^2} + \frac{1}{(u - M_*^2)^2} \right), \tag{3.4.3}$$

while in model 2 it is given by

$$\sum_{\text{spin}} |\mathcal{M}_2|^2 = 2 y_A^2 y_B^2 \left((m_A^2 + m_B^2) tu - m_A^2 m_B^2 \right) \left(\frac{1}{t - M_*^2} + \frac{1}{u - M_*^2} \right)^2. \tag{3.4.4}$$

The dijet invariant mass distributions in the two models are shown by the blue/dashed line (model 1) and red/dot-dashed line (model 2) in Fig. 3.1. Their strikingly different shapes are due to the angular momentum conservation law and to the different helicity structure of the couplings. To understand this, consider this decay in the A rest frame. In this frame, $s = 2 E_1 E_2 (1 - \cos \theta_{12})$. When $s = 0$, the quark and the antiquark travel in the same direction, as illustrated in Fig. 3.2. Since A and B have zero spin, the sum of the quark and antiquark

---

*Since we are concerned with the shapes of the dijet invariant mass distributions in various models and not their overall normalizations, all distributions appearing on the plots throughout this chapter are normalized to have the same partial width $\Gamma = \int_0^{s^{\text{max}}} \frac{d\Gamma}{ds} \, ds$.
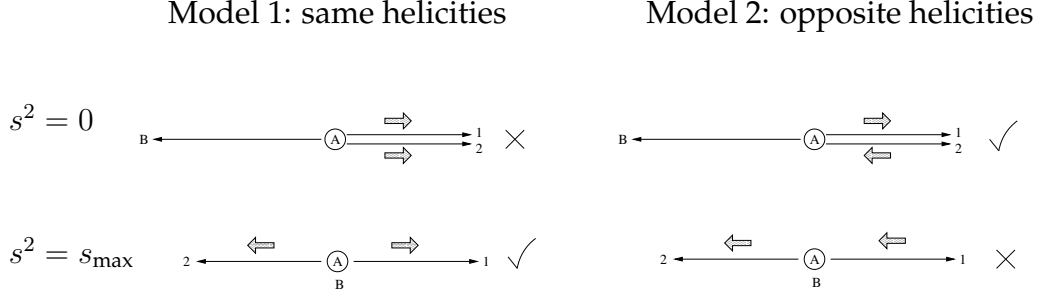
Figure 3.2: Momenta (long arrows) and helicities (short arrows) in the A rest frame for $s = m_{12}^2 = 0$ and $s = m_{12}^2 = s^{\max}$ in the two toy models of section 3.

helicities must vanish for this kinematics. In model 1, the quark and the antiquark have the same helicity, and the decay is forbidden for $s = 0$; in model 2, it is allowed. In contrast, when $s = s^{\max}$, the particle B is at rest, and the quark and the antiquark travel in the opposite directions. By angular momentum conservation, their helicities must be equal. In model 1, this is the case, and the distribution approaches that of pure phase space in the limit $s \to s^{\max}$. In model 2, this kinematics is forbidden, the matrix element vanishes at the endpoint, and the distribution behaves as $d\Gamma/ds \propto (s - s^{\max})^{3/2}$.

3.5   Model Discrimination: SUSY Versus UED

In this Section, we will show that measuring the shape of the dijet invariant mass distribution arising from a three-body decay of a heavy colored particle may allow to determine whether the decaying particle is the gluino of the MSSM or the KK gluon of the UED model. We will begin by comparing the analytic predictions for the shapes of the two distributions at leading order. We will then present a parton-level Monte Carlo study which demonstrates that the discriminating power of this analysis persists after the main experimental complications
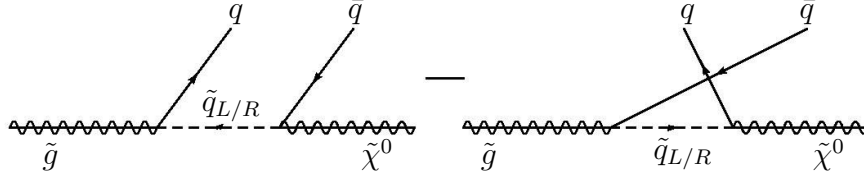
Figure 3.3: The Feynman diagrams for gluino three-body decay in the MSSM. Note that the crossing of the quarks results in a relative minus sign.

(such as the combinatioric background, finite energy resolution of the detector, and cuts imposed to suppress SM backgrounds) are taken into account.

3.5.1 Gluino decay in the MSSM

We consider the MSSM in the region of the parameter space where all squarks are heavier than the gluino, forbidding the two-body decays $\tilde{g} \to \tilde{q}q$. In this situation, gluino decays through three-body channels. We study the channel

$$\tilde{g}(p_A) \to q(p_1) + \bar{q}(p_2) + \tilde{\chi}_1^0(p_B), \qquad (3.5.1)$$

where q and $\bar{q}$ are light (1st and 2nd generation) quarks, and $\tilde{\chi}_1^0$ is the lightest neutralino which we assume to be the LSP. (Note that many of our results would continue to hold if $\tilde{\chi}_1^0$ is replaced with a heavier neutralino or a chargino. The only extra complication in these cases would be a possible additional contribution to the combinatoric background from the subsequent cascade decay of these particles.) The leading-order Feynman diagrams for the process (3.5.1) are shown in Fig. 3.3; the vertices entering these diagrams are well known (see for example Ref. [77]). The spin-summed and averaged matrix element-squared has the form (up to an overall normalization constant)

$$\sum_{\text{spin}} |\mathcal{M}_{\text{MSSM}}|^2 = |C_L|^2 F(s,t,u;M_{L*}) + |C_R|^2 F(s,t,u;M_{R*}), \qquad (3.5.2)$$

71

where

$$F(s,t,u;M) = \frac{(m_A^2 - t)(t - m_B^2)}{(t - M^2)^2} + \frac{(m_A^2 - u)(u - m_B^2)}{(u - M^2)^2} + 2\frac{m_A m_B s}{(u - M^2)(t - M^2)} \, .$$

(3.5.3)

Here m_A, m_B, M_{L*} and M_{R*} are the masses of the gluino, the neutralino, the squarks $\tilde{q}_L$ and $\tilde{q}_R$, respectively. In order to keep the analysis general, we will not assume any relationships (such as mSUGRA contraints) among these parameters, and will always work in terms of weak-scale masses. We also define

$$C_L = T_q^3 N_{12} - t_w(T_q^3 - Q_q)N_{11} \, ,$$

$$C_R = t_w Q_q N_{11} \, ,$$

(3.5.4)

where $T_u^3 = +1/2, T_d^3 = -1/2, Q_u = +2/3, Q_d = -1/3, t_w = \tan\theta_w$, and N is the neutralino mixing matrix[†] in the basis $(\tilde{B}, \tilde{W}^3, \tilde{H}_u^0, \tilde{H}_d^0)$. We have neglected the mixing between the left-handed and right-handed squarks, which is expected to be small in the MSSM. Large mixing in the stop sector may be present, and is actually preferred by fine-tuning arguments in the MSSM (see, e.g., Ref. [78]). However, events with top quarks in the final state are characterized by more complicated topologies and can be experimentally distinguished from the events with light quarks that we are focussing on here. Since light up and down type quarks are experimentally indistinguishable, the dijet invariant mass distribution $d\Gamma/ds$ should include both the contributions of up-type and down-type squarks.
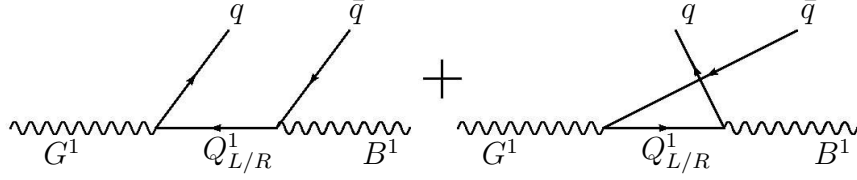
Figure 3.4: The Feynman diagrams for the KK gluon three-body decay in UED. Unlike in the MSSM case, there is no relative minus sign, since what looks like a crossing of the quarks, is actually equivalent to a crossing of the gauge bosons.

3.5.2 Decay of the gluon KK mode in the UED model

The counterpart of the decay (3.5.1) in the universal extra dimensions (UED) model is the decay

$$g^1(p_A) \rightarrow q(p_1) + \bar{q}(p_2) + B^1(p_B), \quad (3.5.5)$$

where g^1 and B^1 are the first-level Kaluza-Klein (KK) excitations of the gluon and the hypercharge gauge boson, respectively. We ignore the mixing between B^1 and the KK mode of the W^3 field, which is small provided that the radius of the extra dimension is small, $R \ll 1/M_W$, and assume that the B^1 is the LTP. As in the MSSM case, the decay (3.5.5) is expected to have a substantial branching fraction when all KK quarks Q_R^1 and Q_L^1 are heavier than the KK gluon. Note that in the original UED model [79], the KK modes of all SM states were predicted to be closely degenerate in mass around $M = 1/R$; it was however later understood [80] that kinetic terms localized on the boundaries of the extra dimension can produce large mass splittings in the KK spectrum. Since such kinetic terms are consistent with all symmetries of the theory, we will assume that they are indeed present, and treat the masses of the g^1, B^1, Q_R^1 and Q_L^1 fields as free parameters.

---

†We assume that N is real. It is always possible to redefine the neutralino fields to achieve this. However one should keep in mind that the neutralino eigenmasses may be negative with this choice.

The leading-order Feynman diagrams for the decay (3.5.5) are shown in Fig. 3.4. (We ignored the contribution of the diagrams mediated by $Q^i_{L/R}$ with $i \geq 2$, which are suppressed by the larger masses of the higher KK modes.) The relevant couplings have the form

$$g_3 G^1_\mu \left[\bar{q}\gamma^\mu P_R Q^1_R + \bar{q}\gamma^\mu P_L Q^1_L + \bar{Q}^1_R \gamma^\mu P_R q + \bar{Q}^1_L \gamma^\mu P_L q \right] +$$

$$g_1 B^1_\mu \left[Y(q_R)\,\bar{q}\gamma^\mu P_R Q^1_R + Y(q_L)\,\bar{q}\gamma^\mu P_L Q^1_L + Y(q_R)\,\bar{Q}^1_R \gamma^\mu P_R q + Y(q_L)\,\bar{Q}^1_L \gamma^\mu \right] \tag{3.5.6}$$

where $Y(q_L) = 1/6, Y(u_R) = +2/3$ and $Y(d_R) = -1/3$ are the hypercharges. The structure of the couplings between the KK gauge bosons and SM (or KK) quarks are unaffected by brane-localized kinetic terms as long as these terms are flavor-independent.

The spin-summed and averaged matrix element-squared has the form (up to an overall normalization constant)

$$\sum_{\text{spin}} |\mathcal{M}_{\text{UED}}|^2 = Y_L^2\, G(s,t,u;M_{L*}) + Y_R^2\, G(s,t,u;M_{R*}), \tag{3.5.7}$$

where M_{L*} and M_{R*} are the masses of the left- and right-handed quark KK modes Q^1_L and Q^1_R, and

$$G(s,t,u;M) = \frac{h_1(s,t,u)}{(t-M^2)^2} + \frac{h_1(s,u,t)}{(u-M^2)^2} + 2\frac{h_2(s,t,u)}{(t-M^2)(u-M^2)}, \tag{3.5.8}$$

with

$$h_1(s,t,u) = 4(tu - m_A^2 m_B^2) + \frac{t^2}{m_A^2 m_B^2}\left(2s(m_A^2 + m_B^2) + tu - m_A^2 m_B^2\right),$$

$$h_2(s,t,u) = 4s(m_A^2 + m_B^2) - \frac{tu}{m_A^2 m_B^2}\left(2s(m_A^2 + m_B^2) + tu - m_A^2 m_B^2\right). \tag{3.5.9}$$
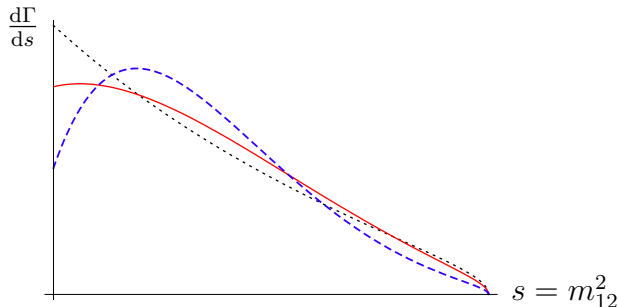
Figure 3.5: Dijet invariant mass distribution for the UED (blue/dashed) and the MSSM (red/solid) models, compared to pure phase space (black/dotted) for $M_{L*}/m_A = M_{R*}/m_A = 1.5$ and $m_B/m_A = 0.1$.

3.5.3 Model Discrimination: a Simplified Analysis

Armed with the expressions (3.5.2) and (3.5.7), it is straightforward to obtain the dijet invariant mass distributions for gluino and KK gluon decays and compare them. For example, the two distributions for a particular choice of parameters, along with the pure phase space distribution, are shown in Fig. 3.5. While not as strikingly different as the two toy models of Section 3.4, the curves predicted by the MSSM and the UED are clearly distinct. (The suppression of the UED distribution compared to phase space around $s = 0$ and $s = s_{max}$ can be easily understood using angular momentum conservation, as explained in Appendix A.1.) In this section, we will perform a simplified analysis of the discriminating power of these distributions, ignoring experimental complications such as cuts, finite energy resolution, combinatoric and SM backgrounds, and systematic errors. We will return to include some of these complications in the following section.

The distrubution in each model depends on a number of parameters, including the mass of the mother particle m_A, the mass of the invisible daughter m_B,

and the masses of intermediate particles: $(\tilde{u}_L, \tilde{d}_L, \tilde{u}_R, \tilde{d}_R)$ in the MSSM case and $(U_L^1, D_L^1, U_R^1, D_R^1)$ in the UED case. We assume that the partners of the up-type quarks of the first two generations and the down-type quarks for all three generations are degenerate, and do not include the diagrams with intermediate stops (or KK tops) since they produce tops in the final state. Furthermore, since the Yukawa couplings for the first two generations are small, it is safe to assume that $m(\tilde{u}_L) = m(\tilde{d}_L)$ in the MSSM and $m(U_L^1) = m(D_L^1)$ in UED. Since an overall rescaling of all masses does not affect the shape of the distribution, we need four dimensionless parameters to specify the mass spectrum in each model; we use the particle masses in units of m_A. Experimentally, these four parameters may be very difficult to obtain independently. A direct measurement of the masses of squarks/KK quarks may well be impossible, since these particles may be too heavy to be produced on-shell. Also, while it is easy to measure $m_A - m_B$ (one can use the endpoint of the dijet invariant mass distribution or other simple observables such as the effective mass [81] or its variations [82,83]), it is much more difficult to measure m_A and m_B individually [84], which would be required in order to obtain m_B/m_A. In this study, we will conservatively assume no prior knowledge of any of these parameters. (Of course, if some independent information about them is available, for example the overall mass scale is constrained by production cross section considerations, this information can be folded into our analysis, increasing its discriminating power.) In addition to the unknown masses, the matrix elements in the MSSM depend on the neutralino mixing matrix elements, N_{11} and N_{12}, although only the ratio N_{11}/N_{12} affects the shape of the distribution. Again, this parameter is difficult to measure at the LHC, and we will assume that it is unknown; fortunately, the effect of varying it is quite small.

To quantify the discriminating power of the proposed observable, we use the following procedure. We assume that the experimental data is described by the MSSM curve with a particular set of parameters. We then ask, how many events (assuming statistical errors only) would be required to rule out the UED as an explanation of this distribution? To answer this question, we scan over 50000 points in the UED parameter space:

$$m_B/m_A = (0\ldots0.5), \quad M(Q^1_L)/m_A = (1.05\ldots3.0),$$
$$M(D^1_R)/m_A = (1.05\ldots3.0), \quad M(U^1_R)/m_A = (1.05\ldots3.0). \quad (3.5.10)$$

For each point in the scan, we compute the Kullback-Leibler (KL) distance (see Appendix A.2) between the UED distribution with the parameters at that point, and the "experimental" distribution. We then find the "best-fit UED" point, which is the point that gives the smallest KL distance among the scanned sample. Finally, we compute the number of events required to rule out the best-fit UED point at a desired confidence level.

The results of this analysis are shown in Fig. 3.6. The MSSM parameters used to generate the "data" are: $m_B = 0.1m_A$, $m(\tilde{u}_R) = m(\tilde{d}_R) \equiv m_R$, $m(\tilde{u}_L) = m(\tilde{d}_L) \equiv m_L$, $N_{11}/N_{12} = 1$. The parameters m_L and m_R were then scanned between $1.05m_A$ and $2m_A$, and for each point in the scan the procedure described in the previous paragraph was performed. Fig. 3.6 shows the number of events required to rule out the UED interpretation of the signal at the 99.9% c.l. (In the language of Appendix A.2, this corresponds to $R = 1000$.) In a typical point in the model parameter space, about 6000 events are required. For comparison, the pair-production cross section for a 1 TeV gluino at the LHC is about 600 fb, corresponding to 12000 gluinos/year at the initial design luminosity of 10 fb^{-1}/year. The number of events useful for the measurement studied here
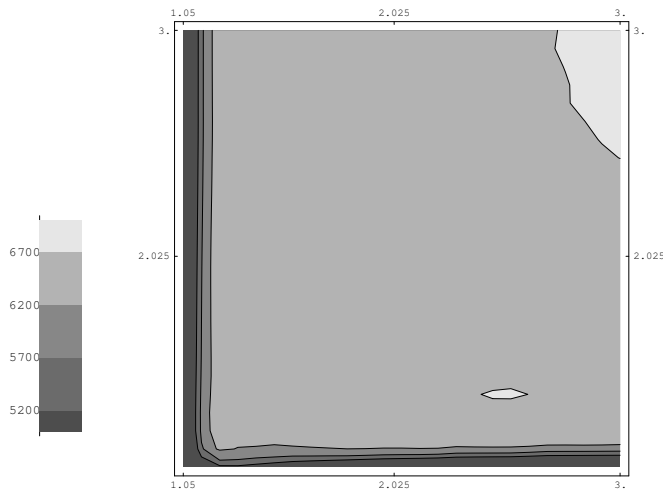
Figure 3.6: Number of events required to distinguish the MSSM and the UED models based on the invariant mass distributions of jets from three-body $\tilde{g}/G^1$ decays.
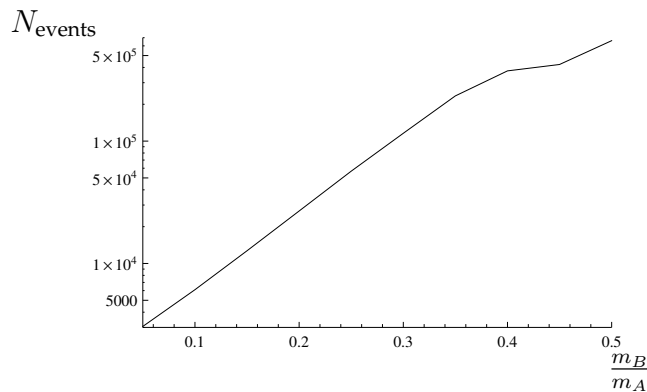
Figure 3.7: Number of events required to distinguish the MSSM and the UED models, as a function of m_B/m_A of the "true" model.

depends on the branching ratio of the decay (3.2.1). Since this branching ratio is generically of order one, we expect $O(10^3)$ useful events/year at the initial stages of the LHC running. Thus, at least under the highly idealized conditions of this simplified analysis, this method of model discrimination is quite promising in a wide range of reasonable model parameters.

We checked that the conclusions of this analysis are approximately indepen-

dent of the value of N_{11}/N_{12} used to generate the "data". They do, however, depend sensitively on the ratio m_B/m_A: as m_B/m_A grows, the MSSM and UED distributions become more and more alike. This is illustrated in Fig. 3.7, which shows the number of events needed to rule out the "wrong" model (assumed to be UED) at the 99.9% c.l., as a function of m_B/m_A of the "true" model (assumed to be the MSSM with $m(\tilde{u}_R) = m(\tilde{d}_R) = m(\tilde{u}_L) = m(\tilde{d}_L) = 1.5m_A$ and $N_{11}/N_{12} = 1$). The UED scan parameters are the same as in Eq. (3.5.10), except that we vary $m_B/m_A = (0 \ldots 0.9)$ in this case. It is clear that the discriminating power of the dijet invariant mass distribution falls rapidly (approximately exponentially) with growing m_B/m_A. This can be understood as follows. The main feature of the invariant mass distributions that allows for model discrimination is the presence of the sharp dip at $s = 0$ in the UED case. According to the Goldstone boson equivalence theorem, if the daughter particle B in the UED case is highly boosted, the decays into its longitudinal component will dominate. The particle B is highly boosted in the vicintiy of $s = 0$, provided that the mass ratio m_B/m_A is small; as m_B/m_A grows, the boost becomes less pronounced and the decays into the longitudinal component of B are less dominant. This is illustrated in Fig. 3.8, which compares the ratio of partial decay rates into the longitudinal and transverse modes of B for $m_B/m_A = 0.1$ and $m_B/m_A = 0.5$. However, it is exactly the decays into the longitudinal mode of B that are mainly responsible for the characteristic dip at $s = 0$; this feature is far less pronounced for the decays into transverse modes. This means that as m_B/m_A is increased, the dip gradually disappears, and the discriminating power of our observable fades away.

We have also checked that the results of our analysis are approximately independent of which model, MSSM or UED, is assumed to be the "true" one giving

$$s = m_{12}^2$$
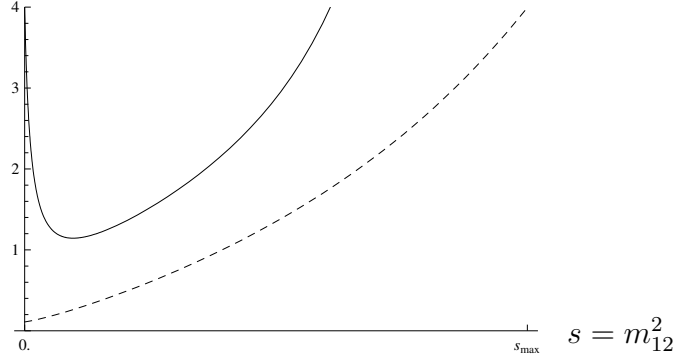
Figure 3.8: Ratio of the decay distributions of A into the longitudinal component of B to the decay distributions into the transverse components of B for $m_B/m_A = 0.1$(solid) and $m_B/m_A = 0.5$(dashed). For low m_B/m_A the daughter particle is highly boosted at $s = 0$ and will mainly be longitudinally polarized. As m_B increases, the transeverse polarization becomes more important.

the experimental data. For this one has to assume that the mass spectrum of the UED model is adjusted to match the MSSM spectrum, which can be achieved by adding large brane-localized kinetic terms for the gluons and quarks.

3.5.4   Model Discrimination: a Test-Case Monte Carlo Study

Given the large number of simplifying assumptions made in the analysis of the previous section, a skeptical reader may well wonder how meaningful the results presented above are. In this section, we will repeat the analysis in a more realistic setting: effects of experimental cuts and combinatoric background will be included. We will also bin the distributions, to approximate the effects of finite jet energy resolution. Since this analysis involves generating large samples of Monte Carlo (MC) events for each model, we were not able to perform a scan over the model parameter space, as we did in the previous section. Instead,

we will present a test case, comparing the MSSM distribution for a single point in the MSSM parameter space with the distribution generated by the "best-fit" UED model for that point.

The chosen MSSM point has the following parameters: $m_A = 1$ TeV, $m_B = 0.1m_A = 100$ GeV, $M(\tilde{Q}_L) = M(\tilde{u}_R) = M(\tilde{d}_R) = 1.5$ TeV. The corresponding "best-fit" UED point, found by the procedure described in the previous section, has the following parameters: $m_A = 1.06$ TeV, $m_B = 0.15m_A = 160$ GeV, $M(Q_L^1) = M(u_R^1) = M(d_R^1) = 1.6$ TeV. (Note that the value of $m_A - m_B$, which can be determined independently, is the same for these two points.) Using `MadGraph/MadEvent v4.1` [85, 86] event generator, we have simulated a statistically significant sample (about 20000) of parton-level Monte Carlo events for each model in pp collisions at $\sqrt{s} = 14$ TeV. The simulated processes are

$$pp \rightarrow q q \bar{q} \bar{q} \chi_1^0 \chi_1^0 \tag{3.5.11}$$

in the MSSM, and its counterpart,

$$pp \rightarrow q q \bar{q} \bar{q} B^1 B^1, \tag{3.5.12}$$

in UED. With the chosen model parameters, the dominant contribution to the processes (3.5.11) and (3.5.12) comes from pair-production of $\tilde{g}/G^1$, followed by the three-body decay (3.2.1), which is of primary interest to us. In the MC simulation, we did not demand that the $\tilde{g}/G^1$ be on-shell; the full tree-level matrix elements for the $2 \rightarrow 6$ reactions (3.5.11) and (3.5.12) were simulated, so that the subdominant contributions with off-shell $\tilde{g}/G^1$ are included. We imposed the following set of cuts on the generated events:

$$\eta_i \leq 4.0; \quad \Delta R(i, j) \geq 0.4; \quad p_{T,i} \geq 100 \text{ GeV}; \quad \not{E}_T \geq 100 \text{ GeV}, \tag{3.5.13}$$

where $i = 1 \ldots 4$, $j = i + 1 \ldots 4$ label the four (anti)quarks in each event. The first three cuts are standard for all LHC analyses, reflecting the finite detector
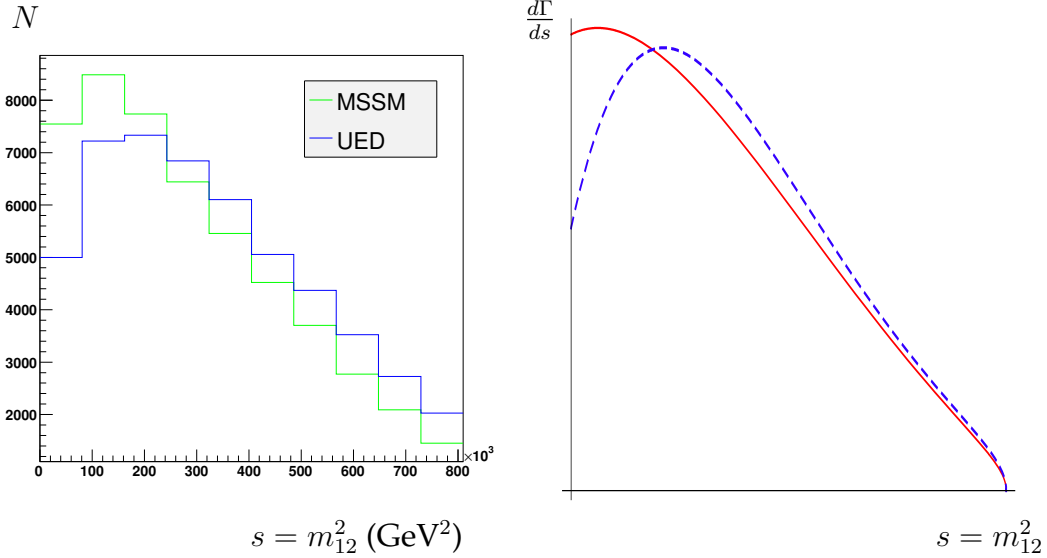
Figure 3.9: Left panel: Dijet invariant mass distributions from the MSSM reaction $pp \to qq\bar{q}\bar{q}\chi_1^0\chi_1^0$ (green/light-gray), and its UED counterpart $pp \to qq\bar{q}\bar{q}B^1B^1$ (blue/dark-gray), including realistic experimental cuts and the combinatoric background (Monte Carlo simulation). Right panel: Theoretical dijet invariant mass distributions from a single gluino/KK gluon decay with the same model parameters and no experimental cuts.

coverage, separation required to define jets, and the need to suppress the large QCD background of soft jets. The $\not{E}_T$ cut is common to all searches for models where new physics events are characterized by large missing transverse energy, such as the MSSM and UED models under consideration. Detailed studies have shown that this cut is quite effective in suppressing the SM backgrounds, including both the physical background, $4j + Z$, $Z \to \nu\bar{\nu}$, and a variety of instrumental backgrounds (see, for example, the CMS study [87]). While we have not performed an independent analysis of the SM backgrounds, based on previous work we expect that, with a sufficiently restrictive $\not{E}_T$ cut, one will be able to obtain a large sample of new physics events with no significant SM contamination.

The dijet invariant mass distruibutions obtained from the MSSM and UED

MC samples are shown in Fig. 3.9. The distributions are normalized to have the same total number of events, since the overall normalization is subject to large systematic uncertainties and we do not use any normalization information in our study. Note that for each MC event, we include all 6 possible jet pairings; 4 out of these correspond to combining jets that do *not* come from the same decay, and thus do not follow the theoretical distributions computed above. In Fig. 3.9, we selected the jet pairs with $s \leq (m_A - m_B)^2$. This selection can be implemented in a realistic experimental situation because $m_A - m_B$ can be measured independently. All pairs with larger values of s arise from the wrong jet pairings. However, some of the wrong jet pairs do have s in the selected range, forming a combinatoric background to the distribution we want to study. Nevertheless, it is clear from Fig. 3.9 that even after realistic cuts (3.5.13) and the combinatoric background are included, the distributions in the two models retain their essential shape difference expected from the simplified theoretical analysis of the previous section. Assuming that the experimental data is described by the MSSM histogram and ignoring systematic uncertainties, we find (using the standard χ^2 test) that about 750 events would be required to rule out the UED curve at the 99.9% c.l. Note that this number is smaller than those obtained in the previous section, indicating that the performed cuts actually enhance the difference between the MSSM and UED distributions. On the other hand, the actual discriminating power of the analysis is likely to be somewhat lower than this estimate, since the systematic uncertainty in the cut efficiencies was not taken into account here.

Our parton-level analysis does not explicitly take into account the smearing effect due to the finite jet energy and direction resolution of a real detector. The hadronic calorimeter energy resolution for a jet of energy E can be approximated

by

$$\frac{\delta E}{E} \approx 0.05 + \left(\frac{1\,\text{GeV}}{E}\right)^{0.5}, \qquad (3.5.14)$$

and is in the $5-15\%$ range for the jets that pass the cuts (3.5.13). We can crudely estimate $\delta s/s$ to be of order $2\delta E/E$, evaluated at $E = \sqrt{s}$. The fractional uncertainty of the measurement of s in our analysis is then roughly between 10% (for points with $s \sim s^{\text{max}}$) and 30% (for points with low s). The bin size used in Fig. 3.9 is of the order of this uncertainty for large s, and larger for small s, so we expect that the smearing introduced by binning in our analysis provides a reasonable, if crude, description of the expected smearing due to finite jet energy resolution. A more detailed investigation of this effect, and other potential detector effects, would be required to fully understand the applicability of the proposed method in a realistic experimental situation.

3.6   Conclusions

In this chapter, we have investigated how the dijet invariant mass distributions from three-body decays of a color-octed TeV-scale new particle, such as the gluino of the MSSM and the KK gluon of the UED model, can be used to determine the nature of this particle. The production cross section for the color-octet state at the LHC is expected to be large, and the branching ratio for the three-body decays is significant whenever all squarks/KK quarks are heavier than the gluino/KK gluon. If this is the case, the dijet invariant mass distribution can be determined accurately at the LHC. The main complication of the analysis is that the distributions in the two models we considered depend on a number of parameters in addition to the spin of the decaying particle. However, even allowing for complete ignorance of these parameters, we found the dijet

invariant mass to be a very promising tool for model discrimination.

The simplified analysis of this chapter did not take into account a number of potentially important effects. Since the particles involved are colored, the QCD loop corrections to the decay amplitudes are expected to be significant, and may modify the tree-level distributions we studied. Also, our analysis is performed at the parton level and does not include detector effects. While we expect that many systematic effects would cancel out since the analysis relies only on the shapes of the distributions and is insensitive to the overall normalization, a better understanding of the systematics is required. We believe that the promising conclusions of this preliminary analysis motivate a more detailed study of these issues.

CHAPTER 4

ODD DECAYS FROM EVEN ANOMALIES: GAUGE MEDIATION SIGNATURES WITHOUT SUSY

4.1 Motivation

A popular solution to the hierarchy problem is gauge-mediated SUSY breaking (GMSB), where the SUSY breaking sector and the MSSM sector decouple in the limit of vanishing SM gauge couplings. Since the gauge couplings are diagonal in flavor space, these models do not give new contributions to flavor changing neutral currents. In these models usually the gravitino is the lightest R-parity odd particle and a stable dark matter candidate. As a result heavier R-odd particles will decay to the gravitino through emission of a hard photon. At the LHC this would yield a lot events with missing energy and (potentially non-pointing) photons, which is a quite striking signature and was believed to be a "smoking gun" for GMSB models.

In this chapter we construct an explicit five dimensional model without supersymmetry which fakes GMSB, i.e. it produces lot of events with (non-pointing) photons and missing energy [25].

4.2 Introduction

Anomalies and the interactions they imply proved crucial in identifying the ultraviolet physics underlying the chiral Lagrangian, playing an important role in the formulation of the dynamical $SU(3)_C$ theory of quarks and gluons [88–92].

From the decay rate of $\pi^0 \to \gamma\gamma$, for example, one can infer the number of colors in the UV theory. This is due to the fact that, in the $SU(3)_C$ model, anomaly cancellation occurs non-trivially with the left and right-handed sectors contributing in equal but opposite non-zero amounts to the anomaly. In the effective field theory at low energies, this non-trivial anomaly cancellation of the UV theory is manifest non-locally in the $SU(3)_L \times SU(3)_R/SU(3)_V$ theory space of the chiral symmetry breaking Lagrangian, and emerges as a topological (and thus quantized) "Wess-Zumino-Witten" term labelled by a winding number that corresponds to the number of colors in the UV theory [56, 93, 94]. Additionally, the $U(1)$ problem of QCD, the unexpectedly large masses of the η and η' mesons have been resolved through non-perturbative instanton contributions through $U(1)$ global anomalies [95].

As we enter the LHC era, we have identified numerous theories which may play some role in stabilizing the weak scale. The most well studied of these physics scenarios is TeV scale supersymmetry [96], however, in recent years, enormous progress has been made on TeV scale extra dimensional theories and effective field theories such as little Higgs models. As was the case with the chiral Lagrangian, these theories may be supplanted at still higher energies by some confining UV dynamics, and anomalies may again play an important role. The study of anomalies in such contexts is in its infancy, but has already produced some important results for the phenomenology of extensions of the Standard Model (SM). To date, most studies have focused on scenarios where all anomalies vanish in the IR. In these models, anomaly cancellation occurs non-locally in an extra dimension [61, 97], or, as happens in the chiral Lagrangian, non-locally in theory space [19]. For consistency, such theories require a Chern-Simons flux or Wess-Zumino-Witten term, respectively. These terms encapsu-

late the integrated out UV dynamics through which anomaly cancellation occurs locally as well as globally.

In this chapter, we study the implications of extra dimensional classical symmetries which contain *non-vanishing* anomalies in the low energy 4D effective theory. Earlier work on such theories (with some overlapping results) has been performed in [98–100]. The Peccei-Quinn (PQ) symmetry [101] which has been originally proposed as a solution to the strong CP problem is a popular and well-motivated example of such a theory, and thus we consider a $U(1)_{\text{PQ}}$ extension of the 5D Universal Extra Dimension model (UED) [79, 102, 103]. In standard UED, the usual 4D SM fields are extended so that they all propagate in the bulk of a compactified extra dimension. This results in a tower of massive Kaluza-Klein (KK) partners of each SM field.

We note that this is only one application of the techniques we develop, and that other constructions are possible that may have novel phenomenology. Examples include warped extra dimensions, or even little Higgs theories, which in certain cases can be related to extra dimensional theories through the language of deconstruction [104, 105].

Even though UED does not explain stability of the weak scale against radiative corrections, there are several compelling reasons to consider such theories. In UED there is remnant of 5D translation invariance known as KK-parity which stabilizes the lightest KK-mode. Due to KK-parity tree-level electroweak precision corrections will be absent (at least from the lightest states), and so these particles can be quite a bit lighter than the TeV scale. The stability of the lightest KK mode (LKP) also results in a realistic dark matter candidate [106, 107]. What makes the theory particularly interesting however is that the UED particle spec-

trum and collider phenomenology may be very similar to that of a generic SUSY theory, and thus UED is a good "straw-man" to pit against supersymmetry [22]. As in SUSY, the collider signatures consist of decay chains that contain high p_T jets in association with large amounts of missing energy. As such, the models may be difficult to differentiate without resorting to observables that are sensitive to spin correlations [23, 69, 70, 84, 108, 108], although techniques are being developed which may be able to discriminate models in early stages of LHC running [109, 110].

In our study of this $U(1)_{\mathrm{PQ}}$ extension of UED (PQ-UED), we find that anomalies can mediate decays of the KK-odd partners of the hypercharge gauge boson which is often the lightest KK-odd particle (LKP), to SM photons and Z's in association with a new KK-odd scalar field that lives in the 5-component of an extra-dimensional gauge field. This B_5 is both stable and neutral, and thus presents as missing energy at colliders. The signal event topologies at a hadron collider generically contain high p_T jets and a pair of neutral SM gauge bosons (either photon or Z). Final state leptons may also make up a portion of the event topology, depending on the spectrum of KK-modes. Such events are also characteristic of gauge mediated SUSY breaking [24, 111–116], where a bino NLSP decays through a Goldstino coupling to the gravitino plus either a photon or Z. We thus overturn the lore that such signatures are a "smoking gun" for supersymmetry.

This chapter is organized as follows. In Section 2, we describe the basic setup of the PQ-UED model. In Section 4.4, we describe in detail the physics underlying anomalies which persist in the 4D effective theory. In particular, we discuss a gauged $U(1)_{\mathrm{PQ}}$ symmetry which is broken by boundary conditions on an S_1/Z_2

orbifold. In Section 4.4.1, we discuss gauge fixing and the residual gauge trans-
formations, showing that a massless Goldstone boson results from this choice
of boundary conditions. In 4.4.2, we discuss the tree-level interactions of the
Goldstone boson. In 4.4.3, we analyze the physics of additional spontaneous
and explicit breaking of the $U(1)_{\mathrm{PQ}}$ symmetry, identifying the spectrum and
the wave functions of the physical scalar modes. In 4.4.4, we discuss quantum
mechanical violation of the $U(1)_{\mathrm{PQ}}$ symmetry, and the interactions of the Gold-
stone modes that are generated by the anomalies. In Section 4.5, we study the
phenomenology of this scenario including collider physics, discussions about
dark matter, and the existing constraints on the model (which turn out not to be
stringent in the parameter space that is most interesting from the perspective of
collider physics).

4.3   Basic Setup

The model is in 5D Minkowski space, with the flat distance element:

$$ds^2 = \eta_{\mu\nu}dx^\mu dx^\nu - dz^2, \tag{4.3.1}$$

where $\eta_{\mu\nu}$ is the metric for 4D Minkowski space. The extra dimensional coor-
dinate z is compactified on an S_1/Z_2 orbifold, and the z-coordinate is taken to
range from $z = [0, L]$. All SM fields are taken to propagate in the bulk, and the
Lagrangian is constructed to obey a discrete Z_2 symmetry known as KK-parity,
a remnant of full 5D translation invariance which is broken by the presence of
the branes at $z = 0, L$ [79]. At the Lagrangian level, KK-parity forbids bulk Dirac
masses for the fermions, requires that brane localized interactions be identical
on the branes at $z = 0, L$, and constrains boundary conditions for bulk fields

to be the same on each brane. Orbifold boundary conditions for the fermions and gauge fields are chosen such that the fermion and gauge boson zero mode spectrum reproduces that of the Standard Model. The bulk Higgs sector then gives masses to these modes in the usual way.

In our setup, we slightly extend UED to incorporate a new bulk gauge symmetry. This gauge symmetry is chosen to be chiral in the zero mode spectrum, with the charges matching those of a Peccei-Quinn global symmetry [101] in Weinberg-Wilczek and DFSZ type axion models [117–120]. In order to do this consistently we must also have up and down-type Higgs doublets, since the SM with one Higgs does not have any such symmetry, even at the global level. In Table 4.3.2, we list the charges of the SM fields under hypercharge and the new gauged PQ symmetry.

$$
\begin{array}{c|c|c|c|c|c|c|c}
 & H_u & H_d & Q & \bar{u} & \bar{d} & L & \bar{e} \\
\hline
Y & 1/2 & -1/2 & 1/6 & -2/3 & 1/3 & -1/2 & 1 \\
\hline
PQ & 1 & 1 & -1/2 & -1/2 & -1/2 & -1/2 & -1/2
\end{array}
\tag{4.3.2}
$$

Note that a bulk μ term, $\mu H_u^T(i\tau_2)H_d$, is forbidden with these charge assignments. On the boundaries, we fix the 4D components of the PQ gauge field, B_M to zero: $B_\mu|_{z=0,L} = 0$. In the absence of other symmetry breaking effects, this leads to a single physical zero mode for the 5-component of the gauge field, B_5 [121, 122]. As is normally the case, the remaining KK tower of B_5 modes can be gauged out of the spectrum as they are Goldstone bosons eaten by the KK tower of massive B_μ fields. We discuss this in further detail in Sections 4.4.1 and 4.4.3, where we also take into account bulk breaking of the gauge symmetry due to the Higgs vacuum expectation values. Additional explicit breaking of the $U(1)_{\mathrm{PQ}}$ symmetry is added in the form of brane localized μ-terms. This is done in order to lift a potential electroweak-scale axion which is ruled out by

experiment [123].

In this theory, all gauge anomalies (cubic anomalies for gauge fields with zero modes) vanish as required for consistency. However global anomalies (e.g. PQ anomalies quadratic in the SM gauge fields) localized on the branes at $z = 0, L$ persist in the theory [61]. These anomalies lead to couplings of the B_5 scalar zero mode to the 5D field strengths and their duals, $G\tilde{G}$, $W\tilde{W}$ and $F\tilde{F}$. These couplings allow a decay of the lightest KK-mode in UED, which is often the first KK mode of the hypercharge gauge boson, down to a photon (or Z), and a PQ B_5 field. This is surprising at first glance, since the B_5 has a flat profile, and is thus naively even under KK-parity. However, we show in Section 4.4.2 that the zero mode B_5 is in fact a KK-odd field in all of its interactions at both the classical and quantum levels.

4.4 The Gauged Peccei-Quinn Symmetry

In this section, we illustrate the physics underlying a gauge symmetry which is broken by boundary conditions at both branes in an extra dimension constructed on an S_1/Z_2 orbifold. First we perform gauge fixing, identifying the residual gauge symmetries. Then we study the interactions of the lowest lying mode, a scalar field arising from the 5-component of the gauge field, and look at the implications of additional spontaneous breaking of the gauge symmetry via a Higgs mechanism. We end with an analysis of anomalies of this symmetry and the interactions they imply.

4.4.1 Residual Gauge Transformations

As described in the previous section, we gauge a $U(1)_{\text{PQ}}$ symmetry in the bulk, and break this symmetry via boundary conditions on the branes at $z = 0$ and $z = L$. In this section, we analyze this theory, identifying the residual gauge symmetry after imposing the boundary conditions on the branes, and adding gauge fixing terms in the bulk which decouple the unphysical modes.

Requiring preservation of the boundary conditions by the gauge transformations, $B_M \to B_M + \partial_M \beta(x, z)$, gives:

$$B_\mu|_{z=0,L} = 0 \quad \implies \quad \partial_\mu \beta(x, z)|_{z=0,L} = 0. \tag{4.4.3}$$

This condition requires that the gauge transformation on the branes is a constant function of the 4D coordinates, or is a global symmetry from the perspective of the 4D theory at $z = 0, L$.

We now turn to gauge fixing the $U(1)_{\text{PQ}}$ in the bulk. The 5D Lagrangian for a free $U(1)$ gauge field is given by:

$$
\begin{aligned}
\mathcal{L}_{U(1)_{\text{PQ}}} &= -\frac{1}{4g_{\text{PQ}}^2} \int dz\, B_{MN} B^{MN} \\
&= -\frac{1}{4g_{\text{PQ}}^2} \int dz\, \left[B_{\mu\nu} B^{\mu\nu} - 2(\partial_5 B_\mu)^2 - 2(\partial_\mu B_5)^2 + 4(\partial_5 B^\mu)(\partial_\mu B_5) \right] \\
&= -\frac{1}{4g_{\text{PQ}}^2} \int dz\, \left[B_{\mu\nu} B^{\mu\nu} - 2(\partial_5 B_\mu)^2 - 2(\partial_\mu B_5)^2 + 4(\partial_\mu B^\mu)(\partial_5 B_5) \right] \\
&\qquad\qquad\qquad\qquad\qquad - \frac{1}{g_{\text{PQ}}^2} B^\mu \partial_\mu B_5 \Big|_0^L ,
\end{aligned}
\tag{4.4.4}
$$

where we have rearranged the interaction that mixes B_μ and B_5 through integration by parts in the last step. Note that the boundary localized term vanishes

93

for the boundary conditions that we have chosen, $B_\mu|_{L,0} = 0$, so there is no brane localized mixing between B_5 and B_μ.

As we gauge fix, it is convenient to remove the terms that mix B_5 and B_μ in the bulk. This is achieved by adding a gauge fixing term to the Lagrangian given by [124, 125]:

$$\mathcal{L}_{\text{GF}} = -\frac{1}{2} \int dz G^2 \equiv -\frac{1}{2g_{\text{PQ}}^2 \xi_B} \int dz \left[\partial_\mu B^\mu - \xi_B \partial_5 B_5\right]^2 . \tag{4.4.5}$$

Note that there is a residual gauge symmetry where the gauge transformation parameter obeys the following equation:

$$\partial_\mu \partial^\mu \beta(x, y) - \xi_B \partial_5^2 \beta(x, y) = 0. \tag{4.4.6}$$

We choose to go to unitary gauge, $\xi_B \to \infty$ where the eaten B_5 modes are projected out of the spectrum. In this limit, the solutions are:

$$\beta(x, z) = \beta^+(x) + \left(\frac{2z - L}{2L}\right)\beta^-(x) \implies \beta_{\text{res}}(x, z) = \beta^+ + \beta^- \left(\frac{2z - L}{2L}\right), \tag{4.4.7}$$

where we have imposed the boundary conditions in Eq. (4.4.3) for the gauge transformation in the second step.

Under this residual transformation, the PQ gauge fields transform as:

$$\begin{aligned} B_\mu &\to B_\mu \\ B_5 &\to B_5 + \frac{\beta^-}{L}. \end{aligned} \tag{4.4.8}$$

Thus the remaining physical B_5 zero mode behaves as a Goldstone boson, undergoing a constant shift under the KK-odd part of the residual gauge transformation. This implies that the choice of these boundary conditions is equivalent to having spontaneously broken a global symmetry. As we will show explicitly in Section 4.4.4, the effective scale of this symmetry breaking is given by

$f_{\rm PQ} = (g_{5D}^{\rm PQ}\sqrt{L})^{-1}$. For the remainder of our analysis, we replace the gauge coupling with this effective breaking scale using this relation.

Note that the constant transformations β^+ correspond to a true (unbroken) PQ global symmetry in terms of the transformation properties of the light SM fields. This residual transformation is unbroken at this stage, and thus the B_5 cannot play the role of a usual axion in resolving the strong CP problem (the B_5 is not a traditional PQ axion).

Before discussing the interactions of the light B_5, it is useful to understand this pattern of symmetry breaking in the language of deconstruction [104, 105]. This model can be deconstructed as a chain of $U(1)$ symmetries linked by scalar fields which each transform under two neighboring $U(1)$ sites. To mimic the choice of boundary conditions we have chosen, we only gauge the internal sites, and the endpoints of the chain are taken to be global symmetries. In total, we have N sites, and $N-2$ of the sites are gauged. There are $N-1$ scalar fields breaking this set of symmetries, so there remains one unbroken $U(1)$ symmetry, corresponding to β^+ in the continuum theory. There are $N-1$ Goldstone bosons, and $N-2$ are eaten since $N-2$ of the sites were gauged. The remaining physical Goldstone mode corresponds to a non-trivial linear combination of $U(1)$'s and becomes a Wilson line for B_5 in the continuum limit.

4.4.2   Tree level interactions of the B_5 zero mode

In this section, we study the interactions of the PQ B_5 with the KK-modes and SM fields. In doing so we dispel the notion that the KK-parity transformation properties of a KK mode are determined solely by the transformation properties

of the wave function.

This can be seen in a simple way. First we note that 5D gauge invariance associates every ∂_5 with a B_5 and vice versa through the covariant derivative:

$$D_5 = \partial_5 - iqB_5. \tag{4.4.9}$$

The form of the 5D flat space metric requires that any index must be repeated an even number of times in any single term in the Lagrangian.* This is because everything must be contracted through the metric tensor (or through the vielbeins). This means that for interactions with an odd number of B_5's, there must be an odd number of ∂_5's (or a $\gamma^5 \equiv e_a^5 \gamma^a$). Since both of these pick up a sign under the transformation $z \to L - z$, the parity transform of the tower of B_5's is effectively the opposite of how the wavefunctions transform. In short, the internal KK parity of the 4D B_5 zero mode is $-$.

As a concrete example, we consider the tree level interactions with a 5D fermion. The interactions arise from the 5D gauge covariant kinetic term:

$$\mathcal{L}_{\text{eff}} = \int dz \, \bar{\Psi} i D_M e_a^M \gamma^a \Psi \supset q \int dz \, \bar{\Psi} B_5 e_a^5 \gamma^a \Psi \tag{4.4.10}$$

The 5D Dirac fermion can be expanded in solutions of the 4D Dirac equation with masses m_n:

$$\Psi = \sum_n \begin{pmatrix} g_n(z) \chi_n(x) \\ f_n(z) \bar{\psi}_n(x) \end{pmatrix} \tag{4.4.11}$$

The boundary conditions that produce a χ_0 massless mode are $f_n(z = 0, L) = 0$. Choosing these boundary conditions, the solutions for f_n and g_n are given by:

$$g_n = A_n \cos \frac{n\pi z}{L}$$
$$f_n = -A_n \sin \frac{n\pi z}{L} \tag{4.4.12}$$

---

*Except in the case of contraction through the 5D Levi-Civita tensor, however such terms explicitly violate KK parity as they correspond to a net $U(1)_{\text{PQ}}$ flux along the extra dimensional coordinate.

with $A_0 = 1/\sqrt{L}$, and $A_n = \sqrt{2/L}$ for $n \neq 0$. This choice reproduces canonically normalized fields in the 4D effective theory.

We now expand Eq. (4.4.10) in KK modes and integrate over z, finding

$$\mathcal{L}_{\text{eff}} = -\frac{1}{f_{\text{PQ}}L} q \sum_{m,n} c_{nm} B_5(x) \left[\psi_n \chi_m - \bar{\chi}_m \bar{\psi}_n \right]$$

$$c_{nm} = \begin{cases} \frac{4}{\pi} \frac{n}{m^2 - n^2} & m + n \text{ odd}, m \neq 0 \\ \frac{2\sqrt{2}}{\pi n} & m + n \text{ odd}, m = 0 \\ 0 & m + n \text{ even} \end{cases} \quad . \tag{4.4.13}$$

The B_5 is thus a KK-odd field in its interactions with fermions. The tree-level interactions with scalars are simpler to calculate, and the result is similar. At tree level, the massless B_5 is KK-odd in all of its interactions.

4.4.3 Spontaneous Breaking in the Bulk

When the SM Higgs fields obtain vacuum expectation values, the $U(1)_{\text{PQ}}$ symmetry undergoes additional spontaneous breaking in the bulk. We show that, in the absence of additional explicit breaking, the Higgsing along with the choice of boundary conditions produces two massless modes. One of these is a KK-even would-be electroweak scale axion that must be lifted, as such a scalar has interactions that are too strong to remain consistent with bounds from nuclear and astro-particle physics [123]. The other is the KK-odd zero mode whose phenomenology we are most interested in. Both modes will now be partly contained in B_5 and in the Goldstone field π in the bulk Higgs. In this subsection we first identify these two modes, and then show that an explicit symmetry breaking term (which is allowed on the boundaries) will give a mass to both

of these states. First we use a simplified version with a single bulk Higgs, and then show that it is easy to find the full answer for the two Higgs doublet case relevant for the bulk $U(1)_{PQ}$ model.

The two Goldstone zero modes

The Lagrangian, before gauge fixing, in our toy model is given by

$$\mathcal{L} = \int dz \left[\frac{1}{L}|D_M H|^2 - V(H) - \frac{f_{\mathrm{PQ}}^2 L}{4} B_{MN} B^{MN} \right] - V_{\mathrm{bound}}(H_{|0}) - V_{\mathrm{bound}}(H_{|L}).$$
(4.4.14)

With the assumption that there are no brane localized scalar potential terms, the Higgs develops a z-independent vev profile. For now, we assume that this is the case, and add brane localized interactions later, treating them perturbatively in the low-energy 4D effective theory.

First, as in Section 4.4.1, we identify the interactions which kinetically mix the gauge bosons with the Goldstone bosons, so that we can remove them with a suitable gauge fixing term. Taking $H \equiv \frac{v}{\sqrt{2}} e^{i\pi/v}$, keeping only the Goldstone fluctuations π, we have:

$$\mathcal{L}_{\mathrm{mix}} = -f_{\mathrm{PQ}}^2 L (\partial_5 B^\mu)(\partial_\mu B_5) - \frac{1}{L} v \partial_\mu \pi B^\mu$$
(4.4.15)

A gauge fixing term that removes the 4D kinetic mixing is:

$$\mathcal{L}_{\mathrm{GF}} = -\frac{1}{2} G^2 = -\frac{f_{\mathrm{PQ}}^2 L}{2\xi} \left[\partial_\mu B^\mu - \xi \left(\partial_5 B_5 - \frac{1}{f_{\mathrm{PQ}}^2 L^2} v\pi \right) \right]^2.$$
(4.4.16)

The residual gauge symmetry obeys the following boundary conditions:

$$\partial_\mu \partial^\mu \beta - \xi \left(\partial_5^2 \beta - \frac{v^2}{f_{\mathrm{PQ}}^2 L^2} \beta \right) = 0$$
(4.4.17)

In the $\xi \to \infty$ limit, with constant v, the solutions to the equation with appropriate boundary conditions are:

$$\beta(x, y) = \beta^+ \cosh(\kappa(z - L/2)) + \beta^- \sinh(\kappa(z - L/2)), \qquad (4.4.18)$$

where we have introduced an expansion parameter $\kappa \equiv v/(f_{\mathrm{PQ}}L)$. We can find the Goldstone-like zero modes which are shifting under β by carefully analyzing the bulk EOM's and the BC's, which is performed in detail in Appendix B.1. The resulting zero modes can be written in terms of KK even and odd combinations. In the case where the B_5 part has a KK-even wave-function (but remembering that the interactions are KK-odd) the B_5 and π zero modes given by

$$
\begin{aligned}
B_5^{(0)\mathrm{odd}} &= A_B' \cosh \kappa(z - L/2)\zeta_-(x) \\
\pi^{(0)\mathrm{odd}} &= A_B' \frac{v}{\kappa} \sinh \kappa(z - L/2)\zeta_-(x)
\end{aligned}
\qquad (4.4.19)
$$

The subtlety about the KK-parity quantum numbers of the B_5 plays out here, as a single zero mode KK-eigenstate has simultaneous KK-even and KK-odd wavefunctions (although the interactions are all consistent, as they must be).

The KK-even modes are given by:

$$
\begin{aligned}
B_5^{(0)\mathrm{even}} &= B_B' \sinh \kappa(z - L/2)\zeta_+(x) \\
\pi^{(0)\mathrm{even}} &= B_B' \frac{v}{\kappa} \cosh \kappa(z - L/2)\zeta_+(x)
\end{aligned}
\qquad (4.4.20)
$$

Imposing canonical normalization for the 4D fields then fixes the overall coefficients A_B' and B_B'. Note that the residual symmetries in Eq. (4.4.18) are consistent with the profiles of these zero modes: the residual gauge transformations are shift symmetries for the 4D massless modes, ζ_- and ζ_+.

Explicit brane localized $U(1)_{\text{PQ}}$ breaking

We now analyze what happens when we add explicit symmetry breaking on the boundaries. We add PQ breaking μ terms of the form $V_{\text{bound}} = -\frac{\mu}{2}(H^2 + H^{*2})$ on each boundary. This is allowed, since the symmetry is only global on the endpoints. Expanding in the Goldstone fluctuations, this leads to brane localized mass terms for the 5D field π:

$$V_{\text{bound}}\Big|_{z=0,L} = \mu\pi^2\Big|_{z=0,L}. \tag{4.4.21}$$

Keeping track of only the (now approximate) zero modes, this becomes:

$$V_{\text{bound}}\Big|_{0,L} = \mu\left[A'_B\frac{v}{\kappa}\sinh\kappa(z-L/2)\zeta_-(x) + B'_B\frac{v}{\kappa}\cosh\kappa(z-L/2)\zeta_+(x)\right]^2\Big|_{0,L}. \tag{4.4.22}$$

The effective 4D potential is obtained by summing over the two boundary contributions, which gives:

$$V_{\text{eff}} = 2\mu A'^2_B\left(\frac{v}{\kappa}\right)^2\sinh^2\frac{\kappa L}{2}\zeta_-^2(x) + 2\mu B'^2_B\left(\frac{v}{\kappa}\right)^2\cosh^2\frac{\kappa L}{2}\zeta_+^2(x) \tag{4.4.23}$$

Expanding in small κ and imposing canonical normalization on the scalar zero modes in the 4D effective theory takes this to:

$$V_{\text{eff}} = 2\mu\zeta_+^2 + \frac{1}{2}\frac{\mu v^2}{f_{\text{PQ}}^2}\zeta_-^2 \tag{4.4.24}$$

The masses of the KK-even and KK-odd modes are then $m_+^2 = 4\mu$, and $m_-^2 = \mu v^2/f_{\text{PQ}}^2$. A full numerical evaluation of the equations of motion, including deformation of the VEV due to the μ-terms, confirms that these approximations hold at the level of 2% for the KK-odd mode, and $< 1\%$ for the KK-even mode for μ as large as $(300\text{ GeV})^2$.

Pseudo-Goldstones in the full 2-Higgs doublet model

The generalization of this model to the two Higgs doublet model (2HDM) of our construction is quite simple. We first write the two Higgs doublets keeping only the Goldstone fluctuations along the $U(1)_{\text{PQ}}$ flat direction, ignoring the 2 neutral Higgses, and the charged Higgs fields. The Goldstone fluctuation π is the neutral pseudoscalar often referred to as A_0 in 2HDMs.

$$H_u = \frac{v_u}{\sqrt{2}} e^{i\pi/V}, \quad H_d = \frac{v_d}{\sqrt{2}} e^{i\pi/V}, \quad \text{with } V \equiv \sqrt{v_u^2 + v_d^2} \tag{4.4.25}$$

In this case, the entire analysis above follows through the same way with the replacements

$$v \to V = \sqrt{v_u^2 + v_d^2}$$
$$\text{and } \mu \to \frac{\mu}{2} \sin 2\beta, \tag{4.4.26}$$

where the angle β is defined in the usual way for a 2HDM, $v_u/v_d \equiv \tan \beta$. The explicit symmetry breaking terms in this case are given by

$$\mathcal{L}_{\text{mix}} = \frac{\mu}{2} H_u^T (i\tau_2) H_d \Big|_{z=0,L} \tag{4.4.27}$$

The final masses are:

$$m_+^2 = 2\mu \sin 2\beta$$
$$m_-^2 = \frac{\mu V^2}{2 f_{\text{PQ}}^2} \sin 2\beta. \tag{4.4.28}$$

Taking $\mu_{\text{eff}} \equiv \frac{\mu \sin 2\beta}{2}$, the numerical expression for the mass of the light pseudo-Goldstone boson is:

$$
\begin{aligned}
m_- &= (f_{\text{PQ}} L)^{-1} \left(\frac{\sqrt{\mu_{\text{eff}}}}{300 \text{ GeV}} \right) (L \cdot 10^3 \text{ GeV}) \cdot 74 \text{ GeV} \\
&= \left(\frac{\sqrt{\mu_{\text{eff}}}}{300 \text{ GeV}} \right) \left(\frac{10^9 \text{ GeV}}{f_{\text{PQ}}} \right) \cdot 74 \text{ keV}.
\end{aligned}
\tag{4.4.29}
$$

For perturbative values of the coupling $(f_{\mathrm{PQ}}L)^{-1}$, and for weak scale μ, the mass of ζ_- is less than the mass of any level one KK-mode, whose masses are generally $m^{(1)} \sim \pi/L$. So for most choices of parameters, this pseudo-Goldstone is the LKP. The reference value of 10^9 GeV in the second expression is chosen to match the point at which the decay length of the NLKP is of order tens of centimeters, as we show in Section 4.5.

4.4.4 $U(1)_{\mathrm{PQ}}$ Anomalies

With the fermion charges given in Table 4.3.2, the $U(1)_{\mathrm{PQ}}$ symmetry is anomalous. However, as we have shown in Section 4.4.1, the residual symmetry after imposing Dirichlet boundary conditions on the 4D components of the PQ gauge field is global on the endpoints of the extra dimension. In this section we calculate the chiral anomalies in this model, emphasizing that the chiral anomalies are localized on the branes [61], where the gauge transformation is global rather than local. As a result, the theory is consistent at the quantum level. However, as is crucial in our model, the anomalies imply effective interactions between the $U(1)_{\mathrm{PQ}}$ B_5 and the SM gauge fields. We focus on anomalies of the form $U(1)_{\mathrm{PQ}} \times \mathrm{SM} \times \mathrm{SM}$, since these lead to the interactions we are most interested in.

An intuitive argument for the localized anomaly terms

First we present an intuitive argument that suggests the required form of the localized anomaly terms based on the shift properties of the action and the Goldstone bosons under the anomalous symmetries. Later we will give a more rig-

orous derivation based on the anomalous transformations of the path integral measure.

Under an anomalous $U(1)_{\mathrm{PQ}}$ transformation $B_M \to B_M + \partial_M \beta(x, z)$, the action shifts by:

$$\delta \mathcal{S} = \int d^4x \int_0^L dz\, \beta \partial_M J^M - \int d^4x\, \beta J^5\big|_0^L \equiv \int d^5x\, \beta \mathcal{A}, \qquad (4.4.30)$$

here J^M is the classically conserved PQ current, and $\mathcal{A}$ is the anomalous divergence. The boundary term vanishes by construction, through the assignment of the orbifold boundary conditions which produce the chiral spectrum in Table 4.3.2. The anomaly is itself purely localized on the branes, and has been calculated in [61] to be:

$$\mathcal{A}(x, z) = \tfrac{1}{2}\left[\delta(z) + \delta(z - L)\right] \sum_f q^f_{\mathrm{PQ}} \left(\tfrac{q^{f2}_Y}{16\pi^2} F \cdot \tilde{F} + \tfrac{\mathrm{Tr}\, \tau^f_a \tau^f_a}{16\pi^2} W \cdot \tilde{W} + \tfrac{\mathrm{Tr}\, t^f_a t^f_a}{16\pi^2} G \cdot \tilde{G} \right)$$

$$\equiv \tfrac{1}{2}\left[\delta(z) + \delta(z - L)\right] \mathcal{Q}_{\mathrm{PQ}}(x, z) \qquad (4.4.31)$$

where F, W, and G are the hypercharge, $SU(2)_L$, and QCD field strengths, and $F \cdot \tilde{F}$ is given by $\tfrac{1}{2}\epsilon^{\mu\nu\rho\sigma} F_{\mu\nu}(x, z) F_{\rho\sigma}(x, z)$ (with similar expressions for $W \cdot \tilde{W}$ and $G \cdot \tilde{G}$).

To reproduce the above shift in the action, the Lagrangian has to contain a coupling involving the Goldstone bosons, whose shifts will exactly correspond to the above change in the action. Remembering that the decomposition of β is

$$\beta = \beta^+ \cosh[\kappa(z - \tfrac{L}{2})] + \beta^- \sinh[\kappa(z - \tfrac{L}{2})] \qquad (4.4.32)$$

and the fact that under this shift $B_5 \to B_5 + \partial_5 \beta$, we can identify the shifts of the fields $\zeta_\pm$. We find, that

$$\zeta_\pm \to \zeta_\pm + v\sqrt{\frac{\sinh \kappa L}{\kappa L}}\, \beta^\pm. \qquad (4.4.33)$$

Therefore the shift in the action is reproduced if the following couplings are added to the Lagrangian:

$$\mathcal{L}^{\text{eff}}_{\text{anomaly}} = \frac{1}{2v} \zeta_- \sqrt{\frac{\kappa L}{\sinh \kappa L}} \sinh \frac{\kappa L}{2} \left[\mathcal{Q}_{\text{PQ}}(x, L) - \mathcal{Q}_{\text{PQ}}(x, 0) \right]$$
$$+ \frac{1}{2v} \zeta_+ \sqrt{\frac{\kappa L}{\sinh \kappa L}} \cosh \frac{\kappa L}{2} \left[\mathcal{Q}_{\text{PQ}}(x, L) + \mathcal{Q}_{\text{PQ}}(x, 0) \right].$$

$$(4.4.34)$$

To lowest order in the bulk PQ gauge coupling, this becomes:

$$\mathcal{L}^{\text{eff}}_{\text{anomaly}} = \frac{1}{4 f_{\text{PQ}}} \zeta_- \left(\mathcal{Q}_{\text{PQ}}(x, L) - \mathcal{Q}_{\text{PQ}}(x, 0) \right) + \frac{1}{2v} \zeta_+ \left(\mathcal{Q}_{\text{PQ}}(x, L) + \mathcal{Q}_{\text{PQ}}(x, 0) \right).$$

$$(4.4.35)$$

Anomalous interactions from the path integral measure

Above we have seen a simple argument for the existence of the brane localized anomalous interactions, motivated by the shifts of the various Goldstone fields. We now present the full derivation of these terms through the shift in the path integral measure as first identified by Fujikawa [91, 92]. For this we add two fermions to the single Higgs toy model described by the effective Lagrangian in Eq. 4.4.14. These fermions have $(\pm, \pm)$ and $(\mp, \mp)$ boundary conditions respectively, such that one fermion has a left handed zero mode, and the other has a right handed zero mode. Additionally, they each carry opposite charge under the $U(1)_{\text{PQ}}$ symmetry, $q_{L,R} = \pm 1/2$. The additional terms in the classical effective Lagrangian are:

$$\mathcal{L}^{\text{fermion}}_{\text{eff}} = \int dz \left\{ \bar{\Psi}_{L5} i \slashed{D} \Psi_{L5} + \bar{\Psi}_{R5} i \slashed{D} \Psi_{R5} + \left(\lambda H \bar{\Psi}_{L5} \Psi_{R5} + \text{h.c.} \right) \right\}. \quad (4.4.36)$$

We now restrict ourselves to the terms in this Lagrangian that involve the Goldstone bosons π and B_5:

$$\mathcal{L}_{\text{eff}}^{\text{fermion}} \supset \int dz \Big\{ \bar{\Psi}_{L5} i \left(\partial_5 - i q_L B_5 \right) \gamma^5 \Psi_{L5} + \bar{\Psi}_{R5} i \left(\partial_5 - i q_R B_5 \right) \gamma^5 \Psi_{R5}$$
$$+ \left(\frac{\lambda v}{\sqrt{2}} e^{i(q_L - q_R)\frac{\pi}{v}} \bar{\Psi}_{L5} \Psi_{R5} + \text{h.c.} \right) \Big\}. \tag{4.4.37}$$

We now perform a redefinition of the fermion fields such that the new fermion degrees of freedom do not transform under the broken $U(1)_{\text{PQ}}$ symmetry. After this is done, the path integral measure itself no longer transforms under rotations, and all interactions of the Goldstone bosons through the anomaly are manifest. The redefinition is given by:

$$\Psi_j = e^{i q_j f(\pi, B_5)} \Psi'_j, \tag{4.4.38}$$

with f transforming as $f \to f + \beta(x, z)$, and $\Psi'_j \to \Psi'_j$. The most general choice of f that satisfies this property is a linear combination of a Wilson line and the 5D field π from the bulk Higgs:

$$f(\pi, B_5) = a \left[\int_{z_0}^z dz' B_5(x, z') + \frac{\pi(z_0, x)}{v(z_0)} \right] + (1 - a) \frac{\pi(z, x)}{v(z)}, \tag{4.4.39}$$

where a is an arbitrary c-number.

In terms of the two physical Goldstone modes, ζ_+ and ζ_-, the function $f(\pi, B_5)$ is given by:

$$f(\pi, B_5) = \frac{1}{v} \sqrt{\frac{\kappa L}{\sinh \kappa L}} \left[\sinh \kappa (z - L/2) \zeta_-(x) + \cosh \kappa (z - L/2) \zeta_+(x) \right] \tag{4.4.40}$$

It is reassuring that this result is completely independent of the two undetermined parameters z_0 and a. These parameters are thus unphysical, and do not affect any interactions after performing the redefinition.

The redefinition does, however, reorganize other interactions in the theory. The 5D fermion kinetic terms are modified in the following way at the classical

level:

$$\bar{\Psi}_j i \slashed{D} \Psi_j = \bar{\Psi}'_j i D_\mu \gamma^\mu \Psi'_j - q_j \left(\partial_\mu f(\pi, B_5) \right) \bar{\Psi}'_j \gamma^\mu \Psi'_j + \bar{\Psi}'_j i \partial_5 \gamma^5 \Psi'_j$$

$$- q_j \left(\partial_5 f(\pi, B_5) - B_5 \right) \bar{\Psi}'_j i \gamma^5 \Psi'_j. \tag{4.4.41}$$

Note that this expression is completely gauge invariant under $U(1)_{\mathrm{PQ}}$. In addition, the Goldstone interactions from the Yukawa term in the Lagrangian become:

$$\frac{\lambda v}{\sqrt{2}} \exp \left[i \left(q_L - q_R \right) \left(\frac{\pi(z, x)}{v(z)} - f(\pi, B_5) \right) \right] \bar{\Psi}'_{L5} \Psi'_{R5} \tag{4.4.42}$$

The argument of this exponential and the coefficient of the 5D pseudoscalar current in Eq. (4.4.41) are both invariant under all $U(1)_{\mathrm{PQ}}$ gauge transformations, and thus these expressions do not involve either of the physical Goldstone bosons. This can be verified using the wave functions derived in the previous section.

It is instructive to compute the effective 4D currents corresponding to the broken symmetries associated with the KK-even and KK-odd pseudo-Goldstone bosons. At lowest order in the 5D PQ gauge coupling, the ζ_+ couples diagonally due to wave function orthogonality, and the current corresponding to this symmetry is

$$j_+^\mu = \sum_{j,n} q_j \bar{\Psi}_{j,n}^{4D} \gamma^\mu \Psi_{j,n}^{4D}, \quad \Psi_{j,n \neq 0}^{4D} = \begin{pmatrix} \chi_{j,n}(x) \\ \bar{\psi}_{j,n}(x) \end{pmatrix}, \quad \Psi_{j,0}^{4D} = P_j \begin{pmatrix} \chi_{j,0}(x) \\ \bar{\psi}_{j,0}(x) \end{pmatrix}$$

$$\tag{4.4.43}$$

which can be determined by reading off the coupling of the ζ_+ in the 4D effective theory (arising from the second term in 4.4.41):

$$\mathcal{L}_+ = -\frac{1}{v} \left(\partial_\mu \zeta_+(x) \right) j_+^\mu, \tag{4.4.44}$$

where j labels the species of fermion, and n labels the KK-level. The projector, P_j is either P_+, or P_-, depending on whether Ψ_j contains a right- or left-handed

zero mode. With the charge assignments we have chosen, from the perspective of the zero modes, this is an axial-vector current. The KK-odd current is more involved:

$$j_-^\mu = \sum_{m,n,j} q_j c_{mn} \bar{\Psi}_{j,m}^{4D} \gamma^\mu \left[(m-n)^{-2} + (m+n)^{-2} \gamma^5 \right] \Psi_{j,n}^{4D}.$$

$$c_{mn} \equiv \begin{cases} 0 & m+n \text{ even} \\ 2/\pi^2 & m+n \text{ odd}, m, n \neq 0 \\ \sqrt{2}/\pi^2 & m+n \text{ odd}, m \cdot n = 0 \end{cases} \tag{4.4.45}$$

where the coupling is

$$\mathcal{L}_- = -\frac{1}{f_{\mathrm{PQ}}} \left(\partial_\mu \zeta_-(x) \right) j_-^\mu. \tag{4.4.46}$$

Note that we have finally explicitly identified the effective symmetry breaking scale associated with the B_5 Goldstone boson, justifying our identification $g_{5D}\sqrt{L} \equiv f_{\mathrm{PQ}}^{-1}$.

Due to the anomaly, the redefinition (4.4.38) produces a non-trivial Jacobian in the path integral measure [91,92]. The couplings of the Goldstone bosons due to the anomaly can then be found by expanding

$$\mathcal{L}_{\mathrm{anomaly}}^{\mathrm{eff}} = \int dz f(\pi, B_5) \mathcal{A} \tag{4.4.47}$$

in terms of the scalar zero modes. Using again the expression of the anomaly from [61] in (4.4.31) we reproduce the expressions (4.4.34)-(4.4.35) for the brane localized anomalous couplings of the Goldstone bosons.

The interactions of ζ_-

We now turn our focus to the interactions of the KK-odd Goldstone, ζ_-, in the effective action Eq. 4.4.35. Using the KK decomposition of the 5D hypercharge

gauge boson (in the absence of electroweak symmetry breaking), we get

$$F_{\mu\nu}(x,z) = g'_{5D}\sqrt{\frac{1}{L}}F^{(0)}_{\mu\nu}(x) + g'_{5D}\sum_{n\geq 1}\sqrt{\frac{2}{L}}\cos\left(\frac{n\pi z}{L}\right)F^{(n)}_{\mu\nu}(x),\qquad (4.4.48)$$

with similar expansions for the $SU(2)_L$ and $SU(3)_C$ field strengths. The normalization coefficients are chosen to produce a canonically normalized 4D effective theory. This yields

$$\begin{aligned}
\mathcal{L}^{\text{eff}}_{B_5AA} &= \frac{1}{16\pi^2}\frac{1}{f_{\text{PQ}}}\frac{g'^2_{5D}}{L}\zeta_-(x)\sum_{m\geq n\geq 0}c_{nm}F^{(n)}\cdot\tilde{F}^{(m)}\\
&= \frac{\alpha_1}{4\pi}\frac{1}{f_{\text{PQ}}}\zeta_-(x)\sum_{m\geq n\geq 0}c_{nm}F^{(n)}\cdot\tilde{F}^{(m)},
\end{aligned}\qquad (4.4.49)$$

where $\alpha_1 = \frac{g'^2}{4\pi}$, $g' = g'_{5D}/\sqrt{L}$ is the usual 4D effective hypercharge gauge coupling, $f_{\text{PQ}} \equiv 1/(g^{\text{PQ}}_{5D}\sqrt{L})$ is the effective PQ decay constant, and the coefficients c_{nm} are given by

$$c_{nm} = \begin{cases} 0 & n+m \text{ even}\\ 2\sum_f q^f_{\text{PQ}}q^{f2}_Y & n+m \text{ odd}, n,m\geq 1\\ \sqrt{2}\sum_f q^f_{\text{PQ}}q^{f2}_Y & n+m \text{ odd}, n\cdot m = 0. \end{cases}\qquad (4.4.50)$$

4.5 B_5 Phenomenology

In this section, we perform a study of the basic phenomenology of this new model. The collider signatures are quite dramatic: nearly all final state signal events contain high p_T photons or Z bosons along with large amounts of missing energy. Even more remarkable is that for some ranges of the extra dimensional $U(1)_{\text{PQ}}$ gauge coupling, the photons or Z's do not generally point back to the original interaction vertex (that is, the photons or Z's are "delayed"). Such signatures have long been considered a smoking gun for supersymmetry broken by low scale gauge mediation, and so our analysis suggests that more detailed

experimental analyses may be necessary to distinguish supersymmetry from this model. We calculate the lifetime of the lightest KK-mode and the displacement of the decay vertex from the interaction point. We assume here that the lightest KK-mode is the level-1 partner of the hypercharge gauge boson. We also consider the possibility that the ζ_- Goldstone boson may constitute a large fraction of the observed relic abundance of dark matter, calculating the relic abundance over a range of free parameters in the model.

4.5.1 Decays of the NLKP

We presume that the NLKP is the first KK-mode of the hypercharge gauge boson. This is often the case in UED, since mass splittings in the level 1 KK sector are achieved at the quantum level through brane localized kinetic terms. The small value of α_1 implies a smaller contribution to the mass of the level-1 hypercharge gauge boson.[†] Using the effective Lagrangian in Eq. (4.4.49), we evaluate the matrix element between the level one hypercharge gauge boson, the ζ_-, and a SM photon or Z. The final polarization averaged and summed amplitude squared for the decay of the level-1 KK-mode of the hypercharge gauge boson is given by:

$$\frac{1}{3}\sum_{\text{pol}}|i\mathcal{M}_{\gamma,Z}|^2 = \frac{8}{3}\lambda_{\gamma,Z}^2\left[\left(p^{(0)}\cdot p^{(1)}\right)^2 - p^{(0)2}p^{(1)2}\right] = \frac{2}{3}\lambda_{\gamma,z}^2 m^{(1)4}\left[1 - \left(\frac{m^{(0)}}{m^{(1)}}\right)^2\right]^2$$

(4.5.51)

[†]The level 1-KK mode of the PQ gauge boson may be lighter, however this mode is *even* under KK-parity, and additionally has a very small coupling to SM fields. This particle is thus rarely produced, and does not appear substantially in the decay products of the KK-modes of SM fields.

where $p^{(0)}$ is the momentum of the photon or Z, and $\lambda_{\gamma,Z}$ is given by

$$\lambda_{\gamma,Z} = \frac{\alpha_1}{4\pi}\frac{1}{f_{\mathrm{PQ}}}\sqrt{2}\sum_f q_{\mathrm{PQ}}^f q_Y^{f2} \cdot (c_w, s_w). \tag{4.5.52}$$

In the last step, we have evaluated the products of momenta in the rest frame of the decaying KK-mode, and we have neglected the mass of the B_5.

For $1/L \gg v$, we can ignore the mass of the Z boson, and the partial widths in this limit are given by:

$$\Gamma_{\gamma,Z} \approx \frac{\alpha^2}{192\pi^3 c_w^4 f_{\mathrm{PQ}}^2}m^{(1)3}\left(\sum_f q_{\mathrm{PQ}}^f q_Y^{f2}\right)^2 (c_w^2, s_w^2). \tag{4.5.53}$$

The sum over charges as can be read in Table 4.3.2 is $\sum_f q_{\mathrm{PQ}}^f q_Y^{f2} = -5$. We express the final width numerically for reference values of the free parameters as:

$$\Gamma_{\mathrm{tot}} \approx 4.3 \cdot 10^{-7}\ \mathrm{eV}\left(\frac{m^{(1)}}{10^3\ \mathrm{GeV}}\right)^3\left(\frac{10^9\ \mathrm{GeV}}{f_{\mathrm{PQ}}}\right)^2, \tag{4.5.54}$$

with branching fractions given by

$$R_\gamma \approx c_w^2 \qquad R_Z \approx s_w^2 \tag{4.5.55}$$

up to terms of order $m_Z^2/m^{(1)2}$. The total width corresponds to a lifetime for the NLKP equal to

$$\tau = 1.5 \cdot 10^{-9}\ \mathrm{s}\left(\frac{10^3\ \mathrm{GeV}}{m^{(1)}}\right)^3\left(\frac{f_{\mathrm{PQ}}}{10^9\ \mathrm{GeV}}\right)^2. \tag{4.5.56}$$

he NLKP is at the bottom of a decay chain of exotica produced at a collider experiment, and the NLKP may travel some measurable distance before decaying, producing a rather spectacular signature of high energy photons or Z's which decay to jets or leptons that do not point back to a central interaction vertex. The distance traveled by the NLKP is given by:

$$\Delta x = \gamma v\tau \approx 46\ \mathrm{cm}\left(\frac{10^3\ \mathrm{GeV}}{m^{(1)}}\right)^3\left(\frac{f_{\mathrm{PQ}}}{10^9\ \mathrm{GeV}}\right)^2\sqrt{\left(\frac{E}{m^{(1)}}\right)^2 - 1}. \tag{4.5.57}$$

Where γ is the relativistic time-dilation factor, and v is the velocity. The typical range for the energy E of the NLKP in a collider experiment is both model and analysis dependent. For larger mass splittings between the different members of the level-1 KK sector, E will typically be larger, as a greater portion of the parent exotica is converted to kinetic energy. Also the analyses performed at collider experiments require specific cuts on the sample. For example, an analysis may focus on a trigger sample in which events are required to contain large amounts of missing transverse energy. Such requirements again bias towards larger E for the NLKP, and thus longer decay lengths.

4.5.2 B_5 Dark Matter

In the scenario we study, the B_5 is most likely the LKP for all perturbative choices of the 5D PQ coupling, and is thus a dark matter candidate when KK-parity is preserved. In this section, we discuss the constraints on parameter space based on over-closure considerations, and the potential of the B_5 to make up a significant fraction of the dark matter relic abundance. We vary the scale f_{PQ} over a large range, from a standard $\mathcal{O}(1)$ weak coupling to a very high suppression. An excellent review that describes the analysis in these different cases can be found in [126].

The case with weak scale m_-

The gauge coupling may not be very small, in which case the decays will be prompt, and the ζ_- may be a more standard dark matter candidate, being in thermal equilibrium prior to decoupling. In this case, one can evaluate the an-

nihilation cross section, and follow the usual prescription to evaluate the relic abundance. The annihilation to SM particles primarily takes place via s-channel Higgs exchange. For our calculation, we assume large $\tan\beta = v_u/v_d$, and that the heavy neutral Higgs is much more massive that the light neutral Higgs: $m_{H_0} \gg m_{h_0}$.

The thermally averaged non-relativistic annihilation cross section to massive SM gauge fields is given in this limit by:

$$\langle \sigma v \rangle_{W^{\pm},Z} = \frac{2m_-^6}{\pi v_{\rm eff}^4} \frac{1}{(4m_-^2 - m_H^2)^2 + m_H^2 \Gamma_H^2} \left(1 - \frac{m_V^2}{m_-^2} + \frac{3m_V^4}{4m_-^4}\right) \sqrt{1 - \frac{m_V^2}{m_-^2}}, \quad (4.5.58)$$

where $v_{\rm eff} = 246$ GeV is the effective electroweak symmetry breaking scale and $m_V = m_{W,Z}$ is the mass of the massive SM gauge bosons into which the ζ_- annihilates. The annihilation cross section into fermions via the s-channel Higgs in the large $\tan\beta$ and $m_{H_0} \gg m_{h_0}$ limit is given by:

$$\langle \sigma v \rangle_{\bar{f}f} = \frac{m_-^4 m_f^2}{\pi v_{\rm eff}^4} \frac{1}{(4m_-^2 - m_H^2)^2 + m_H^2 \Gamma_H^2} \left(1 - \frac{m_f^2}{m_-^2}\right)^{3/2}. \quad (4.5.59)$$

The annihilation into vectors is rather efficient, even relatively far off of the light Higgs resonance. Thus the preferred band in which the ζ_- relic abundance saturates the WMAP bound in this mass range is close to the threshold for annihilation into W bosons. For the annihilation into light fermions, the cross section is suppressed by the fermion mass, and the WMAP window is saturated on the tails of the Higgs resonance.

There are additional channels where the ζ_- annihilates to photons or gluons, however these are essentially two loop diagrams, since each vertex arises through the anomaly. These annihilation channels can thus be ignored. The results for the relic abundance calculation are shown in Figure 4.1. We plot con-
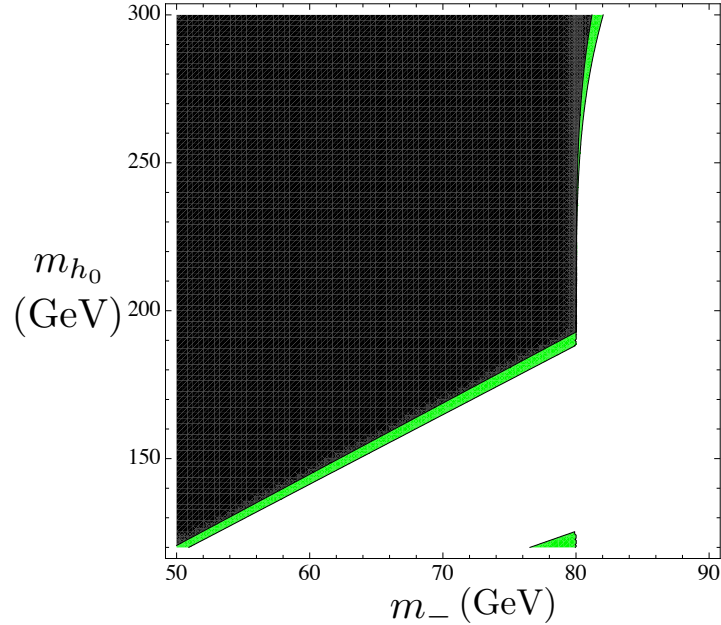
Figure 4.1: In this Figure, we plot contours of the relic abundance, $\Omega_{\mathrm{dm}}h^2$, of the ζ_- dark matter candidate in the case that the mass of the ζ_- is near the electroweak scale. The narrow gray band corresponds to the WMAP 2σ band, where we take the density of non-baryonic dark matter to be $\Omega_{\mathrm{nbdm}} = .106 \pm .008$ [123]. The white area corresponds to an under-density of ζ_- dark matter where it annihilates efficiently, and the dark area corresponds to an over-density.

tours for when the WMAP result for the relic abundance is saturated (within the

2σ band), as well as contours where there is less or more dark matter.

The case with low $T_{\mathbf{reheat}}$, small $(f_{\mathbf{PQ}}L)^{-1}$

In the case that the reheating temperature is very low (on order the mass of the

level 1 KK-modes), and the PQ gauge coupling is small, the KK-odd Goldstone

boson is never in equilibrium with the thermal bath, and the relic abundance of

the B_5 in this case originates primarily from decays of the NLKP. The final relic

abundance is then given by:

$$\Omega_{B_5} h^2 = \frac{m_{B_5}}{m_{\mathrm{NLKP}}} \Omega_{\mathrm{NLKP}} h^2. \tag{4.5.60}$$

The NLKP abundance has been calculated as a function of mass, and splittings between KK-modes [106, 107, 127]. Unless the the relic abundance of the NLKP is anomalously large, this is clearly not enough dark matter to saturate the measured relic abundance. Of course, in such scenarios, there may be another dark matter candidate (such as a standard pseudo-scalar axion) which can make up the remainder. We note that baryogenesis and leptogenesis are very problematic in such scenarios, as they must also occur at this low scale of reheating.

The case with larger $T_{\mathbf{reheat}}$, small $(f_{\mathbf{PQ}}L)^{-1}$

In the case where the gauge coupling is small, the universe is overclosed if the B_5 was in thermal equilibrium. This implies that some intervening era of inflation must dilute the initial relic abundance, and that post-reheating, the dark matter never reached thermal equilibrium with the bath. The reheat temperature is likely significantly higher than the mass of the level-1 KK-modes, as is necessary for generating a baryon asymmetry. In this case the situation is considerable more complicated than the previous ones. The relic abundance in such a scenario can be found as a function of the reheating temperature and the couplings to the species which are in equilibrium. The relic abundance in this case primarily arises through thermal production via scattering processes that occur in the bath.

This has been calculated to leading order in the QCD gauge coupling for the scenario of a supersymmetric axino DM candidate [128] in supersymmetric extensions of the SM [129], and the calculation is quite involved. In the PQ-UED

model, the situation is even more complicated due to the fact that not only are level-1 KK modes present in the thermal bath, but the entire tower of KK-modes contributes at a given reheat temperature. Additionally, the 5D theory is non-renormalizable, and perturbative unitarity is lost at energies of order $4\pi/L$. The 5D theory must be UV completed at some relatively low scale, and the characteristics of this UV completion will likely play a crucial role in the final relic abundance. These complications do not by themselves rule out the potential of the KK-odd Goldstone as a DM candidate in this region of parameter space, but the calculation is clearly beyond the scope of this analysis. We note that it is quite easy to construct a model that is very similar to that of the MSSM by deconstructing the extra dimension into a simple 2-site model. If the symmetry breaking in this scenario is achieved by a linear sigma model, then the results would likely be very similar to those in [129], with differences arising only from spin statistics in the production matrix elements, and an extended scalar sector.

In the case of very small $(f_{\rm PQ}L)^{-1}$, one might also worry about constraints from big-bang nucleosynthesis, or perturbations in the cosmic microwave background due to the late injection of electromagnetic energy from NLKP decays. Neither of these are relevant for the range of couplings we are most interested in. BBN is safe so long as the lifetime of the NLSP is less than 1 second, the time at which BBN takes place. This limit on the lifetime, for weak scale μ, corresponds to a limit on the PQ scale of $f_{\rm PQ} < 10^{14}$ GeV. The CMB constraints are even more relaxed, requiring a lifetime of not more than 10^{4-5}s, conservatively. For these large values of the PQ scale, the NLKP decays far outside of the detector, and does not play a role in collider physics.

4.5.3 Electroweak precision and direct collider constraints

We estimate the size of shifts in electroweak precision observables due to the variation in the vev due to the localized μ terms. The terms in the 5D Lagrangian relevant to EWP are:

$$\int dz \frac{g^2 v^2(z)}{8} \left[W_\mu^{(1)2} + W_\mu^{(3)2} - 2\frac{g'}{g} W_\mu^{(3)} B^\mu \right] \tag{4.5.61}$$

We expand the Lagrangian in terms of the KK-modes, examining the terms which give mass mixing between the lowest lying modes and the higher KK-modes. We treat the vev perturbatively, expanding it as $v(z) = v_0 + \delta v(z)$.

$$\sum_n \int dz \frac{g^2 v_0 \delta v(z)}{2} \left[W_{0\mu}^{(1)} W_n^{(1)\mu} + W_{0\mu}^{(3)} W_n^{(3)\mu} - \frac{g'}{g} W_{0\mu}^{(3)} B_n^\mu \right] \tag{4.5.62}$$

The diagrams involving heavy W exchange cancel in calculating $\Pi_{11} - \Pi_{33}$, so we need only calculate the diagrams mixing the heavy B with $W_0^{(3)}$ the last term in Eq. (4.5.62).

We Taylor expand the vev about the midpoint of the extra dimension, $\delta v(z) = 1/2 v''(z = L/2)(z - L/2)^2$, and we input the canonically normalized gauge boson wave functions to find the relevant overlap integrals for the mixing terms:

$$\frac{g g' v_0 v''_{L/2}}{2\sqrt{2}L} \int dz (z - L/2)^2 \cos \frac{n\pi z}{L} = \frac{g g' L^2 v_0 v''_{L/2}}{\sqrt{2} n^2 \pi^2} \cdot \begin{cases} 1 & n \text{ even} \\ 0 & n \text{ odd} \end{cases} \tag{4.5.63}$$

The diagrams then evaluate to:

$$g^2 \left(\Pi_{11} - \Pi_{33} \right) = \sum_{n \text{ even}} \frac{g^2 g'^2 L^6 v_0^2 (v''_{L/2})^2}{2 n^6 \pi^6} = \frac{g^2 g'^2 L^6 v_0^2 (v''_{L/2})^2}{120,960} \tag{4.5.64}$$

where we have used the fact that the masses of the hypercharge gauge boson KK-modes are approximately given by $m_n = \frac{n\pi}{L}$. $\Delta\rho$ is then given by:

$$\Delta\rho = \alpha T = \frac{4}{v_0^2} \left(\Pi_{11} - \Pi_{33} \right) = \frac{g'^2 L^6 (v''_{L/2})^2}{30,240} \approx 8 \cdot 10^{-9} \left(\frac{L}{1 \text{ TeV}} \right)^6 \left(\frac{\mu}{300^2 \text{ GeV}^2} \right)^2, \tag{4.5.65}$$

well within current experimental limits. To understand the overall scaling with L and μ, remember that $v'|_{0,L} = \mp \mu L v|_{0,L}$, and thus $v'' \approx \frac{v'|_L - v'|_0}{L} \approx 2\mu v$.

Regarding direct collider constraints, it is unlikely that the Tevatron experiments searching for GMSB-like scenarios [130, 131] place any limits on this scenario. This is due to the fact that there are indirect electroweak precision constraints on the extra dimensional model in addition to the ones calculated above. These arise from higher dimensional operators in the non-renomalizable 5D theory that are suppressed by the cutoff scale. Electroweak precision constraints require that this cutoff scale must be at least 5 TeV. These limit the size of the extra dimension to be about $L \lesssim (400 \text{ GeV})^{-1}$. Searches for parity odd quarks in the acoplanar dijet topology at the Tevatron do not yet probe this region of parameter space [32, 132], and the searches for GMSB like scenarios place even less stringent limits. The upcoming LHC experiments will have much greater kinematic access to the region which is allowed by electroweak precision constraints. However, distinction between GMSB scenarios and this extra dimensional model may be difficult given a discovery of an excess of this type of signal.

4.6   Conclusions

We have performed an analysis of spontaneously broken anomalous global symmetries in the context of one universal extra dimension compactified on an S_1/Z_2 orbifold. A light pseudo-Goldstone scalar field arises from a 5D gauge symmetry that is broken by orbifold boundary conditions. Anomalous couplings to the unbroken gauge field strengths emerge after performing a 5D field

redefinition that produces a non-trivial Jacobian. Over a large range of couplings and explicit symmetry breaking terms, the resulting effective action permits decays of the lightest level one SM KK-mode (of the hypercharge gauge boson) to a scalar field associated with the 5-component of an extra dimensional gauge field along with either a photon or Z-boson. In particularly interesting regions of parameter space, the decays occur on detector sized length scales with sizable displaced vertices. Such signals were long thought to be a smoking gun signature of SUSY models in which the soft masses are generated through gauge mediation, and in which the NLSP decays to a light gravitino in association with a photon or Z-boson. We have calculated constraints on this extra dimensional scenario, finding these to be minimal, and irrelevant for the range of couplings most interesting from the perspective of collider phenomenology. This pseudo-Goldstone scalar field is a potential dark matter candidate, and it may be possible for it to saturate the relic abundance observed by WMAP and numerous other astrophysical experiments. We have performed a standard relic abundance calculation for the case in which the extra dimensional gauge coupling is $\mathcal{O}(1)$. For small values of the gauge coupling, the relic abundance calculation is intensive, model dependent, and depends on unknown details of early cosmology such as the reheat temperature. It is unlikely that this region of parameter space is ruled out by overclosure of the universe, however the calculation is beyond the scope of this analysis. BBN and the CMB spectrum do not place any constraints on the parameter space most relevant for collider physics.

APPENDIX A

TESTING GLUINO SPIN WITH THREE-BODY DECAYS

A.1   Polarization Analysis of the UED case

The main feature of the invariant mass distribution of the UED case, which makes it distingishable from SUSY, is the dip at $s = 0$. This feature can be understood by analyzing the decay amplitudes of the individual polarization components of the mother and daughter particles and considering conservation of angular momentum. As shown with the two toy models in Section 3.4, conservation of angular momentum can lead to suppression of the invariant mass distributions with respect to the pure phase space distribution (3.3.8) at $s = 0$, as well as at $s = s^{\max}$. The couplings in the UED case have the same chiral structure as the second toy model of Section 3.4, with the quark and antiquark having opposite helicities. The added complication in the UED case is that the mother and daughter particles are massive spin one particles. We use $m_z(A)$ and $m_z(B)$ to denote the projections of the A and B spins on the direction of the momentum p_1 of the quark q. These operators have eigenvalues $m_z(A), m_z(B) = -1, 0, +1$; the corresponding eigenstates have polarization vectors ϵ_-, ϵ_L, and ϵ_+. The transitions among these eigenstates are described by a 3×3 matrix of decay amplitudes. Using the UED lagrangian (3.5.6), we have evaluated these amplitudes and obtained the dijet invariant mass distribution corresponding to each entry.[*] These distributions, divided out by the pure phase space distribution (3.3.8), are plotted in Fig. A.1. At $s = 0$ the spin projections of the quark-antiquark pair sums

---

[*] For clarity, we only included the contribution of the diagrams with Q_L^1 in the intermediate state. The diagrams with Q_R^1 lead to distributions that are identical, up to a parity reflection, to the ones presented here.
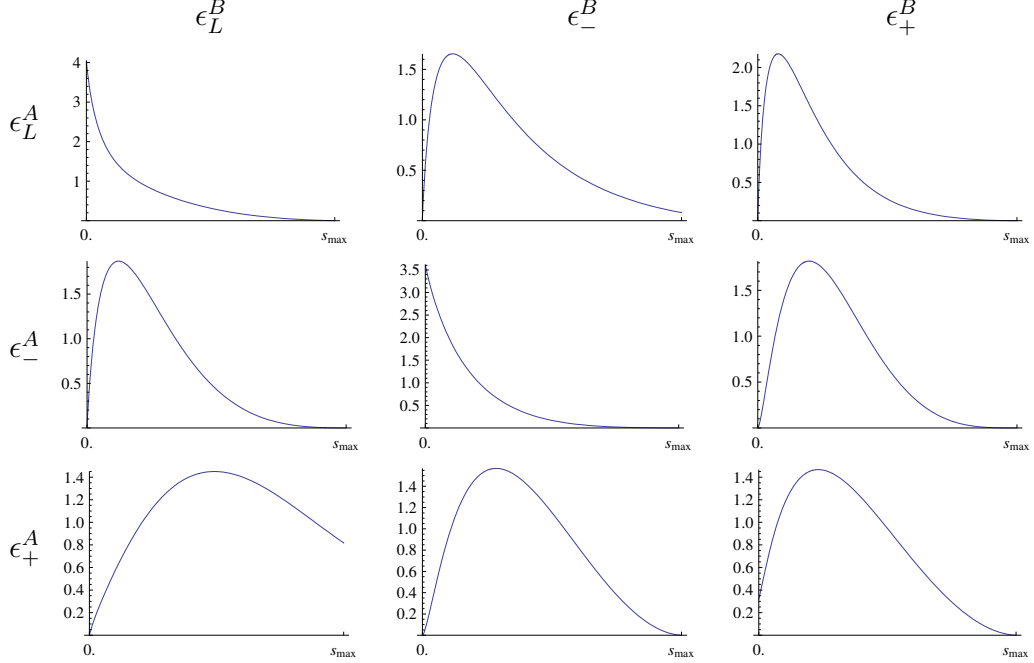
119

Figure A.1: The invariant mass distributions for the decay of individual polarizations, divided by the phase space distribution, for $m_B/m_A = 0.1$ and $M/m_A = 1.5$ in arbitrary units. The polarization vectors are along the momentum p_1 of the outgoing quark q. Notice that at $s = m_{12}^2 = 0$ only the diagonal elements are unsuppressed due to angular momentum conservation, resulting in a dip of the distribution.

up to zero, and the final state has no angular momentum (see the right panel of Fig. 3.2). Therefore the polarizations of A and B must be the same. This will result in a suppression of all non-diagonal components in the transition matrix at $s = 0$, resulting in a dip there. At $s = s^{\mathrm{max}}$, however, the spin projections of the quark-antiquark pair add up to $m_z = +1$ (see Fig. 3.2). Thus the only allowed decays at s_{max} are the longitudinal component of A to $m_z(B) = -1$ and $m_z(A) = +1$ to the longitudinal component of B. Both features at the ends of the distribution can be nicely observed in Fig. A.1.

A.2 The Kullback-Leibler distance

A convenient measure to quantify how much two continuous probability distributions differ from each other is the *Kullback-Leibler distance*. (For a recent application in the collider phenomenology context, see Ref. [72].) In this appendix, we will briefly review this measure.

Suppose that the data sample consists of N events distributed according to the theoretical prediction of model T. Consider a second model, S, which predicts a distribution different from T. We can quantify the discriminating power of our data sample by the ratio of conditional probabilities for S and T to be true, given the data:

$$\kappa = \frac{p(S \text{ is true} | N \text{ events from } T)}{p(T \text{ is true} | N \text{ events from } T)}. \tag{A.2.1}$$

This equation can be rewritten using Bayes' theorem:

$$\begin{aligned} \kappa &= \frac{p(S | N \text{ events from } T)}{p(T | N \text{ events from } T)} \\ &= \frac{p(S) p(N \text{ events from } T | S)}{p(T) p(N \text{ events from } T | T)} \end{aligned} \tag{A.2.2}$$

where $p(S)$ and $p(T)$ are the priors – probabilities for S and T to be true before the experiment at hand is conducted. (In this paper, we assumed that the MSSM and UED are *a priori* equally likely, so we set $p(S) = p(T) = 1$.) Suppose that each event i ($i = 1 \ldots N$) is characterized by a single variable s_i (in our case, the dijet invariant mass). Since the N events are independent, we have

$$\begin{aligned} \kappa &= \frac{p(S) \prod_{i=1}^{N} p(s_i^{(T)} | S)}{p(T) \prod_{i=1}^{N} p(s_i^{(T)} | T)} \\ &= \frac{p(S)}{p(T)} \exp\left(\sum_{i=1}^{N} \log\left(\frac{p(s_i^{(T)} | S)}{p(s_i^{(T)} | T)} \right) \right). \end{aligned} \tag{A.2.3}$$

For large N we can approximate $\sum_N \approx \int ds \frac{dN}{ds}$ and use the normalization condition $\frac{dN}{ds} = Np(s|T)$ to obtain

$$
\begin{aligned}
\kappa &\approx \frac{p(S)}{p(T)} \exp\left(N \int ds \log\left(\frac{p(s|S)}{p(s|T)} \right) p(s|T) \right) \\
&= \frac{p(S)}{p(T)} \exp\left(-N \, \mathrm{KL}(T, S) \right),
\end{aligned}
\tag{A.2.4}
$$

where the *Kullback-Leibler distance* (also called *relative entropy*) is defined as

$$
\mathrm{KL}(T, S) := \int ds \log\left(\frac{p(s|T)}{p(s|S)} \right) p(s|T).
\tag{A.2.5}
$$

It follows that the number of events needed to constrain the probability of model S being true, relative to the probability of T being true, to be less than $1/R$, is given by

$$
N \approx \frac{\log R + \log \frac{p(S)}{p(T)}}{\mathrm{KL}(T, S)}.
\tag{A.2.6}
$$

This number provides a convenient and physically meaningful measure of how different the S and T distributions are.

Two properties of the Kullback-Leibler distance are worth mentioning in our context. First, while this is not manifest from its definition, the KL distance is non-negative, and zero if and only if $T = S$. Second, it is invariant under transformations $s \to f(s)$: for example, it does not matter whether we consider the jet invariant mass distribution in terms of s or $m_{jj} = \sqrt{s}$.

APPENDIX B

ODD DECAYS FROM EVEN ANOMALIES: GAUGE MEDIATION SIGNATURES WITHOUT SUSY

B.1   The Goldstone Wave Functions with a Bulk Higgs VEV

The full classical equations of motion for B_5 and π are given by:

$$\Box\pi - \pi'' + \xi\kappa^2\pi + \frac{v''}{v}\pi + (1-\xi)vB_5' - 2v'B_5 = 0$$

$$\Box B_5 - \xi B_5'' + \kappa^2 B_5 - (1-\xi)\frac{\kappa^2}{v}\pi' + (1+\xi)\frac{\kappa^2}{v^2}v'\pi = 0$$

(B.1.1)

where we have kept the terms containing the derivatives of v for completeness. After enforcing $B_\mu|_{z=0,L} = 0$, the boundary conditions for π and B_5 are given by:

$$\pi' - vB_5 - \frac{v'}{v}\pi \pm L\frac{\delta V_{\text{bound}}}{\delta\pi}\bigg|_{z=0,L} = 0$$

$$B_5' - \frac{\kappa^2}{v}\pi\bigg|_{z=0,L} = 0.$$

(B.1.2)

In the cases where $v' = 0$, we can decouple the second order bulk equations by taking the first equation, solving for B_5',

$$B_5' = \frac{1}{v(\xi - 1)}\left[\Box\pi - \pi'' + \xi\kappa^2\pi\right],$$

(B.1.3)

taking the z-derivative of the second equation, and substituting using the above formula. The result is a 4-th order equation for π:

$$\pi'''' - 2\kappa^2\pi'' + \kappa^4\pi + m^2\left\{(1+1/\xi)\pi'' + \left[m^2/\xi - \kappa^2(1+1/\xi)\right]\pi\right\} = 0 \quad \text{(B.1.4)}$$

The same 4-th order equation can be obtained for B_5. Note that the only dependence on ξ is in the mass terms. One can immediately find the physical states (those that don't depend on ξ). For solutions to the second order equation

$$\pi'' + (m^2 - \kappa^2)\pi = 0,$$

(B.1.5)

123

there is no ξ dependence in the second half of the equation, and the bulk eom is also automatically satisfied. This means that the remaining two solutions to the full fourth order equation must be the ones that are eaten/unphysical.

For zero modes, there is trivially no ξ dependence, since ξ appears only in the mass terms. The most general solutions for the massless case are:

$$\pi = A_\pi e^{\kappa z} + B_\pi e^{-\kappa z} + C_\pi z e^{\kappa z} + D_\pi z e^{-\kappa z},$$
$$B_5 = A_B e^{\kappa z} + B_B e^{-\kappa z} + C_B z e^{\kappa z} + D_B z e^{-\kappa z}.$$

(B.1.6)

We first eliminate 4 of these 8 coefficients by requiring that the original second order coupled equations are satisfied. Satisfying the boundary conditions further requires that there are no solutions of the form $z e^{\pm \kappa z}$. Two undetermined coefficients remain, implying that there are two physical scalar zero modes in the spectrum. The full massless solution is given by:

$$B_5 = A_B e^{\kappa z} + B_B e^{-\kappa z}$$
$$\pi = -\frac{v}{\kappa} \left[A_B e^{\kappa z} - B_B e^{-\kappa z} \right].$$

(B.1.7)

By rewriting these in KK even and odd combinations we obtain the final Goldstone wave functions in eqns. (4.4.19) and (4.4.20).

BIBLIOGRAPHY

[1] J. Alcaraz, "Precision Electroweak Measurements and Constraints on the Standard Model," 2009.

[2] Maxim Markevitch et al., "Direct constraints on the dark matter self-interaction cross-section from the merging galaxy cluster 1E0657-56," *Astrophys. J.*, vol. 606, pp. 819–824, 2004.

[3] Henning Flacher et al., "Gfitter - Revisiting the Global Electroweak Fit of the Standard Model and Beyond," *Eur. Phys. J.*, vol. C60, pp. 543–583, 2009.

[4] Marcela S. Carena et al., "Report of the Tevatron Higgs working group," 2000.

[5] R. Barate et al., "Search for the standard model Higgs boson at LEP," *Phys. Lett.*, vol. B565, pp. 61–75, 2003.

[6] T. Aaltonen et al., "Combination of Tevatron searches for the standard model Higgs boson in the W+W- decay mode," *Phys. Rev. Lett.*, vol. 104, pp. 061802, 2010.

[7] John R. Ellis, Giovanni Ridolfi, and Fabio Zwirner, "Higgs boson properties in the standard model and its supersymmetric extensions," *Comptes Rendus Physique*, vol. 8, pp. 999–1012, 2007.

[8] M. J. G. Veltman, "Second Threshold in Weak Interactions," *Acta Phys. Polon.*, vol. B8, pp. 475, 1977.

[9] Benjamin W. Lee, C. Quigg, and H. B. Thacker, "Weak Interactions at Very High-Energies: The Role of the Higgs Boson Mass," *Phys. Rev.*, vol. D16, pp. 1519, 1977.

[10] Benjamin W. Lee, C. Quigg, and H. B. Thacker, "The Strength of Weak Interactions at Very High-Energies and the Higgs Boson Mass," *Phys. Rev. Lett.*, vol. 38, pp. 883–885, 1977.

[11] C. E. Vayonakis, "New Threshold of Weak Interactions," 1977, Print-77-0432 (ATHENS).

[12] Martin Schmaltz and David Tucker-Smith, "Little Higgs Review," *Ann. Rev. Nucl. Part. Sci.*, vol. 55, pp. 229–270, 2005.

[13] Maxim Perelstein, "Little Higgs models and their phenomenology," *Prog. Part. Nucl. Phys.*, vol. 58, pp. 247–291, 2007.

[14] J. Goldstone, "Field Theories with Superconductor Solutions," *Nuovo Cim.*, vol. 19, pp. 154–164, 1961.

[15] Jeffrey Goldstone, Abdus Salam, and Steven Weinberg, "Broken Symmetries," *Phys. Rev.*, vol. 127, pp. 965–970, 1962.

[16] Yoichiro Nambu, "Quasi-particles and gauge invariance in the theory of superconductivity," *Phys. Rev.*, vol. 117, pp. 648–663, 1960.

[17] Sidney R. Coleman, J. Wess, and Bruno Zumino, "Structure of phenomenological Lagrangians. 1," *Phys. Rev.*, vol. 177, pp. 2239–2247, 1969.

[18] Curtis G. Callan, Jr., Sidney R. Coleman, J. Wess, and Bruno Zumino, "Structure of phenomenological Lagrangians. 2," *Phys. Rev.*, vol. 177, pp. 2247–2250, 1969.

[19] Christopher T. Hill and Richard J. Hill, "T^- parity violation by anomalies," *Phys. Rev.*, vol. D76, pp. 115014, 2007.

[20] N. Arkani-Hamed, A. G. Cohen, E. Katz, and A. E. Nelson, "The littlest Higgs," *JHEP*, vol. 07, pp. 034, 2002.

[21] Csaba Csaki, Johannes Heinonen, Maxim Perelstein, and Christian Spethmann, "A Weakly Coupled Ultraviolet Completion of the Littlest Higgs with T-parity," *Phys. Rev.*, vol. D79, pp. 035014, 2009.

[22] Hsin-Chia Cheng, Konstantin T. Matchev, and Martin Schmaltz, "Bosonic supersymmetry? Getting fooled at the CERN LHC," *Phys. Rev.*, vol. D66, pp. 056006, 2002.

[23] Csaba Csaki, Johannes Heinonen, and Maxim Perelstein, "Testing Gluino Spin with Three-Body Decays," *JHEP*, vol. 10, pp. 107, 2007.

[24] G. F. Giudice and R. Rattazzi, "Theories with gauge-mediated supersymmetry breaking," *Phys. Rept.*, vol. 322, pp. 419–499, 1999.

[25] Csaba Csaki, Johannes Heinonen, Jay Hubisz, and Yuri Shirman, "Odd Decays from Even Anomalies: Gauge Mediation Signatures Without SUSY," *Phys. Rev.*, vol. D79, pp. 105016, 2009.

[26] Nima Arkani-Hamed, Andrew G. Cohen, and Howard Georgi, "Electroweak symmetry breaking from dimensional deconstruction," *Phys. Lett.*, vol. B513, pp. 232–240, 2001.

[27] Hsin-Chia Cheng and Ian Low, "TeV symmetry and the little hierarchy problem," *JHEP*, vol. 09, pp. 051, 2003.

[28] Hsin-Chia Cheng and Ian Low, "Little hierarchy, little Higgses, and a little symmetry," *JHEP*, vol. 08, pp. 061, 2004.

[29] Ian Low, "T parity and the littlest Higgs," *JHEP*, vol. 10, pp. 067, 2004.

[30] Jay Hubisz, Patrick Meade, Andrew Noble, and Maxim Perelstein, "Electroweak precision constraints on the littlest Higgs model with T parity," *JHEP*, vol. 01, pp. 135, 2006.

[31] Masaki Asano, Shigeki Matsumoto, Nobuchika Okada, and Yasuhiro Okada, "Cosmic positron signature from dark matter in the littlest Higgs model with T-parity," *Phys. Rev.*, vol. D75, pp. 063506, 2007.

[32] Marcela S. Carena, Jay Hubisz, Maxim Perelstein, and Patrice Verdier, "Collider signature of T-quarks," *Phys. Rev.*, vol. D75, pp. 091701, 2007.

[33] Jay Hubisz and Patrick Meade, "Phenomenology of the littlest Higgs with T-parity," *Phys. Rev.*, vol. D71, pp. 035016, 2005.

[34] Alexander Belyaev, Chuan-Ren Chen, Kazuhiro Tobe, and C. P. Yuan, "Phenomenology of littlest Higgs model with T-parity: Including effects of T-odd fermions," 2006, Moscow 2006, ICHEP (1113-1116).

[35] Andreas Birkedal, Andrew Noble, Maxim Perelstein, and Andrew Spray, "Little Higgs dark matter," *Phys. Rev.*, vol. D74, pp. 035002, 2006.

[36] Maxim Perelstein and Andrew Spray, "Indirect detection of little Higgs dark matter," *Phys. Rev.*, vol. D75, pp. 083519, 2007.

[37] Richard J. Hill, "Topological physics in the standard model and beyond," 2007.

[38] David Krohn and Itay Yavin, "Anomalies in Fermionic UV Completions of Little Higgs Models," *JHEP*, vol. 06, pp. 092, 2008.

[39] Emanuel Katz, Jae-yong Lee, Ann E. Nelson, and Devin G. E. Walker, "A composite little Higgs model," *JHEP*, vol. 10, pp. 088, 2005.

[40] Jesse Thaler and Itay Yavin, "The littlest Higgs in anti-de Sitter space," *JHEP*, vol. 08, pp. 022, 2005.

[41] Kaustubh Agashe, Adam Falkowski, Ian Low, and Geraldine Servant, "KK Parity in Warped Extra Dimension," *JHEP*, vol. 04, pp. 027, 2008.

[42] Andreas Birkedal, Z. Chacko, and Mary K. Gaillard, "Little supersymmetry and the supersymmetric little hierarchy problem," *JHEP*, vol. 10, pp. 036, 2004.

[43] Zurab Berezhiani, Piotr H. Chankowski, Adam Falkowski, and Stefan Pokorski, "Double protection of the Higgs potential," *Phys. Rev. Lett.*, vol. 96, pp. 031801, 2006.

[44] Tuhin S. Roy and Martin Schmaltz, "Naturally heavy superpartners and a little Higgs," *JHEP*, vol. 01, pp. 149, 2006.

[45] Csaba Csaki, Guido Marandella, Yuri Shirman, and Alessandro Strumia, "The super-little Higgs," *Phys. Rev.*, vol. D73, pp. 035006, 2006.

[46] Kaustubh Agashe, Roberto Contino, and Alex Pomarol, "The Minimal Composite Higgs Model," *Nucl. Phys.*, vol. B719, pp. 165–187, 2005.

[47] Lisa Randall and Raman Sundrum, "A large mass hierarchy from a small extra dimension," *Phys. Rev. Lett.*, vol. 83, pp. 3370–3373, 1999.

[48] Z. G. Berezhiani and G. R. Dvali, "Possible solution of the hierarchy problem in supersymmetrical grand unification theories," *Bull. Lebedev Phys. Inst.*, vol. 5, pp. 55–59, 1989.

[49] Riccardo Barbieri, G. R. Dvali, Alessandro Strumia, Zurab Berezhiani, and Lawrence J. Hall, "Flavor in supersymmetric grand unification: A Democratic approach," *Nucl. Phys.*, vol. B432, pp. 49–67, 1994.

[50] Zurab Berezhiani, Csaba Csaki, and Lisa Randall, "Could the super-

symmetric Higgs particles naturally be pseudoGoldstone bosons?," *Nucl. Phys.*, vol. B444, pp. 61–91, 1995.

[51] David E. Kaplan and Martin Schmaltz, "The little Higgs from a simple group," *JHEP*, vol. 10, pp. 039, 2003.

[52] Martin Schmaltz, "The simplest little Higgs," *JHEP*, vol. 08, pp. 056, 2004.

[53] N. Seiberg, "Electric - magnetic duality in supersymmetric nonAbelian gauge theories," *Nucl. Phys.*, vol. B435, pp. 129–146, 1995.

[54] Igor R. Klebanov and Matthew J. Strassler, "Supergravity and a confining gauge theory: Duality cascades and chiSB-resolution of naked singularities," *JHEP*, vol. 08, pp. 052, 2000.

[55] J. Wess and B. Zumino, "Consequences of anomalous Ward identities," *Phys. Lett.*, vol. B37, pp. 95, 1971.

[56] Edward Witten, "Global Aspects of Current Algebra," *Nucl. Phys.*, vol. B223, pp. 422–432, 1983.

[57] Yoshiharu Kawamura, Hitoshi Murayama, and Masahiro Yamaguchi, "Low-energy effective Lagrangian in unified theories with nonuniversal supersymmetry breaking terms," *Phys. Rev.*, vol. D51, pp. 1337–1352, 1995.

[58] Adam Falkowski, "Note on little SUSY," 2005, (unpublished).

[59] Csaba Csaki, Christophe Grojean, Hitoshi Murayama, Luigi Pilo, and John Terning, "Gauge theories on an interval: Unitarity without a Higgs," *Phys. Rev.*, vol. D69, pp. 055006, 2004.

[60] Csaba Csaki, Christophe Grojean, Luigi Pilo, and John Terning, "Towards a realistic model of Higgsless electroweak symmetry breaking," *Phys. Rev. Lett.*, vol. 92, pp. 101802, 2004.

[61] Nima Arkani-Hamed, Andrew G. Cohen, and Howard Georgi, "Anomalies on orbifolds," *Phys. Lett.*, vol. B516, pp. 395–402, 2001.

[62] Csaba Csaki, Jay Hubisz, Graham D. Kribs, Patrick Meade, and John Terning, "Big corrections from a little Higgs," *Phys. Rev.*, vol. D67, pp. 115002, 2003.

[63] Gustavo Burdman, Maxim Perelstein, and Aaron Pierce, "Collider tests of the little Higgs model," *Phys. Rev. Lett.*, vol. 90, pp. 241802, 2003.

[64] Maxim Perelstein, Michael Edward Peskin, and Aaron Pierce, "Top quarks and electroweak symmetry breaking in little Higgs models," *Phys. Rev.*, vol. D69, pp. 075002, 2004.

[65] Jay Hubisz, Seung J. Lee, and Gil Paz, "The flavor of a little Higgs with T-parity," *JHEP*, vol. 06, pp. 041, 2006.

[66] Monika Blanke et al., "Particle antiparticle mixing, epsilon(K), Delta(Gamma(q)), A(SL)(q), A(CP)(B/d –¿ psi K(S)), A(CP)(B/s –¿ psi Phi) and B –¿ X/s,d gamma in the littlest Higgs model with T- parity," *JHEP*, vol. 12, pp. 003, 2006.

[67] Monika Blanke et al., "Rare and CP-Violating K and B Decays in the Littlest Higgs Model with T-Parity," *JHEP*, vol. 01, pp. 066, 2007.

[68] Monika Blanke, Andrzej J. Buras, Bjoern Duling, Anton Poschenrieder, and Cecilia Tarantino, "Charged Lepton Flavour Violation and $(g - 2)_\mu$ in the Littlest Higgs Model with T-Parity: a clear Distinction from Supersymmetry," *JHEP*, vol. 05, pp. 013, 2007.

[69] A. J. Barr, "Using lepton charge asymmetry to investigate the spin of supersymmetric particles at the LHC," *Phys. Lett.*, vol. B596, pp. 205–212, 2004.

[70] Jennifer M. Smillie and Bryan R. Webber, "Distinguishing Spins in Supersymmetric and Universal Extra Dimension Models at the Large Hadron Collider," *JHEP*, vol. 10, pp. 069, 2005.

[71] AseshKrishna Datta, Kyoungchul Kong, and Konstantin T. Matchev, "Discrimination of supersymmetry and universal extra dimensions at hadron colliders," *Phys. Rev.*, vol. D72, pp. 096006, 2005.

[72] Christiana Athanasiou, Christopher G. Lester, Jennifer M. Smillie, and Bryan R. Webber, "Distinguishing spins in decay chains at the Large Hadron Collider," *JHEP*, vol. 08, pp. 055, 2006.

[73] Lian-Tao Wang and Itay Yavin, "Spin Measurements in Cascade Decays at the LHC," *JHEP*, vol. 04, pp. 032, 2007.

[74] Can Kilic, Lian-Tao Wang, and Itay Yavin, "On the Existence of Angular Correlations in Decays with Heavy Matter Partners," *JHEP*, vol. 05, pp. 052, 2007.

[75] Alexandre Alves, Oscar Eboli, and Tilman Plehn, "It's a gluino," *Phys. Rev.*, vol. D74, pp. 095010, 2006.

[76] Manuel Toharia and James D. Wells, "Gluino decays with heavier scalar superpartners," *JHEP*, vol. 02, pp. 015, 2006.

[77] Howard E. Haber and Gordon L. Kane, "The Search for Supersymmetry: Probing Physics Beyond the Standard Model," *Phys. Rept.*, vol. 117, pp. 75–263, 1985.

[78] Maxim Perelstein and Christian Spethmann, "A collider signature of the supersymmetric golden region," *JHEP*, vol. 04, pp. 070, 2007.

[79] Thomas Appelquist, Hsin-Chia Cheng, and Bogdan A. Dobrescu, "Bounds on universal extra dimensions," *Phys. Rev.*, vol. D64, pp. 035002, 2001.

[80] Marcela S. Carena, Timothy M. P. Tait, and C. E. M. Wagner, "Branes and orbifolds are opaque," *Acta Phys. Polon.*, vol. B33, pp. 2355, 2002.

[81] I. Hinchliffe, F. E. Paige, M. D. Shapiro, J. Soderqvist, and W. Yao, "Precision SUSY measurements at CERN LHC," *Phys. Rev.*, vol. D55, pp. 5520–5540, 1997.

[82] C. G. Lester and D. J. Summers, "Measuring masses of semiinvisibly decaying particles pair produced at hadron colliders," *Phys. Lett.*, vol. B463, pp. 99–103, 1999.

[83] Alan Barr, Christopher Lester, and P. Stephens, "m(T2) : The Truth behind the glamour," *J. Phys.*, vol. G29, pp. 2343–2363, 2003.

[84] Patrick Meade and Matthew Reece, "Top partners at the LHC: Spin and mass measurement," *Phys. Rev.*, vol. D74, pp. 015010, 2006.

[85] Fabio Maltoni and Tim Stelzer, "MadEvent: Automatic event generation with MadGraph," *JHEP*, vol. 02, pp. 027, 2003.

[86] Johan Alwall et al., "MadGraph/MadEvent v4: The New Web Generation," *JHEP*, vol. 09, pp. 028, 2007.

[87] G. L. Bayatian et al., "CMS technical design report, volume II: Physics performance," *J. Phys.*, vol. G34, pp. 995–1579, 2007.

[88] J. S. Bell and R. Jackiw, "A PCAC puzzle: pi0 $\rightarrow$ gamma gamma in the sigma model," *Nuovo Cim.*, vol. A60, pp. 47–61, 1969.

[89] Stephen L. Adler, "Axial vector vertex in spinor electrodynamics," *Phys. Rev.*, vol. 177, pp. 2426–2438, 1969.

[90] William A. Bardeen, "Anomalous Ward identities in spinor field theories," *Phys. Rev.*, vol. 184, pp. 1848–1857, 1969.

[91] Kazuo Fujikawa, "Path Integral Measure for Gauge Invariant Fermion Theories," *Phys. Rev. Lett.*, vol. 42, pp. 1195, 1979.

[92] Kazuo Fujikawa, "Path Integral for Gauge Theories with Fermions," *Phys. Rev.*, vol. D21, pp. 2848, 1980.

[93] J. Wess and Bruno Zumino, "Lagrangian method for chiral symmetries," *Phys. Rev.*, vol. 163, pp. 1727–1735, 1967.

[94] O. Kaymakcalan, S. Rajeev, and J. Schechter, "Nonabelian Anomaly and Vector Meson Decays," *Phys. Rev.*, vol. D30, pp. 594, 1984.

[95] Gerard 't Hooft, "Computation of the quantum effects due to a four- dimensional pseudoparticle," *Phys. Rev.*, vol. D14, pp. 3432–3450, 1976.

[96] Stephen P. Martin, "A Supersymmetry Primer," 1997.

[97] Christopher T. Hill, "Anomalies, Chern-Simons terms and chiral delocalization in extra dimensions," *Phys. Rev.*, vol. D73, pp. 085001, 2006.

[98] Ben Gripaios, "Anomaly Holography, the Wess-Zumino-Witten Term, and Electroweak Symmetry Breaking," *Phys. Lett.*, vol. B663, pp. 419–423, 2008.

[99] Ben Gripaios and Stephen M. West, "Anomaly Holography," *Nucl. Phys.*, vol. B789, pp. 362–381, 2008.

[100] Thomas Flacke, Ben Gripaios, John March-Russell, and David Maybury, "Warped axions," *JHEP*, vol. 01, pp. 061, 2007.

[101] R. D. Peccei and Helen R. Quinn, "CP Conservation in the Presence of Instantons," *Phys. Rev. Lett.*, vol. 38, pp. 1440–1443, 1977.

[102] Hsin-Chia Cheng, Konstantin T. Matchev, and Martin Schmaltz, "Radiative corrections to Kaluza-Klein masses," *Phys. Rev.*, vol. D66, pp. 036005, 2002.

[103] Ki-woon Choi, "A QCD axion from higher dimensional gauge field," *Phys. Rev. Lett.*, vol. 92, pp. 101602, 2004.

[104] Nima Arkani-Hamed, Andrew G. Cohen, and Howard Georgi, "(De)constructing dimensions," *Phys. Rev. Lett.*, vol. 86, pp. 4757–4761, 2001.

[105] Christopher T. Hill, Stefan Pokorski, and Jing Wang, "Gauge invariant effective Lagrangian for Kaluza-Klein modes," *Phys. Rev.*, vol. D64, pp. 105005, 2001.

[106] Geraldine Servant and Timothy M. P. Tait, "Is the lightest Kaluza-Klein particle a viable dark matter candidate?," *Nucl. Phys.*, vol. B650, pp. 391–419, 2003.

[107] Hsin-Chia Cheng, Jonathan L. Feng, and Konstantin T. Matchev, "Kaluza-Klein dark matter," *Phys. Rev. Lett.*, vol. 89, pp. 211301, 2002.

[108] Lian-Tao Wang and Itay Yavin, "A Review of Spin Determination at the LHC," *Int. J. Mod. Phys.*, vol. A23, pp. 4647–4668, 2008.

[109] Jay Hubisz, Joseph Lykken, Maurizio Pierini, and Maria Spiropulu, "Missing energy look-alikes with 100 pb^{-1} at the LHC," *Phys. Rev.*, vol. D78, pp. 075008, 2008.

[110] Gregory Hallenbeck, Maxim Perelstein, Christian Spethmann, Julia Thom, and Jennifer Vaughan, "Model Discrimination with the CMS Detector: a Case Study," *Phys. Rev.*, vol. D79, pp. 075024, 2009.

[111] Michael Dine and Willy Fischler, "A Phenomenological Model of Particle Physics Based on Supersymmetry," *Phys. Lett.*, vol. B110, pp. 227, 1982.

[112] Michael Dine and Willy Fischler, "A Supersymmetric GUT," *Nucl. Phys.*, vol. B204, pp. 346, 1982.

[113] Luis Alvarez-Gaume, Mark Claudson, and Mark B. Wise, "Low-Energy Supersymmetry," *Nucl. Phys.*, vol. B207, pp. 96, 1982.

[114] Savas Dimopoulos and Stuart Raby, "Geometric Hierarchy," *Nucl. Phys.*, vol. B219, pp. 479, 1983.

[115] Michael Dine, Ann E. Nelson, and Yuri Shirman, "Low-energy dynamical supersymmetry breaking simplified," *Phys. Rev.*, vol. D51, pp. 1362–1370, 1995.

[116] Michael Dine, Ann E. Nelson, Yosef Nir, and Yuri Shirman, "New tools for low-energy dynamical supersymmetry breaking," *Phys. Rev.*, vol. D53, pp. 2658–2669, 1996.

[117] Steven Weinberg, "A New Light Boson?," *Phys. Rev. Lett.*, vol. 40, pp. 223–226, 1978.

[118] Frank Wilczek, "Problem of Strong p and t Invariance in the Presence of Instantons," *Phys. Rev. Lett.*, vol. 40, pp. 279–282, 1978.

[119] Michael Dine, Willy Fischler, and Mark Srednicki, "A Simple Solution to the Strong CP Problem with a Harmless Axion," *Phys. Lett.*, vol. B104, pp. 199, 1981.

[120] A. R. Zhitnitsky, "On Possible Suppression of the Axion Hadron Interactions. (In Russian)," *Sov. J. Nucl. Phys.*, vol. 31, pp. 260, 1980.

[121] Yoshiharu Kawamura, "Triplet-doublet splitting, proton stability and extra dimension," *Prog. Theor. Phys.*, vol. 105, pp. 999–1006, 2001.

[122] Roberto Contino, Yasunori Nomura, and Alex Pomarol, "Higgs as a holographic pseudo-Goldstone boson," *Nucl. Phys.*, vol. B671, pp. 148–174, 2003.

[123] Claude Amsler and A. Masoni, "The $\eta(1405)$, $\eta(1475)$, $f_1(1420)$, and $f_1(1510)$," .

[124] Giacomo Cacciapaglia, Csaba Csaki, Christophe Grojean, Matthew Reece,

134

and John Terning, "Top and bottom: A brane of their own," *Phys. Rev.*, vol. D72, pp. 095018, 2005.

[125] Alexander Muck, Apostolos Pilaftsis, and Reinhold Ruckl, "Minimal Higher-Dimensional Extensions of the Standard Model and Electroweak Observables," *Phys. Rev.*, vol. D65, pp. 085037, 2002.

[126] Jonathan L. Feng, "Supersymmetry and cosmology," 2003.

[127] Kyoungchul Kong and Konstantin T. Matchev, "Precise calculation of the relic density of Kaluza-Klein dark matter in universal extra dimensions," *JHEP*, vol. 01, pp. 038, 2006.

[128] Toru Goto and Masahiro Yamaguchi, "Is axino dark matter possible in supergravity?," *Phys. Lett.*, vol. B276, pp. 103–107, 1992.

[129] Arnd Brandenburg and Frank Daniel Steffen, "Axino dark matter from thermal production," *JCAP*, vol. 0408, pp. 008, 2004.

[130] V. M. Abazov et al., "Search for long-lived particles decaying into electron or photon pairs with the D0 detector," *Phys. Rev. Lett.*, vol. 101, pp. 111802, 2008.

[131] T. Aaltonen et al., "Search for Heavy, Long-Lived Neutralinos that Decay to Photons at CDF II Using Photon Timing," *Phys. Rev.*, vol. D78, pp. 032015, 2008.

[132] V. M. Abazov et al., "Search for scalar leptoquarks and T-odd quarks in the acoplanar jet topology using 2.5 fb^{-1} of $p\bar{p}$ collision data at $\sqrt{s} =$ 1.96-TeV," *Phys. Lett.*, vol. B668, pp. 357–363, 2008.